学位論文

Dynamics of black holes and holography
（ブラックホールの動力学とホログラフィー）

平成２５年１２月博士（理学）
申請

東京大学大学院理学系研究科
物理学専攻
宇賀神　知紀

Abstract

In this thesis, we study black holes in three dimensional anti de Sitter spaces by using AdS_3/CFT_2 correspondence.

Quantum quenches are interesting time dependent processes of CFT_2s. Especially global quneches can be regarded as toy models of thermalizations. In the first original part of the thesis, We propose a systematic construction of holographic duals of two dimensional quantum quenches. We discuss time evolutions of holographic entanglement entropy in these backgrounds and compare them with CFT results. We show how information of bulk holographic geometries, such as horizon interiors are encoded in time evolutions of entanglement entropy under quantum quenches [1].

In the second part, we then analytically calculate the time evolution of entanglement entropy for a free Dirac fermion on a circle following a global quench [2]. This is interpreted as a toy holographic dual of black hole creations and annihilations.

Higher spin theories are toy models of string theory in highly curved spacetimes. In higher spin theories, an event horizon of a black hole is a gauge dependent concept because of the large amount of gauge symmetries. In the final part, we derive an entropy formula for general higher spin black holes in three dimensions [3] . This entropy formula is shown to satisfy correct first law of thermodynamics.

Contents

1 Introduction

Although almost hundred years have passed since discovery of Schwarzchild black holes[4], black holes are still surrounded by a lot of mysteries, and have been a most fascinating subject of theoretical physics. These mysteries have stimulated many physicists to bring a lot of ideas, and we are very sure that they are going to continue to play a central role for advances of theoretical physics. This is because they provide important clues for understanding quantum gravity, toward which we have no experimental suggestions so far. Among these mysteries of black holes, following three problems are most important in my opinion.

(1) Why black holes are thermal?: A black hole is merely a spacetime which is a solution of classical equations of motion, therefore a coherent state in the corresponding quantum theory. But due to the epoch-making work of Bekenstein[5], as well as Badeen, Carter and Hawking [6] which were stimulated by the entropy paradox raised by Wheeler, established the fact that black holes have temperature and thermal entropy. This means that we regard them as coarse grained objects. But how do we coarse grain them? Some progress have been made since the era of the secondary revolution of string theory. Especially, Strominger and Vafa [7] identified the microstates of some special black holes, and found that the enumeration of these microstates yields the Bekenstein Hawking formula of the black hole entropy. However the applicability of their analysis is quite limited to near supersymmetric or extremal black holes. The goal of the study in this direction is to find all the microstates of all black holes, which would have tremendous impacts on our view of nature.

(2) Information loss problem of black holes: Since black holes are themal, they emit thermal radiations like usual black bodies. The radiations are known as Hawking radiations. However the emissions of thermal radiations are problematic. This is because the emissions appear to mean that pure states on black holes can evolve to mixed states. This seems to break unitarity of quantum field theories on them. The paradox is called as information loss problem [8] and has been extensively discussed since its discovery. A product of the long-term discussion is the idea of "black hole complementarity"[11] which suggests highly nonlocal entangling structures of quantum states in black hole backgrounds. More recently, it is suggested that the unitarity of the radiations appears to contradict with the regularity of event horizons [9] (black hole fire walls). The core of the argument is the tension between the special types of entanglement in the presence of event horizons and the fast scrambling natures of black holes[10]. The argument triggered various studies, especially relations between entanglement involving black holes and spacetime structures.

(3)Black holes in quantum gravity, especially in string theory: We know black holes in classical general relativity very well. However the descriptions of them in general relativity are still incomplete in two reasons. The first reason of the incompleteness is

that all classical black hole solutions contain a singularity inside of their horizons where general relativity itself breaks down. Second reason is that general relativity can not be a complete theory when it is quantized, because of its non- renormalizability. String theory is a promising candidate of quantum theory of gravity, and it corrects general relativity in various ways. Thus it is nice to know how these stringy effects correct properties of black holes we know, especially the singularities of the black holes.

One can easily specify a peculiar feature of black holes behind these problems. That is, black holes have event horizons, and inside of the horizons is invisible from the outside of the event horizon. Obviously, the thermal nature of black holes which causes various confusions, is strongly tied to our lack of information because of the presence of the event horizons. The existence of the singularity is also correlated to the existence of event horizons. In a usual classical field theory, a solution with singularities is merely unphysical. However it is believed in the name of cosmic censorship conjecture, that in general relativity, a solution with singularities is still physical, if they are hidden by event horizons.

Taking into account these motivations, in this thesis we would like to make small steps toward complete descriptions of event horizons and inside regions behind them .

Our main tool to study them is gauge/gravity duality, a version of holography [20]. The duality states that a quantum or classical gravity on d+1 dimensional asymptotically anti de Sitter space (AdS_{d+1}) is equivalent to a d dimensional conformal field theory, defined on the boundary of the AdS_{d+1}. Since the boundary CFT constitutes a non-perturbative definition of the bulk quantum gravity, the correct description of the event horizons in the bulk has to be encoded in the CFT observables. The real problem is how we extract the correct structure of an event horizon from the observables. See related discussions regarding bulk reconstruction from the boundary CFT [12, 13, 14, 15, 16, 17]

Here we would like to remark an important fact that to probe the inside of event horizons from the boundary CFT, one needs to consider time dependent observables. As we can see from the figure 1 of the Penrose diagram of an eternal AdS black hole , the static time slice does not probe inside of the event horizon. If we choose another time slice which does probe the inside of the horizon, the eternal black hole looks time dependent because of the expansion of the event horizon. [2] Hence the problem is what is the CFT interpretation of the time dependence of the black hole in the slice and what kind of observables in the CFT are useful to hologaphically probe inside of the horizon.

In the remarkable recent paper [32], Hartman Maldacena answered the question. They showed that the time dependence of the black hole is identical to that of a global quench process [75] of the dual CFT. They further showed that some properties of the event horizon are encoded in the evolution of entanglement entropy in the CFT under these processes.

A global quench is a time dependent process which can be regarded as a toy model of thermalization. In a global quench we prepare a gapped Hamiltonian and its vacuum.

[2]This is quite similar to the relation between the conformal coordinate and the static coordinate of a de Sitter space.

Figure 1: Penrose diagram of an eternal AdS black hole. Two null lines (black) in the diagrams are the event horizons of the black hole. The intersection of the two null lines is the bifurcation surface of the black hole. Left: A static timeslice (blue) does not probe the inside of the event horizon. Right: A timeslice which probes the inside of the event horizon. In this time slice the black hole looks time dependent.

At $t = 0$, we suddenly make the Hamiltonian gappless, so that the vacuum state becomes a homogeneously excited state. Analyzing the process looks a difficult task, particularly when we compare the field theory result with the holographic gravity result, where the strong coupling comes into play. However in two dimensional conformal field theories, one can treat these processes even analytically with the help of conformal symmetry and the boundary state formalism [75].

Entanglement entropy is the particularly interesting observable to probe global quenches. There are multiple reasons for this : The first reason is that entanglement entropy can be defined for any quantum field theory. Because of the ubiquitous nature, it is anticipated that it captures universal natures of global quenches. Indeed we find a universal behavior of entanglement entropy toward thermalization in two dimensional conformal field theories in these quenches. As we will see later, the universality allow us to compare the CFT result to the holographic gravity result. Second reason is that entanglement entropy is a non-equilibrium generalization of usual thermal entropy. Actually, it was shown [75] that at late time of global quenches, entanglement entropy take thermal value with emergent temperature related to the energy scale of the quench. It is also important to note that local observables, like one point functions, turn out to be immediately thermalized after the quench therefore they do not contain useful information. [3]

There various are types of quantum quenches actually. For example, we can consider a quench where one injects energy only at one point of space. This is known as a local quench. Similarly by changing the inhomogeneity on the initial time slice, one can realize various types of quantum quenches. In 2d CFTs, there is a dictionary between these quantum quenches and Riemann surfaces with boundaries. By making use of the dictionary, we can calculate evolutions of entanglement entropy under these quenches.

[3]This is particularly clear from gravity point of view, because correlation functions only probe near the conformal boundary of anti de Sitter space.

A purpose of this thesis is to show how to systematically construct holographic duals of quantum quenches in two dimensional conformal field theories. The main ingredient of the construction is the introduction of a space time boundary, which is the gravity counterpart of a boundary state in the dual CFT. We will see how information of bulk geometries are encoded in the evolution of corresponding quenches.

So far we only address quantum quenches on non compact spaces. When the spatial direction is compact, the time evolution after a quench is more interesting because it contains additional physics, like a recurrence of excited quasi particles. In the bulk point of view, the non-compactness of the spatial direction correspond to taking the high temperature limit of black holes. In the situation quantum effects of these black holes, like Hawking radiations, do not play important roles. To consider these quantum effects, we compute the evolution of entanglement entropy of a free massless Dirac fermion theory under global quenches when the spatial direction is a circle. We find a gravitational interpretation of the result, by successive creations and evaporations of the bulk black holes.

Another insight on event horizons comes from black holes in higher spin theories. A higher spin theory describes the interactions between gravity (spin two field) and massless fields whose spin are larger than two (higher spin fields). Each higher spin field have its own gauge symmetry (higher spin symmetry), which is a generalization of diffeomorphism invariance of the spin two field (gravitions). The full nonlinear equations of motion of the higher spin fields are in general highly complicated. But in three dimensional anti de Sitter spaces , since all the higher spin fields are topological, they are described by certain Chern Simons theories with some gauge groups G which contain $\mathrm{SL}(2,\mathbb{R})$ as a subgroup. These theories are particularly interesting for two reasons. One reason is that they can be regarded as toy models of string theory in spacetimes with sufficiently high curvature. Another reason is that there are several conjectural holographic relations between higher spin theories in AdS and exactly solvable conformal field theories [97, 93]. Especially, asymptotic symmetries of these higher spin theories in AdS_3 turned to be $\mathcal{W}$ algebras, which are generalizations of Virasoro algebra. From this fact, it is conjectured that a certain higher spin theory in AdS_3 is dual to a large N limit of $\mathcal{W}_N$ minimal model [97]. For evidences in favor of the conjecture, see [97, 101, 102, 103, 104]

There is an significant implication of the higher spin symmetries for black holes in higher spin theories. Higher spin symmetries transform the metric of a black hole non trivially. This means that a metric with event horizons can be mapped to another metric without event horizons via the gauge symmetries of the higher spin fields. As a consequence, the notion of an event horizon is a gauge dependent concept in these theories. As we have pointed out, almost all properties as well confusions about black holes in general relativity comes from the existence of event horizons. However, in higher spin theories, properties of black holes are not tied to event horizons. We have not fully understand the implications of the fact yet, hence it is important to study them.

Kraus and his collaborators found three dimensional black holes with higher spin charges [108]. The black holes have natural CFT interpretations as saddle points of grand canonical

partition functions with certain chemical potentials in the high temperature limit. Surprisingly, they found that in a simple gauge, these black holes do not have event horizons. This is because of the higher spin symmetries which we have pointed out, and later, they find a gauge where these black holes have event horizons [110].

To consider thermodynamics, they defined a regularity condition of the Euclidean black holes in terms of holonomy of the Chern Simons connections of these black holes. By solving the condition, and using first law of thermodynamics, they very indirectly computed entropy of these black holes. The results for certain black holes were compared to CFT results, and found that they perfectly agree [115, 116].

In the absence of event horizons what kind of formula does compute the thermal entropy of higher spin black holes? We find a general entropy formula by applying so called conical singularity approach which was developed by Fursaev and Solodukhin [122] to Chern Simons theories. Similar technique were used to prove the Ryu Takayanagi formula for entanglement entropy recently [29]. Furthermore we find that the entropy formula satisfies the desired first law. This means that black hole entropy computed by the formula in some case has a microscopic explanation[115, 116] .

Organizations of this thesis

Organizations of this thesis is as follows. In section 2, we mainly review calculations of entanglement entropy in two dimensional CFTs. In the last part of this section we briefly comment on entanglement entropy in higher dimensional CFTs. In section 3, we review quantum quenches in 2d CFT s. We mainly focus on time evolutions of entanglement entropy under these processes. In section 4, after introducing gauge/gravity duality, we explain holographic calculations of entanglement entropy. In section 5, we see holographic relations between global quenches in CFTs and eternal black holes. In section 6 we discuss a systematic construction of holographic duals of 2d quantum quenches . In section 7, we apply our new construction to various examples, including local quenches, and an finite inhomogeneous quench. We discuss how information of the dual spacetimes are encoded in time evolution of entanglement entropy under these quenches. Section 6 and section 7 are based on the author's work [1]. In section 8, we then analytically calculate the time evolution of entanglement entropy for a free Dirac fermion on a circle following a global quantum quenches. We holographically interpret the result by black hole creations and annihilations. This section is based on the author's work with T.Takayanagi [2]. In section 9, we review higher spin theories in three dimensions. We then consider black hole solutions in the higher spin theories (higher spin black holes) and their thermodynamics. Finally, in section 10 we derive a general entropy formula for higher spin black holes by making use of conical singularity approach. We also see the entropy formula satisfies the first law of thermodynamics correctly. This section is besed on the author's work with P.Kraus [3]

2 Entanglement entropy in field theories

Entanglement is a useful concept to characterize a given state. Entanglement entropy measures how much the state is entangled. Suppose total Hilbert space H_{tot} is divided into a sub Hilbert space H_A and H_B, so that $H_{tot} = H_A \otimes H_B$. Entanglement entropy for a given state $|\psi\rangle$ is defined as follows. First, we define reduced density matrix ρ_A by tracing out the sub Hilbert space H_B

$$\rho_A = \mathrm{tr}_{\mathrm{H_B}}\rho, \quad \rho = |\psi\rangle\langle\psi|, \tag{1}$$

Entanglement entropy is defined as the von Neumann entropy of the reduced density matrix ρ_A

$$S_A = -\mathrm{Tr}\ \rho_{\mathrm{A}} \log \rho_{\mathrm{A}} \qquad \mathrm{Tr}\ \rho_{\mathrm{A}} = 1. \tag{2}$$

Suppose the quantum field theory we consider is defined on a globally hyperbolic manifold $R_t \times \Sigma$, where R_t and Σ denote the time direction and the spatial manifold respectively. We divide Σ into region A and its complement B. In local quantum field theories one can consider an associated sub Hilbert space H_A for region A and its complement H_B. Below we consider this entanglement entropy.

In this section, we review computations of entanglement entropy of vacuum in conformal field theories. These computations are performed by making use of the replica method. The entanglement entropy S_A can be written as follows.

$$S_A = -\frac{\partial}{\partial n}\mathrm{Tr}\ \rho_{\mathrm{A}}^{\mathrm{n}}\Big|_{\mathrm{n}=1}. \tag{3}$$

The $\mathrm{Tr}\,\rho_{\mathrm{A}}^{\mathrm{n}}$ in the left hand side can be regarded as a partition function on a certain singular manifold $\mathcal{R}_n$. This makes a path integral expression of the entanglement entropy possible.

Furthermore, in two dimensional conformal field theories, these computations of $\mathrm{Tr}\ \rho_{\mathrm{A}}^{\mathrm{n}}$ reduce to correlation functions of certain twisted operators. In the subsection 2.2, we explain this approach, and compute entanglement entropy of 2d CFT s on the complex plane $\mathbb{C}$. The result only depends on the central charge of the CFT. In subsection 2.4 we also explain the computation of entanglement entropy of free fermion theory on tori by making use of bosonizations. In subsection 2.5 we comment on higher dimensional results.

2.1 Replica method for entanglement entropy

In this subsection we introduce the replica method. The matrix element of the reduced density matrix $\langle\phi_+|\rho_A|\phi_-\rangle$ can be written as

$$\langle\phi_+|\rho_A|\phi_-\rangle = \int D\phi_B \langle\phi_+|e^{-iHt}|\psi\rangle\langle\psi|e^{iHt}|\phi_-\rangle \tag{4}$$

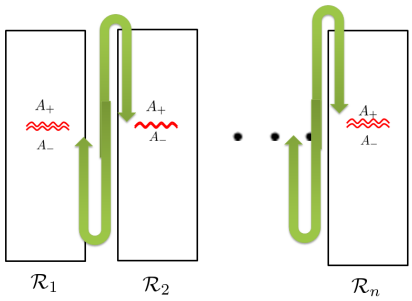

Figure 2: The construction of $\mathcal{R}_n$.We glue each of A_- of i-th sheet to A_+ of i+1 th sheet together.

Two components in the integrand are transition amplitudes, therefore have following path integral representations.

$$\begin{aligned}\langle\phi_-|e^{-iHt}|\psi\rangle &= \int_{\mathcal{R}_-} D\phi\Big|_{\phi(0)=\phi_-} e^{-S[\phi]}\langle\phi(-t)|\psi\rangle \\ \langle\phi_+|e^{iHt}|\psi\rangle &= \int_{\mathcal{R}_+} D\phi\Big|_{\phi(0)=\phi_+} e^{-S[\phi]}\langle\phi(+t)|\psi\rangle. \end{aligned} \tag{5}$$

where regions of integral $\mathcal{R}_-$ and $\mathcal{R}_+$ are upper and lower half space of the spacetime respectively:

$$\mathcal{R}_+ = \{\ (T,x)\mid 0\le T\le t\ , x\in\Sigma\},\quad \mathcal{R}_- = \{\ (T,x)\mid\ -t\le T\le 0\ , x\in\Sigma\}. \tag{6}$$

We then glue the region B of $\mathcal{R}_+$at $t=0$ together with region B of $\mathcal{R}_+$at $t=0$ Therefore, $\langle\phi_+|\rho_A|\phi_-\rangle$ can be computed by a path integral on the region $\mathcal{R}_+\cup\mathcal{R}_-\backslash A$. Below we call this region as a "sheet". The sheet contains two edges, namely region A at $t=0$ of $\mathcal{R}_+$ and region A at $t=0$ of $\mathcal{R}_-$. Below we denote them as A_+ and A_- respectively. Similarly the trace of n-th power of the reduced density matrix tr $\rho_{\mathrm{A}}^{\mathrm{n}}$ is also computed by a path integral on a certain manifold $\mathcal{R}_n$. This $\mathcal{R}_n$ is constructed as follows. First we prepare n copies of sheets. Then we glue each of A_- of i-th sheet to A_+ of i+1 th sheet together, and A_- of n th sheet to A_+ of first sheet. See figure 2. By taking an analytic continuation of tr $\rho_{\mathrm{A}}^{\mathrm{n}}$ with respect to n, and substituting the result into (3) we get the entanglement entropy S_A.

To summarize, via the replica method a computation of entanglement entropy is accomplished by computing path integrals on manifolds $\mathcal{R}_n$ with a branch cut along the subsystem A.

2.2 Entanglement entropy of 2d CFTs on planes

In the previous section we see that it is convenient to analyze $\mathrm{tr}\,\rho_{\mathrm{A}}^{\mathrm{n}}$ to compute entanglement entropy S_A. In this section, we argue that in two dimensional conformal field theories, a computation of $\mathrm{tr}\ \rho_{\mathrm{A}}^{\mathrm{n}}$ is further reduced to a computation of a correlation function of so called twisted vertex operator $\mathcal{O}_n$ [50].

Suppose we take the subsystem A to an interval $[u, v]$. Then the corresponding singular manifold $\mathcal{R}_n$ is mapped to a complex plane $\mathbb{C}$ via the map,

$$w = \left(\frac{z-u}{z-v}\right)^{\frac{1}{n}}. \tag{7}$$

In 2d CFTs, the one point function $\langle T_{zz}(z)\rangle_{\mathcal{R}_n}$ of the holomorphic part of the stress tensor on the singular manifold $\mathcal{R}_n$, is related to that of on the complex plane $\langle T_{ww}(w)\rangle_{\mathbb{C}}$ in following way.

$$\langle T(z)_{zz}\rangle_{\mathcal{R}_n} = \left(\frac{dw}{dz}\right)^2 \langle T_{ww}(w)\rangle_{\mathbb{C}} + \frac{c}{12}\{w, z\}, \quad \{w, z\} = \frac{2w'''(z)w'(z) - 3w''(z)^2}{2w'(z)^2}, \tag{8}$$

where c in the expression denotes the central charge of the CFT we consider. Since one can set $\langle T_{ww}(w)\rangle_{\mathbb{C}}$ to be zero without loss of generality, we find,

$$\langle T_{zz}(z)\rangle_{\mathcal{R}_n} = \frac{c(1-n^{-2})}{24}\frac{(u-v)^2}{(z-u)^2(z-v)^2}. \tag{9}$$

Here we introduce the twisted operator $\mathcal{O}_n$ with scaling dimensions $h_n = \bar{h}_n = \frac{c}{24}(1-\frac{1}{n^2})$. The two point function of the operator is

$$\langle \mathcal{O}_n(u)\mathcal{O}_n(v)\rangle = \frac{1}{(u-v)^{2h_n}(\bar{u}-\bar{v})^{2\bar{h}_n}}. \tag{10}$$

From the definition one can show the following identity.

$$\langle T(z)_{zz}\rangle_{\mathcal{R}_n} = \frac{\langle T_{zz}(z)\mathcal{O}_n(u)\mathcal{O}_n(v)\rangle_{\mathbb{C}}}{\langle \mathcal{O}_n(u)\mathcal{O}_n(v)\rangle_{\mathbb{C}}}. \tag{11}$$

This follows from the Virasoro Ward indentity,

$$\langle T_{zz}(z)\mathcal{O}_n(u)\mathcal{O}_n(v)\rangle_{\mathbb{C}} = \sum_{w_i=u,v}\left(\frac{h_n}{(z-w_i)^2} + \frac{1}{(z-w_i}\frac{\partial}{\partial w_i}\right)\langle \mathcal{O}_n(u)\mathcal{O}_n(v)\rangle_{\mathbb{C}} \tag{12}$$

$$= \frac{h_n(u-v)^2}{(z-v)^2(z-u)^2}\langle \mathcal{O}_n(u)\mathcal{O}_n(v)\rangle_{\mathbb{C}}. \tag{13}$$

The identity (11) tell us that the trace of the reduced density matrix tr $\rho_{\rm A}^{\rm n}$ and n-th power of the two point function of the twisted operator $\langle \mathcal{O}_n(u)\mathcal{O}_n(v)\rangle_{\mathbb{C}}$ have the same transformation properties under all holomorphic maps. Therefore, they are actually same up to some position independent constant,

$$\mathrm{tr}\ \rho_{\rm A}^{\rm n} = {\rm c_n}\left(\frac{|{\rm u}-{\rm v}|}{\rm a}\right)^{-\frac{\rm c}{6}({\rm n}-\frac{1}{\rm n})}. \tag{14}$$

In the expression we introduced a UV cut off a By differentiating it, we obtain the expression of entanglement entropy of 2d CFTs on a plane $\mathbb{C}$,

$$S_A = -\frac{\partial}{\partial n}\mathrm{tr}\ \rho_{\rm A}^{\rm n} = \frac{\rm c}{3}\log\frac{|{\rm u}-{\rm v}|}{\rm a} + \text{const.} \tag{15}$$

2.3 Entanglement entropy on cylinders

In the previous subsection we consider entanglement entropy of general 2d CFT defined on complex planes. We find the expression only depends on the central charge of the CFT we consider. We can see entanglement entropy also depends only on the central charge when the CFT is defined on a cylinder. This is because a cylinder can be mapped to a complex plane via a conformal map. The circle S^1 direction in a cylinder can be either the spatial direction or the Euclidean timelike direction. When the S^1 direction is the spatial direction, the cylinder is mapped to a complex plane via

$$w = \exp\left(\frac{2\pi i z}{L}\right), \tag{16}$$

where we denote L the circumference of the circle. Entanglement entropy is derived by making use of the transformation property of the two point function of the twisted operator.

$$S_A(L) = \frac{c}{3}\log\left[\frac{L}{a\pi}\sin\frac{\pi l}{L}\right], \tag{17}$$

where l denotes the size of the subsystem A. $l = |A|$. Note that in the short distance limit $l \ll L$ the expression is reduced to (15).

To find the expression of entanglement entropy at finite temperature with a non-compact spatial direction, we need to consider a cylinder where the S^1 direction is the Euclidean timelike direction. The circumference β of the cylinder is the inverse of the temperature of the system. The cylinder is mapped to a complex plane via

$$w = \exp\left(\frac{2\pi i z}{\beta}\right), \tag{18}$$

Therefore the entanglement entropy is

$$S_A(\beta) = \frac{c}{3}\log\left[\frac{\beta}{\pi a}\sinh\frac{\pi l}{\beta}\right]. \tag{19}$$

In the high temperature limit $l \gg \beta$, the entanglement entropy become thermal entropy (plus a divergent term)

$$S_A(\beta) \to \frac{c\pi}{3\beta} l + S_{div}. \tag{20}$$

2.4 Entanglement entropy of free Dirac fermion theory on tori

In previous subsection we derive expressions of entanglement entropy on cylinders where one direction is non-compact by making use of conformal maps. The results are universal in the sense that among all parameters which are needed to specify the CFT, they depend only on the central charge. However when both spatial and time like direction are a circle S^1 (ie, the Euclidean space time is a torus), the technique developed in the previous sections can not be applied, and actually entanglement entropy does depend on full operator contents of the CFT. Therefore, calculations of the entanglement entropy become much more difficult, and only few results are known. In this section we review the calculation of entanglement entropy for massless free Dirac fermion on tori [80]. In the discussion below we take the subsystem A to be a segment $[u, v] = [0, L]$

We have argued that entanglement entropy S_A is derived by evaluating the partition function on n-fold covering of the Euclidean spacetime (in this case, a torus) $\mathcal{R}_n$ with branch cuts along the subsystem A.

A path integral of *single* field $\Psi(x)$ on the n sheets spacetime $\mathcal{R}_n$ with identifications along the cuts is equivalent to the path integral of n *copies of fields* $\{\Psi_k\}_{k=1}^n$ on a *single sheet* spacetime with cuts. These fields satisfy the following boundary conditions.

$$\Psi_k(e^{2\pi i}(z-u)) = \Psi_{k+1}((z-u)), \quad \Psi_k(e^{2\pi i}(z-v)) = \Psi_{k-1}((z-v)) \quad 1 \le k \le n. \tag{21}$$

If we define new fields $\Phi_k(z)$ by

$$\Phi_k(z) = \sum_{l=1}^{n} e^{\frac{2\pi i k l}{n}} \Psi_l(z), \qquad 1 \le k \le n. \tag{22}$$

The boundary conditions become twisted boundary conditions.

$$\Phi_k(e^{2\pi i}(z-u)) = e^{-2\pi \frac{ik}{n}} \Phi_k((z-u)), \quad \Phi_k(e^{2\pi i}(z-v)) = e^{2\pi \frac{ik}{n}} \Phi_k((z-v)), \quad 1 \le k \le n. \tag{23}$$

One can convert these multi valued fields to single valued fields by introducing vertex like background U(1) gauge fields $\{A_\mu^k\}_{k=1}^n$ which satisfy,

$$\epsilon^{\mu\nu} \partial_\nu A_\mu^k = \frac{2\pi k}{n} \left[\delta(x-u) - \delta(x-v)\right], \tag{24}$$

or equivalently,

$$\oint_{\mathcal{C}} A^k = -\frac{2\pi k}{n} \qquad \oint_{\mathcal{C}} A^k = \frac{2\pi k}{n}. \tag{25}$$

Hence, we find the partition function Z_n on n-fold cover $\mathcal{R}_n$ is reduced to a path integral of n decoupled fields on the backgound with the U(1) fluxes.

$$Z_n = \prod_{k=-\frac{n-1}{2}}^{\frac{n-1}{2}} \left\langle \exp \int A_\mu^k \, j^\mu \right\rangle. \tag{26}$$

In two dimensions, a free massless Dirac fermion theory is equivalent to a compactified boson theory with radius $R = 1$. The fermion field ψ is related to the boson field ϕ by the relation $\psi = e^{i\phi}$. $U(1)$ current of the Dirac fermion can be written by the bosonic field as

$$\jmath^\mu = \epsilon^{\mu\nu}\partial_\nu \phi. \tag{27}$$

By substituting the background flux (24) into (26), the partition function Z_n is expressed by the products of the correlation functions

$$Z_n = \prod_{k=-\frac{n-1}{2}}^{k=\frac{n-1}{2}} \left\langle e^{\frac{ik}{n}\phi(u)} e^{-\frac{ik}{n}\phi(v)} \right\rangle \tag{28}$$

When the theory is defined on a plane, by making use of the boson propergator

$$\langle \phi(x)\phi(y)\rangle = -\frac{1}{2\pi}\log|x-y|, \tag{29}$$

we recover the entanglement entropy on a plane (15) with $c = 1$.

To proceed, we introduce $\mathcal{O}_{(n,m)}$ which are primary operators of the compactified boson theory with momentum n and winding number w. The scaling dimension of these operators are $h_{(n,m)} = \frac{1}{2}\left(\frac{n}{R} + \frac{wR}{2}\right)^2$, $\bar{h}_{(n,m)} = \frac{1}{2}\left(\frac{n}{R} - \frac{wR}{2}\right)^2$. Their two point function on a torus with the moduli parameter τ is

$$\langle \mathcal{O}_{(n,m)}(z)\mathcal{O}_{(n,m)}(0)\rangle = \left(\frac{2\pi\eta(\tau)^3}{\theta_1(z|\tau)}\right)^{2\Delta_{m,n}} \overline{\left(\frac{2\pi\eta(\tau)^3}{\theta_1(z|\tau)}\right)^{2\bar{\Delta}_{m,n}}} \frac{\sum_{m,n} q^{\Delta_{m,n}} q^{\bar{\Delta}_{m,n}} e^{4\pi i(\alpha_{n,w}\alpha_{m,l} - \alpha_{n,w}\alpha_{m,l})z}}{\sum_{m,n} q^{\Delta_{m,n}} q^{\bar{\Delta}_{m,n}}}. \tag{30}$$

where $\alpha_{n,w} = \frac{1}{\sqrt{2}}\left(\frac{n}{R} + \frac{wR}{2}\right)$,$\bar{\alpha}_{n,w} = \frac{1}{\sqrt{2}}\left(\frac{n}{R} - \frac{wR}{2}\right)$, and $q = e^{2\pi i\tau}$. About the definition of the eta function $\eta(\tau)$ and theta functions $\theta_i(\nu|\tau)$, we followed the convention in [82].

The operators appearing in (28) is identified to be $\mathcal{O}_{(\frac{k}{n},0)}$. In the computation below, we impose anti periodic boundary conditions for our Dirac fermion on both the spatial and the temporal cycle. In that case, the expression correlation function is given by

$$\langle O_{(\frac{k}{n},0)}(L,L)O_{(-\frac{k}{n},0)}(0,0)\rangle_{NS} = \left|\frac{2\pi\eta(\tau)}{\theta_1(L|\tau)}\right|^{4\Delta_k} \frac{|\theta_3(\frac{kL}{N}|\tau)|^2}{|\theta_3(0|\tau)|^2} \tag{31}$$

By substituting this correlation function into (28), we obtain a expression of the entanglement entropy,

$$S_A = \frac{1}{3}\log\left[\frac{\beta}{\pi a}\sinh\left(\frac{\pi L}{\beta}\right)\right] + \frac{1}{3}\sum_{m=1}^{\infty}\log\left[\frac{(1-e^{2\pi\frac{L}{\beta}}e^{-2\pi\frac{m}{\beta}})(1-e^{-2\pi\frac{L}{\beta}}e^{-2\pi\frac{m}{\beta}})}{(1-e^{-2\pi\frac{m}{\beta}})^2}\right] + 2\sum_{l=1}^{\infty}\frac{(-1)^l}{l}\frac{\frac{\pi lL}{\beta}\coth\left(\frac{\pi lL}{\beta}\right)-1}{\sinh\left(\frac{\pi lL}{\beta}\right)}. \tag{32}$$

We immediately see the expression reduces to the temporal cylinder result (19) in the high temperature limit $\beta \to 0$.

Yet an another equivalent expression of the result is obtained by performing a modular transformation,

$$S_A = \frac{1}{3}\log\left[\frac{1}{\pi a}\sin\left(\pi L\right)\right] + \frac{1}{3}\sum_{m=1}^{\infty}\log\left[\frac{(1-e^{2\pi iL}e^{2\pi\beta m})(1-e^{-2\pi L}e^{-2\pi\beta m})}{(1-e^{-2\pi\beta m})^2}\right] + 2\sum_{l=1}^{\infty}\frac{(-1)^l}{l}\frac{1-\pi lL\cot\left(\pi lL\right)}{\sin\left(\pi lL\beta\right)}. \tag{33}$$

The expression is appropriate to see the low temperature limit $\beta \to \infty$, where the expression is reduced to the spatial cylinder result (17).

2.5 Entanglement entropy of CFT in higher dimensions

In general it is hard to compute entanglement entropy in higher dimensional conformal field theories. However at least for free field theories, the results have been obtained by applying the heat kernel method (see for example, [121]) to compute the partition function on $\mathcal{R}_n$. The resulting entanglement entropy contain again UV divergent parts, thus we need to regulate them by introducing lattice spacing a (UV cutoff) to get finite results. Remarkably, the most divergent part in d dimension is proportional to the area of the entangling region ∂A,

$$S_A = \frac{\text{Area}(\Sigma)}{a^{d-2}} + \cdots . \tag{34}$$

Sometimes this is called as area law of entanglement entropy [68]. Note that the result have strong similarity to Bekenstein Hawking formula of black hole entropy in general relativity[4]. This leading divergence can be naturally identified to be contributions from ultraviolet modes which localize near the entangling surface ∂A.

[4]Unfortunately the result can not explain black hole entropy when we take ∂A to the bifurcation surface of a black hole, see Figure 1. The reason is that the total entropy depend on the number of fields on the black hole, while the Bekenstein Hawking formula is not. However the entanglement entropy can be interpreted as 1 loop correction of the black hole entropy[121]

The details of the divergence depend on whether the CFT is defined on even dimensions or odd dimensions. In even dimensions, the divergence contains a logarithmically divergent term,

$$S_A = p_0 \left(\frac{R}{a}\right)^{d-2} + p_2 \left(\frac{R}{a}\right)^{d-4} + \cdots p_{d-2} \log \frac{R}{a} + (\text{finite parts}).,\tag{35}$$

where we denote the size of the subsystem A as R. Although the coefficients $p_i, i = 0 \cdots d-4$ do depend on the cutoff, the coefficient of the logarithmic part does not. In two dimensions, we saw that the coefficient is proportional to the central charge of the theory. Similarly in four dimensions, this term is strongly related to the trace anomaly of the theory. The concrete expression is derived as

$$\begin{aligned} p_{d-2} &= cP_c + aP_a \\ P_c &= -\frac{\pi}{8}\int_{\partial A}\left(R_{ijij} - R_{ii} + \frac{1}{3}R\right) + \left(K^{(i)}_{\mu\nu}K^{(i)\mu\nu} - \frac{1}{2}K^{(i)\mu}_{\mu}K^{(i)\mu}_{\mu}\right) \qquad (36) \\ P_a &= \int_{\partial A} R \qquad (37) \end{aligned}$$

where $n_{i\mu}, i = 1, 2, \mu = 0, 4$ are the unit normal vector fields on ∂A, and $K^{(i)\mu\nu}$ are two extrinsic curvatures of ∂A, $R_{ijij} = R^{\mu\nu\alpha\beta}n_{i\mu}n_{j\nu}n_{i\alpha}n_{j\beta}$, $R_{ii} = R^{\mu\nu}n_{i\mu}n_{i\nu}$, $R^{\mu\nu\alpha\beta}$ is the Riemann tensor of the spacetime. Furthermore R is the intrinsic curvature of ∂A. Therefore roughly speaking this entanglement entropy counts massless degrees of freedom of the conformal field theory in question.

In two dimensions, Zamoldchikov's c theorem states that if we consider RG flows, the central charge of the UV fixed point c_{UV} is always larger than that of the IR fixed point c_{IR}. It is intriguing to note that entanglement entropy provides a c function which connects c_{UV} and c_{IR} in RG flows, and indeed c theorem can be proved by making use of a property of entanglement entropy (strong subadditivity.) [69].

When the spacetime dimensions is odd, the finite part of the entanglement entropy is independent of the UV cutoff a.

$$S_A = p_0 \left(\frac{R}{a}\right)^{d-2} + p_2 \left(\frac{R}{a}\right)^{d-4} + \cdots p_{d-4} \left(\frac{R}{a}\right)^{2} + p_{d-2}.\tag{38}$$

The finite part of the entanglement entropy p_{d-2} for a spherical entangling region $\partial A = S^{d-2}$ turn out to be related to the finite part of the partition function Z_{S^d} of the CFT on d dimensional sphere S^d as $p_{d-2} = \log Z_{S^d}$. Recently it is conjectured that so called F function s $F_d = (-1)^{\frac{d+1}{2}} \log Z_{S^d}$ in odd dimensions are monotonically decreasing along RG flows [70]. The theorem is proved in [71] also by making use of strong subadditivity of entanglement entropy.

3 Quantum quenches in 2d CFTs and evolutions of entanglement entropy

Entanglement entropy is a useful quantity to characterize not only vacuum, but also excited states. It has been shown to be an efficient measure to probe thermalization processes since it can be regarded as a non-equilibrium generalization of thermal entropy.

An interesting toy models of thermalization in two dimensions are proposed in [75], known as global quenches. In a global quench, one prepares a ground state of a gapped Hamiltonian, then excites the system by suddenly changing parameters in the Hamiltonian so that the system becomes gappless, while keeping the translational invariance. The resulting excited state is supposed to have both translational and conformal invariance below the energy scale of the quench, therefore it is well approximated by a boundary state of the gapless theory (CFT_2). The observation about the initial state makes it possible to compute the time evolution of entanglement entropy under the quench by calculating correlation functions of a twisted operator on a strip. The resulting entanglement entropy grows linearly in time and subsequently it is thermalized. The result is interpreted via entangling pairs of quasi particles propagating in opposite direction.

Actually there are a variety of quantum quenches in two dimensional CFTs. For example one can consider quenches where one injects energy only at one point of the initial time slice. These quenches are called local quenches [51]. The time evolution of entanglement entropy was computed by calculating correlation functions of twisted operators which was introduced in the previous section on a plane with slits.

In general, there is one to one correspondence between quantum quenches in 2d CFTs and Riemann surfaces with boundaries. Correlation functions of the twisted operators on these Riemann surfaces are related to time evolutions of entanglement entropy under corresponding quenches. The dictionary relates the energy $\epsilon(x)$ injected at each point x of the initial time slice in the quench to the locations of the boundaries $x \pm \frac{i}{\epsilon(x)}$ in the Riemann surface.

In this section we review various quantum quenches in two dimensional CFTs and time evolutions of entanglement entropy during these processes, which are mainly studied by Cardy and his collaborators.

In a typical quantum quench, we prepare a ground state of a gapped Hamiltonian at the initial time. We then make the system gapless suddenly. In the process, the prepared ground state of the gapped Hamiltonian becomes an excited state of the gappless Hamiltonian, thus it evolves non trivially. We want to compute time dependent entanglement entropy of the excited state. As we have reviewed in the previous section, entanglement entropy $S_A(t)$ of a generic state $|\psi\rangle$ for a subsystem A can be computed by the replica method.

$$S_A(t) = -\frac{\partial}{\partial n}\Big|_{n=1} \mathrm{tr}\rho_A^n(t). \tag{39}$$

The reduce density matrix ρ_A for a subsystem A is defined as

$$\rho_A = \mathrm{tr}_{A^c}[\rho] \qquad \rho = e^{iHt}|\psi\rangle\langle\psi|e^{-iHt}, \tag{40}$$

where A^c denotes the complement of a subsystem A. Actual computations are performed in the Euclidean signature $t \to -i\tau$.

We have also seen that in two dimensional CFTs on a Riemann surface Σ, traces of reduced density matrices tr ρ_A^n can be computed by correlation functions of a twisted operator on Σ. For example, when the subsystem A is an interval $[l_1, l_2]$, the relation is

$$\mathrm{tr}\ \rho_A^n(\tau) = \langle \mathcal{O}(l_1, \tau)\mathcal{O}(l_2, \tau)\rangle_\Sigma. \tag{41}$$

The conformal weights of the operator are $\Delta_n = \bar{\Delta}_n = \frac{c}{24}\left(n - \frac{1}{n}\right)$, where c is the central charge of the CFT. As we will see below, by changing the background Riemann surface Σ one can change the way to quench the system. We then analytically continue the imaginary time $\tau \to it$ and derive real time evolution of entanglement entropy.

3.1 Global quenches

In this subsection we review global quenches. In these quenches we excite each points of the spatial direction homogeneously. The resulting initial states $|\psi\rangle$ are translational and conformal invariant below the energy scale of the quench $4/\beta$, thus they can be written by a boundary states $|B\rangle$ of the CFT as $|\psi\rangle = e^{-\frac{\beta}{4}H}|B\rangle$. The factor in front of the boundary state manifests the energy scale of the quench. The matrix element of the density matrix $\langle\phi_1|\rho|\phi_2\rangle$ can be written as

$$\begin{aligned}
\langle\phi_1|\rho|\phi_2\rangle &= \langle\phi_1|e^{-iHt}|\psi\rangle\langle\psi|e^{iHt}|\phi_2\rangle \\
&= \langle\phi_1|e^{-iHt}e^{-\frac{\beta H}{4}}|B\rangle\langle B|e^{-\frac{\beta H}{4}}e^{iHt}|\phi_2\rangle \\
&= \langle B|e^{-\left\{\frac{\beta}{4}-it\right\}H}|\phi_2\rangle\langle\phi_1|e^{-H\left\{it-(-\frac{\beta}{4})\right\}}|B\rangle.
\end{aligned} \tag{42}$$

If we regard t to be a pure imaginary, the matrix element can be interpreted as Euclidean transition amplitude where the boundary state $|B\rangle$ at $\tau = -\frac{\beta}{4}$ goes back to itself at $\tau = \frac{\beta}{4}$. The amplitude can be written by path integral on a strip with width $\frac{\beta}{2}$. Hence a trace of a reduced density matrix tr $\rho_A^n(\tau)$ of these excited states can be computed by a partition function of the CFT on the strip whose width is $\frac{\beta}{2}$ with boundary conditions at $\tau \pm \frac{\beta}{4}$ and a branch cut along the subsystem A at imaginary time it . The partition function is equivalent to a correlation function of a twisted operator, which can be computed by mapping the strip to a half plane. The strip and a half plane are related via

$$w = \frac{\beta}{2\pi}\log z. \tag{43}$$

The two point function of the twisted operator on a half plane have following form

$$\langle \mathcal{O}_n(w_1)\mathcal{O}_n(w_2)\rangle_{HP} = \left(\frac{|w_1+\bar{w_2}||w_2+\bar{w_1}|}{|w_1-w_2||\bar{w_1}-\bar{w_2}||w_1+\bar{w_1}||w_2+\bar{w_2}|}\right)^{2\Delta_n}. \tag{44}$$

Generically the two point function contains a function that depends on cross ratio. However in sufficiently early time $t \ll |l_2 - l_1|$ or late time $t \gg |l_2 - l_1|$, the two point function is factorized. Therefore contributions from the function can be negligible in these limit. See for example [52] and explicit calculations [2]. Below we assume this. By the same reason the result does not depend on the choice of the boundary state in this limit. The trace of the reduced density matrix $\mathrm{tr}\rho_A^n(t)$ on the strip when the subsystem A is a interval is given by applying the conformal map (43),

$$\mathrm{tr}\rho_A^n(t) = \langle \mathcal{O}_n(\frac{l}{2}+it)\mathcal{O}_n(-\frac{l}{2}+it)\rangle_{\text{strip}} = c_n \left(\frac{\sinh(\frac{2\pi l}{\beta})+\cosh(\frac{4\pi t}{\beta})}{\sinh^2(\frac{\pi l}{\beta})\cosh^2(\frac{2\pi t}{\beta})}\right)^{2\Delta_n}, \tag{45}$$

where c_n is a constant which does not depend on l, t or β. Because of homogeneity of the quench, one can take the subsystem A to be $[-\frac{l}{2}, \frac{l}{2}]$ without loss of generality. If we take the high temperature limit $\beta \to 0$, entanglement entropy behaves like

$$S_A(t) = \frac{2\pi ct}{3\beta}\theta(\frac{l}{2}-t) + \frac{\pi cl}{3\beta}\theta(t-\frac{l}{2}). \tag{46}$$

Where the $\theta(x)$ is the step function. From the expression we see that when $t \leq \frac{l}{2}$ $S_A(t)$ grows linearly in time , and when $t \geq \frac{l}{2}$ it takes thermal value with the inverse temperature β. The stress energy tensors on the strip is given by

$$\langle T_{zz}\rangle = \frac{c}{24}\left(\frac{2\pi}{\beta}\right)^2 \qquad \langle \bar{T}_{\bar{z}\bar{z}}\rangle = \frac{c}{24}\left(\frac{2\pi}{\beta}\right)^2. \tag{47}$$

Thus the width of the strip β can be identified as inverse of effective temperature induced by the quench.

3.2 Inhomogeneous quenches

Having identified the width of the strip with an inverse of effective temperature after the thermalisation, one can also consider various generalizations of the global quenches where the energy density $1/\beta$ one injects depend on the positions in the spatial direction x. These quenches are called inhomogeneous quenches [53]. To treat them we need to deal with wavy strips whose width depend on the position in the spatial direction.

Let us consider a wavy strip extending along the x direction, and at each x, width is given by $\frac{1}{2}(\beta + h(x))$. If inhomogeneity is infinitesimally small, $h(x) \ll \beta$, the conformal

map which maps the wavy strip with coordinate z to the ordinary strip with width $\frac{\beta}{2}$ with coordinate w is given by $w = z - f(z)$, where the $f(z)$ is

$$f(z) = \int_{-\infty}^{\infty} F(s-z)h(s)ds. \tag{48}$$

The karnel $F(s-z)$ is

$$F(z) = \frac{1}{2\beta}\left(\tanh\frac{2\pi z}{\beta} + 1\right), \tag{49}$$

the detail of the construction is in [53]. One can get a simpler expression when z lies in the real axis of the wavy strip and high temperature limit is taken $\beta \to 0$, because the kernel reduces to a step function. Then the $f(x)$ reduces to

$$f(x) = \frac{1}{\beta}\int_{-\infty}^{x} h(s)ds. \tag{50}$$

One can compute correlation functions of the twisted operator in the wavy strip by using the map $w = z - f(z)$ with (50) for arbitrary $h(x)$ .The final expression of the entanglement entropy in high temperature limit is

$$\begin{aligned} S(l_1, l_2, t) = & S_0(l_1, l_2, t) \\ & - \frac{c\pi}{6\beta^2}\theta(\frac{l_2 - l_1}{2} - t)\left[\left(\int_{l_1-t}^{l_1+t} + \int_{l_2-t}^{l_2+t}\right) h(s)ds\right] \\ & - \frac{c\pi}{6\beta^2}\theta(t - \frac{l_2 - l_1}{2})\left[\left(\int_{l_1-t}^{l_2-t} + \int_{l_1+t}^{l_2+t}\right) h(s)ds\right] \\ & + \frac{c}{12}\left(h(l_1 - t) + h(l_1 + t) + h(l_2 - t) + h(l_2 + t)\right), \end{aligned} \tag{51}$$

Where $S_0(x_1, x_2, t)$ denotes the time evolution of entanglement entropy in the unperturbed global quench. The second and the third term can be interpreted by the quasi particle picture. The quasi particles which contribute to entanglement at fixed time $t < \frac{l_1 - l_2}{2}$ are lie in the segment $[l_1 - t, l_1 + t]$ and $[l_2 - t, l_2 + t]$ at the initial time. The total contributions of them to entanglement entropy is

$$\frac{c\pi}{6}\left(\int_{l_1-t}^{l_1+t} + \int_{l_2-t}^{l_2+t}\right)\frac{ds}{\beta + h(x)}. \tag{52}$$

If we set $h(x) = 0$, the expression reproduces the linear grow of the global quench in the early time. Thus one can regard it a direct generalization of the global quench. Since we are assuming $h(x) \ll \epsilon$ we get the second term of (51). Third term can be interpreted by a similar manner.

The time evolutions of stress energy tensors are

$$\langle T_{++}(x,t)\rangle = (1-2f'(x+t))\frac{c}{24}\left(\frac{2\pi}{\beta}\right)^2 + \frac{c}{24}f'''(x+t) \tag{53}$$
$$\langle T_{--}(x,t)\rangle = (1-2f'(x-t))\frac{c}{24}\left(\frac{2\pi}{\beta}\right)^2 + \frac{c}{24}f'''(x-t).$$

3.3 Local quenches

We can consider a quench where we inject energy $1/\epsilon$ only at one point of the initial time slice[51]. Therefore in the quench the corresponding Riemann surface is the plane with two slits which extend along $[-i\infty, -i\epsilon]$ and $[i\epsilon, i\infty]$. The Riemann surface is mapped to the half plane via [51]

$$w = \frac{z}{\epsilon} + \sqrt{\left(\frac{z}{\epsilon}\right)^2 + 1}. \tag{54}$$

Suppose we take the subsystem A to be a finite interval $[l_1, l_2]$. The time evolution of the entanglement entropy under the quench can be computed by substituting the analytic continuation of the map (54) into the general formula (330) of the Appendix.

$$\begin{aligned} S_A(l_1,l_2,t) = &\frac{c}{6}\log\left[\left(2l_1 + \sqrt{(l_1+t)^2+\epsilon^2} + \sqrt{(l_1-t)^2+\epsilon^2}\right)(l_1 \leftrightarrow l_2)\right] \\ &+ \frac{c}{6}\log\left[\left((l_2-l_1) + \sqrt{(l_2+t)^2+\epsilon^2} - \sqrt{(l_1+t)^2+\epsilon^2}\right)(t \leftrightarrow -t)\right] \\ &- \frac{c}{6}\log\left[\left((l_1+l_2) + \sqrt{(l_1+t)^2+\epsilon^2} + \sqrt{(l_2-t)^2+\epsilon^2}\right)(t \leftrightarrow -t)\right] \\ &- \frac{c}{12}\log\left[a_{LQ}^2\left(1+\frac{l_1+t}{\sqrt{(l_1+t)^2+\epsilon^2}}\right)\left(1+\frac{l_1-t}{\sqrt{(l_1-t)^2+\epsilon^2}}\right)(l_1 \leftrightarrow l_2)\right] \end{aligned} \tag{55}$$

.

Figure 3 show the plot of the time evolution of entanglement entropy for several values of ϵ. At the late time $t \to \infty$ the expression settles down to the vacuum value

$$S_A(l_1,l_2,t) \to \frac{c}{3}\log\frac{|l_1-l_2|}{a_{LQ}}, \qquad t \to \infty. \tag{56}$$

The early time behavior of (55) depends on the sign of l_1. In the high energy limit $\epsilon \to 0$, when $0 < l_1 < l_2$,

$$S_A(t) = \frac{c}{6}\log\left[\frac{8l_1l_2(l_1-l_2)^2}{(l_1+l_2)^2}\right], \quad t \sim 0. \tag{57}$$

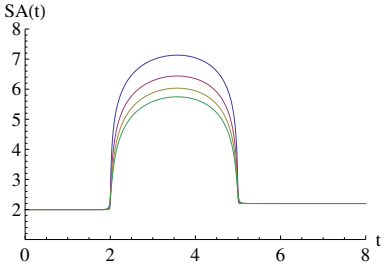

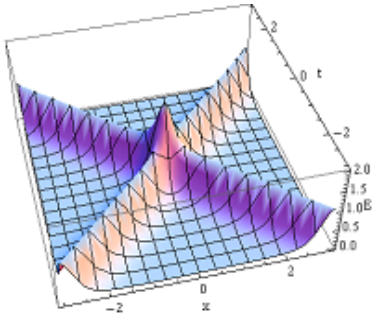

Figure 3: Left:Plot of the time evolution of entanglement entropy under local quenches for various values of ϵ.As we decrease ϵ, maximum value of entanglement entropy become larger. We take $l_1 = 2, l_2 = 5, c = 6$. Right: Plot of the time evolution of energy density $\langle T_{tt}(x,t)\rangle$ during the quench. We take $\epsilon = \frac{1}{2}, c = 2$.

When $l_1 < 0 < l_2$,

$$S_A(t) = \frac{c}{6}\log\frac{4|l_1|l_2}{a_{LQ}^2}, \quad t \sim 0. \tag{58}$$

Time dependence of entanglement entropy $S_A(t)$ in the process can be explained by the quasi particle picture. Let us consider the $l_1 < 0 < l_2$ case for example. In the local quench, an entangled pair of quasi particles with speed of light is created at $t = 0, x = 0$ where the quench happens. When $0 < t < \min\{|l_1|, l_2\}$, the entangled pair completely lie inside of the subsystem A, thus entanglement between the subsystem A and its complement does not increase. When $\min\{|l_1|, l_2\} \leq t < \max\{|l_1|, l_2\}$ one of the quasi particle lie outside of the subsystem A. Because of this, entanglement between A and its complement increases, and S_A shows nontrivial time dependence. At late time $\max\{|l_1|, l_2\} \leq t$, both quasi particles lie outside of the subsystem A, hence S_A does not increase.

4 Holographic entanglement entropy

The idea of holography [18, 19] is a statement that a d+1 dimensional quantum gravity on a region $\mathcal{M}_{d+1}$ is equivalent to a d dimensional quantum field theory *without* gravity living on the boundary of the region $\partial\mathcal{M}_d$.

A concrete example of holography is so called AdS/CFT correspondence. This is the equivalence between quantum theories of gravity (in particular, string theory) in a d+1 dimensional anti de Sitter space AdS_{d+1} and gauge theories with conformal symmetry living on the boundary of the AdS_{d+1}. The correspondence can be naturally generalized to dualities between theories of gravity on *asymptotically* AdS_{d+1} spacetimes and gauge theories *without* conformal symmetry. Therefore the correspondence is more broadly refereed as gauge/gravity duality.

Many studies were devoted to elaborate the duality since the discovery of AdS/CFT correspondence. Among them, Ryu and Takayanagi conjectured that entanglement entropy of a boundary d dimensional gauge theory is related to areas of extremal surfaces in the dual asymptotically AdS_{d+1} spacetime. The conjecture can be regarded as a natural generalization of Bekenstein Hawking formula of black hole entropy.

In this section, after a brief introduction of AdS/CFT correspondence, We explain precise relations between entanglement entropy and extremal surfaces of the dual spacetime. We also address the proof of the conjecture and generalizations of the formula to theories of gravity with higher curvature interactions.

4.1 Introduction to gauge/gravity dualities

4.1.1 IIB string on $AdS_5 \times S^5$ vs $\mathcal{N} = 4$ SYM

A typical example of gauge/gravity duality is the equivalence between type IIB string theory on $AdS_5 \times S^5$ and $\mathcal{N} = 4$ super Yang Mills theory with gauge group $SU(N)$ [20]. This duality was derived by noting that there are two descriptions of dynamical degrees of freedoms of N coincident D3 branes, which are non-perturbative solitons of type IIB string theory. In the closed string picture the coincident D3 branes is described by a ten-dimesional spacetime with an event horizon, and the excitations around this spacetime are described by closed strings (IIB string theory). On the other hand, in the open string picture the coincident D3 branes is described by four dimensional object which are decoupled from gravity, and their dynamics are described by opens strings attaching on the branes ($\mathcal{N} = 4$ $SU(N)$ super Yang Mills theory). Since in the colosed string picture the near horizon limit ofthe spacetime $AdS_5 \times S^5$, one is led to the conjecture of [20].

IIB string theory on the background contains two parameters, namely the closed string coupling g_s and curvature radius of the AdS_5 in the string unit L/l_s. While $\mathcal{N} = 4SU(N)$ super Yang Mills theory also contains two parameters, that are the rank of the gauge group N and t'Hooft coupling $\lambda = g_{YM}^2 N$ where g_{YM} denotes gauge coupling, and it is related to

the string coupling by $g_s = g_{YM}^2$. The curvature radius of the AdS_5 is related to the t'Hooft coupling of dual gauge theory by $\lambda = L^4/l_s^4$

In the $g_s \to 0$ and $L/l_s \to \infty$ limit, IIB string theory on the background is reduced to classical IIB supergravity. In the dual gauge theory side the limit corresponds to large N, large t' Hooft coupling limit. Hence one can see that the strongly coupled large N $\mathcal{N} = 4$ super Yang Mills theory is equivalent to weakly coupled typed IIB supergravity on $AdS_5 \times S^5$. The observation makes it possible to convert difficult gauge theory problems involving strong coupling into easy classical problem of gravity. Below we mainly consider gauge/gravity duality in this regime.

By using the gauge/gravity duality we can also derive various insights regarding quantum gravity and black holes. A most impressible one is the implication for the black hole information loss problem. Since evolutions in gauge theories are always unitary, evaporations of black holes must also be unitary.

4.1.2 Matching of Symmetries

There are a lot of evidences of the AdS/CFT correspondence. The most simple one is the matching of symmetries of both sides. We know that the isometry group of a d+1 dimensional anti de Sitter space is $SO(2, d)$ which is also the symmetry of vacuum of d dimensional conformal field theories. To be specific, let us define so called Poincare coordinate of the d+1 dimensional anti de Sitter space (z, x^μ), $\mu = 0, \cdots d-1$, where the metric of the spacetime is

$$ds^2 = \frac{L^2(dz^2 + \eta_{\mu\nu}dx^\mu dx^\nu)}{z^2}. \tag{59}$$

L appearing the metric is proportional to the curvature radius of the spacetime. Furthermore, (59) satisfy Einstein equation with negative cosmological constant.

$$R_{\mu\nu} = -\frac{d(d-1)}{L^2} g_{\mu\nu}. \tag{60}$$

The flat Minkowski space at $z = 0$ is the boundary of the AdS_{d+1}, where the dual conformal field theory is defined. The metric 59 is invariant under the following coordinate transformations.

$$z \to \Lambda z \quad x^\mu \to \Lambda x^\mu. \tag{61}$$

In the boundary directions these transformations are nothing but scale transformations. Therefore this element of isometries correspond to the actions of the dilatation operator of the dual conformal field theory. As a byproduct, it turns out that the emergent z direction corresponds to the energy scale of the dual CFT.

4.1.3 Bulk-boundary relation and dictionary

In gravity side, the excitations around an anti de Sitter space are described by various supergravity fields $\{\phi\}$. On the other hand, the excitations around the vacuum of the

dual conformal field theory are dominated by operators $\{\mathcal{O}\}$ with low scaling dimensions . Hence there must be a dictionary between the supergravity fields$\{\phi\}$ and low dimensional operators in the CFT $\{\mathcal{O}\}$. Indeed, there is a dictionary between the bulk fields and operators in the boundary theory as follows,

- Boundary scalar operator $\mathcal{O} \longleftrightarrow$ Bulk scalar field ϕ.
- Boundary current J_μ of global symmetry G $\longleftrightarrow$ Bulk G valued gauge field A_μ
- Boundary stress energy tensor $\longleftrightarrow$ Bulk gravitational field $g_{\mu\nu}$

Suppose ϕ is a minimally coupled scalar field in the bulk. To specify a theory in the bulk, one needs to impose boundary conditions on ϕ at the boundary of the bulk $z = 0$. By solving the equation of motion of the scalar field (Klein -Gordon equation), one can specify the near boundary behavior of the field,

$$(\Box - m^2)\phi(z, x^\mu) = 0 \longrightarrow \phi(z, x^\mu) \sim \phi_0(x^\mu) z^{d-\Delta} + \beta(x^\mu) z^\Delta, \quad z \sim 0 \tag{62}$$

Where the Δ appearing in (62) is related to the mass m of the scalar field as

$$\Delta = \frac{d}{2} + \sqrt{\frac{d^2}{4} + m^2}. \tag{63}$$

Since turning non zero $\phi_0(x^\mu)$ breaks the asymptotic AdS condition, this corresponds to a deformation of the bulk theory. In dual CFT side, this is supposed to be related to the deformation in terms of external field $\phi_0(x^\mu)$, $I_{CFT} \to I_{CFT} + \int dx^d \phi_0(x)\mathcal{O}(x)$.

Since two theories are equivalent, it is natural to assume that partition functions of both sides are equal,

$$Z_{gravity}[\phi_0(x^\mu)] = \left\langle e^{\int dx^d \phi_0(x)\mathcal{O}(x)} \right\rangle_{gauge}. \tag{64}$$

where $\phi_0(x^\mu)$ appearing in the left hand side makes the boundary condition of the bulk theory manifest. The equation (64) is called as bulk to boundary relation or GKP-W relation[88], and it plays a central role in studies of gauge/gravity duality since their seminal works.

When the classical approximation is valid in the bulk, the left hand of (64) can be evaluated by computing the on-shell actions of the bulk fields, while the right hand side is a highly quantum object, and hard to compute in traditional techniques. This fact makes the bulk to boundary relation (64) to be the strongest tool for studies of field theoretical phenomena involving strong couplings.

An example of the use of the relation (64) is the reproductions of two point functions of CFT operators $\mathcal{O}(x)$. The two point functions are completely fixed by the conformal symmetry,

$$\langle \mathcal{O}(x)\mathcal{O}(y)\rangle = \frac{1}{|x-y|^{2\Delta}}. \tag{65}$$

By substituting the near boundary solution (**??**) into the on shell bulk scalar action, we can reproduce the two point function holographically.

4.1.4 Black branes in bulk and their CFT interpretations

In non-abelian gauge theories, there are various phases. A typical example is the confining phases where the all particles with color charges are confined, and only colorless excitations are allowed. There are also the deconfining phases, where the colorful, gapless excitations are allowed. At finite temperature, the free energies of the deconfining phases are proportional to N^2, where N denotes the rank of the gauge group we consider. The free energies of AdS black branes also scale like N^2 (inverse of Newton constant), it is natural to identify these black branes as gravity duals of deconfining phases at finite temperature. One can also check that both free energies have the same temperature dependence because of the conformal invariance.

In the field theory side, it is known that below some critical temperature, the deconfining phases are disfavored, and the confining phases are realized. Accordingly, in the gravity side at some critical temperatures there are a sharp first order phase transitions between the AdS black branes and the AdS solitons which is a gravity dual of confining phase. These transitions between two spacetimes are known as Hawking-Page transitions [35].

So far we have discussed that a AdS black brane is a gravity realization of a thermal ensemble $\rho = \sum_n e^{-\beta E_n}|E_n\rangle\langle E_n|$ of the dual CFT at sufficiently high temperature regime (a deconfining pahse). E_n denotes each energy spectrum of the CFT. There is an alternative description of the thermal density matrix ρ in terms of a pure state, by doubling the CFT Hilbert space. Consider the following state (the thermo field double state).

$$|\psi\rangle = \sum_n e^{-\frac{\beta}{2}E_n}|E_n\rangle_R|E_n\rangle_L. \tag{66}$$

Here we prepare a pair of identical Hilbert spaces $\mathcal{H}_R = \mathcal{H}_L = \mathcal{H}_{CFT}$, and the state $|\psi\rangle$ belongs to the tensor product of the Hilbert space $\mathcal{H}_{tot} = \mathcal{H}_L \otimes \mathcal{H}_R$.

Since the thermo field double state $|\psi\rangle$ involves two Hilbert spaces $\mathcal{H}_R$ and $\mathcal{H}_L$, its gravity dual has to contain two boundaries. Also, by tracing out a half of the total Hilbert space H_R or H_L, we get a single boundary black brane. Therefore it is natural to guess that the gravity dual of the state is the maximal extension of the AdS black brane. (eternal black brane) [34]. The eternal black brane is parametrized by the Kruskal coordinates U, V and the boundary spatial coordinates.(figure 1)

The thermo field double state $|\psi\rangle$ is invariant under the time evolution by the total Hamiltonian $H = H_R - H_L$. H_R and H_L denotes the CFT Hamiltonian. Accordingly, the eternal black brane is static under the Lorentz boost of the Kruskal coordinates $U \to Ue^tV \to Ve^{-t}$, see the left panel of figure 1. On the other hand if we employ a Hamiltonian $H = H_R + H_L$, the thermo field double state becomes a time dependent state. In the gravity side, this corresponds to the right figure of figure 1. Thermal entropy of the ensemble is

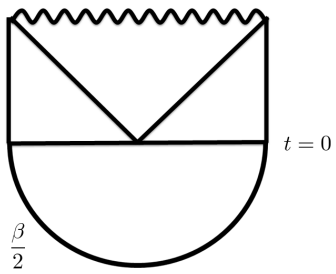

Figure 4: A Hartle Hawking state is derived by a path integral along a half of a Euclidean timelike cycle. The Hartle Hawking state is connected to the Lorentzian space times at $t = 0$

equivalent to the entanglement entropy of the state $|\psi\rangle$ derived by tracing out a half of the total Hilbert space.

A thermal ensemble density matrix $\rho = e^{-\beta H}$ is realized by a path integral along the Euclidean timelike circle with period β. Similarly, A thermo field double state can be realized by integrating along the half of the Euclidean timelike circle. The construction is very much similar to that of a Hartle Hawking state on a black brane. Indeed a Hartle Hawking state is derived by the path integral on half of a Euclidean black brane solution. See figure 4. It is also intriguing to note that Israel has pointed out Hartle Hawking states in eternal black holes can be written as the thermofield double states (66) (66) [126].

4.2 Holographic entanglement entropy

In the papers[21], it was proposed that entanglement entropy with subsystem A of strongly coupled large N gauge theories which have bulk duals can be computed by the area of an extremal surface in the dual holographic spacetime.

$$S_A = \underset{\gamma_A \sim A}{\text{Ext}} \frac{\text{Area}(\gamma_A)}{4G_N}. \tag{67}$$

Here γ_A in the expression denotes codimension two surfaces which end on the conformal boundary of AdS at ∂A of the subsystem. Furthermore $\gamma_A \sim A$ means that γ_As are homologous to the subsystem A. When there are several extremal surfaces we take the minimal area surface.

Area of extremal surfaces are divergent at the conformal boundary of the AdS, therefore we need to introduce a cutoff to regulate them. The same property is appearing in CFT entanglement entropy. We immediately find that the holographic formula pases two nontrivial tests .

- The area law divergence of entanglement entropy is manifest in the holographic side, because the extremal surface intersects with conformal boundary at ∂A
- The holographic formula satisfies the strong subadditivity of entanglement entropy [26, 27],

  $S_{A\cup B} + S_{B\cup C} \geq S_{A\cup B\cup C} + S_B, \quad S_{A\cup B} + S_{B\cup C} \geq S_A + S_C.$

The necessary and sufficient conditions for a codimension two surface $X^\mu(\xi^i)$, $i = 1\cdots d-1$ to be a saddle point of the area functional are the traces of two extrinsic curvatures of the surface vanish, $= K_i^{(a)i} = 0$, $a = 1, 2$. To see this, we consider general functionals $L(h_{ij})$ of the induced metric h_{ij} on the surface,

$$S = \int L(h_{ij})\, d\xi^{d-2} \quad h_{ij} = g_{\mu\nu}\frac{\partial X^\mu}{\partial \xi^i}\frac{\partial X^\nu}{\partial \xi^j}. \tag{68}$$

The greek indices denote spacetime coordinates and alphabet indices denote coordinates on the surface we consider. Taking variation in terms ofX^μ,

$$\begin{aligned}\delta S &= \int d\xi^{d-1}\frac{\delta L}{\delta h_{ij}}\left[2g_{\mu\nu}\frac{\partial \delta X^\mu}{\partial \xi^i}\frac{\partial X^\mu}{\partial \xi^j}\right] \\ &= -\int d\xi^{d-1}\delta X^\mu\left[\frac{\partial}{\partial \xi^i}\left(\frac{\delta L}{\delta h_{ij}}\right)g_{\mu j} + \frac{\delta L}{\delta h_{ij}}\frac{\partial g_{\mu j}}{\partial \xi^i}\right] \\ &.\end{aligned} \tag{69}$$

By using the fact that the variation of the functional $\frac{\delta L}{\delta h_{ij}}$ and the spacetime metric $g_{\mu i}$ vanish by applying the covariant derivative ∇_i, ie $\nabla_i \frac{\delta L}{\delta h_{ij}} = \nabla_i g_{\mu j} = 0$, we find,

$$\Pi_\mu = \frac{\delta S}{\delta X^\mu} = \frac{\delta L}{\delta h_{ij}}\Gamma^k_{i\mu}g_{kj} - \Gamma^i_{ik}\frac{\delta L}{\delta h_{kj}}g_{\mu j}. \tag{70}$$

In an extremal surface these quantities Π_μ are vanish. Since the extremal surfaces are codimension two surfaces, there are two normal vector fields on the surface $n_\mu^{(a)}$ $a = 1, 2$, which are orthogonal to the surface. Contracting Π_μ by $n_\mu^{(a)}$, we get,

$$0 = \frac{\delta L}{\delta h_{ij}}\Gamma^k_{i\mu}n^{(a)\mu}g_{kj} \tag{71}$$

Substituting the area functional $L(h_{ij}) = \det h_{ij}$, we obtain the expected conditions,

$$0 = \frac{\delta L}{\delta h_{ij}}\Gamma^k_{i\mu}n^{(a)\mu}g_{kj} = K_i^{(a)i}. \tag{72}$$

Hence we see that on an extremal surface, traces of two extrinsic curvatures vanish.

4.3 Holographic computation of entanglement entropy of CFT_2

In this subsection we would like to re-derive the entanglement entropy of CFT_2 vacuum on complex planes holographically . The dual spacetimes are the Poincare AdS_3s, whose metrics are given by (129), with $\mu = 0, 1$. Here we take the subsystem A to be an interval $-\frac{l}{2} \leq x \leq \frac{l}{2}$, located at $t = 0$. We assume that the extremal surface is entirely lying in the time slice $t = 0$ and symmetric under the parity transformation $x \to -x$. We parametrize the surface by the radial coordinate z as $x = x(z)$, together with the boundary conditions.

$$x(z_m) = 0, \qquad x(a) = \frac{l}{2}. \tag{73}$$

We introduced a UV cutoff a and maximal value of the radial coordinate z_m.

The length of a given curve $x = x(z)$ in the Poincare AdS_3 is given by

$$A[\gamma] = 2L \int_a^{z_m} \frac{\sqrt{1 + x'(z)^2}}{z} dz. \tag{74}$$

Te factor 2 in front of the integral comes from the parity invariance of the surface. Since the functional does not depend on the $x(z)$, there is a conserved quantity,

$$\frac{x'(z)}{z\sqrt{x'(z)^2 + 1}} = \frac{1}{z_m}. \tag{75}$$

By solving it in terms of $x'(z)$, we find the following relations ,

$$l = 2 \int_a^{z_m} \frac{z}{\sqrt{z_m^2 - z^2}} dz, \quad A_{\min} = 2L \int_a^{z_m} \frac{z_m}{z} \frac{dz}{\sqrt{z_m^2 - z^2}}. \tag{76}$$

After integrations, we find the following result for holograhic entanglement entropy.

$$S_{HEE} = \frac{A_{\min}}{4G_N} = \frac{c}{3} \log \frac{l}{a}, \quad \text{with } c = \frac{3L}{2G_N} \tag{77}$$

The central charge appearing in the above expression perfectly agrees with that of derived from the asymptotic symmetry algebra [28] or the holographic weyl anomaly in two dimensions[47, 48, 49]. Therefore we see the proposal does pass the nontrivial test.

4.4 Cylinder entanglement entropy and global AdS_3

One can also reproduce the entanglement entropy on a cylinder which is periodic along the spatial direction $x \sim x + R$ by calculating length of the extremal surfaces in global AdS_3s. Let us find the length of them. The extremal surfaces connect two endpoints of the subsystem A at the cutoff surface $z = a_{\mathrm{gAdS}_3}$.The metric of the global AdS_3 is given by

$$ds^2 = l^2 \left[\frac{dz^2}{z^2} + 2 \left(\frac{dx^+}{z} - \frac{\pi^2 z}{2R^2} dx^- \right) \left(\frac{dx^-}{z} - \frac{\pi^2 z}{2R^2} dx^+ \right) \right], \tag{78}$$

here we employed a null coordinate on the boundary cylinder $x^{\pm} = x \pm t$. Since the spacetime is static, it is convenient to work with the Euclidean metric by taking an analytic continuation $t \to it$. Because Einstein gravity in three dimension is a topological theory, the Euclidean global AdS_3 and a Euclidean Poincare AdS_3 is related via a coordinate transformation. Let $w, \bar{w}$ be complex coordinates of the boundary plane, and u be the radial coordinate of the Poincare AdS_3.

$$ds^2 = \frac{du^2 + dwd\bar{w}}{u^2}. \tag{79}$$

Near the boundary, the two coordinates are related via [46]

$$w = e^{\frac{2\pi i}{R}(x+it)}, \quad \bar{w} = e^{\frac{2\pi i}{R}(x-it)}, \quad u = |w|z. \tag{80}$$

We take the subsystem A to be $-\frac{l}{2} \leq x \leq \frac{l}{2}$ The location of the cutoff surface of the Poincare AdS_3 $u = a_{\mathrm{PAdS}_3}$ and that of the global AdS_3, $z = a_{\mathrm{PAdS}_3}$ is related by the relation.

$$a_{\mathrm{PAdS}_3} = e^{-\frac{2\pi t}{R}} a_{\mathrm{gAdS}_3}. \tag{81}$$

The each endpoint of the subsystem A at the cutoff surface $u = a_{\mathrm{PAdS}_3}$ is mapped to the point P_1, P_2 of the Poincare AdS_3,

$$P_1 : (w_1, \bar{w}_1, a_{\mathrm{PAdS}_3}) = (e^{\frac{\pi i l}{R}}, e^{\frac{-\pi i l}{R}}, a_{\mathrm{gAdS}_3}) \quad P_2 : (w_2, \bar{w}_2, a_{\mathrm{PAdS}_3}) = (e^{-\frac{\pi i l}{R}}, e^{\frac{\pi i l}{R}}, a_{\mathrm{gAdS}_3}). \tag{82}$$

Hence the holographic entanglement entropy is given by

$$S_A = \frac{c}{3} \log \frac{R}{\pi a_{\mathrm{gAdS}_3}} \sin \frac{\pi l}{R} \tag{83}$$

We can immediately see that the holographic result agree with the CFT result (17).

4.5 Entanglement entropy at finite temperature and black holes

As we have seen, black holes (or black branes) in anti de Sitter spaces correspond to thermal ensembles of dual gauge theories. Here we show how entanglement entropy at finite temperatures are reproduced from the areas of the extremal surfaces in the dual AdS black hole geometries.

First of all, let us consider $\mathrm{AdS}_3/\mathrm{CFT}_2$ correspondence. The metrics of three dimensional black holes (BTZ black holes) are given by

$$ds^2 = l^2 \left[\frac{dz^2}{z^2} + \left(\frac{dx^+}{z} + \frac{z\pi^2}{2\beta^2} dx^- \right) \left(\frac{dx^-}{z} + \frac{z\pi^2}{2\beta^2} dx^+ \right) \right]. \tag{84}$$

These metrics are derived by the modular transformations of the global AdS_3 (78), $R \to i\beta$. Hence the resulting holographic entanglement entropy is

$$S_A(\beta) = \frac{c}{3} \log \left[\frac{\beta}{\pi a} \sinh \frac{\pi l}{\beta} \right] \tag{85}$$

The result agree with the CFT result (19).

When the size of the subsystem A gets large, the finite part of the entanglement entropy is reduced to the thermal entropy. Holographically, the fact can be understood since in this limit the extremal surface wraps the event horizon of the bulk black brane. The metric of the black brane is given by

$$ds^2 = -\frac{f(z)}{z^2} + \frac{1}{f(z)z^2}dz^2 + \frac{dx_1^2 + \cdots dx_{d-1}^2}{z^2}, \quad f(z) = 1 - \left(\frac{z}{z_H}\right)^d \tag{86}$$

For latter convenience we compactify the boundary spatial directions except x_1, $x_i \sim x_i + L_0, i = 2, \cdots d-1$. We take the subsystem A to be a strip,

$$A = \left\{ (t, x_1, x_2, \cdots x^{d-1}) \middle| t = 0, \ -\frac{l}{2} \le x_1 \le \frac{l}{2} \right\}. \tag{87}$$

As before we parametrize the corresponding extremal surface as $x_1 = x(z)$, and assume that the surface has a turning point at $z_m = z$. The area functional of the surface is

$$Area = \int_a^{z_m} \frac{dz}{z^{d-1}} \sqrt{\frac{1}{f(z)} + x'(z)^2}. \tag{88}$$

Substituting the conserved charge, we find the size of the subsystem and the area of the surface in terms of z_m

$$\frac{l}{2} = \int_a^{z_m} \frac{z^{d-1}dz}{\sqrt{f(z)\left(z_m^{d-1} - z^{d-1}\right)}}, \quad S = 2L_0^{d-2} \int_a^{z_m} \left(\frac{z_m}{z}\right)^{d-1} \frac{dz}{\sqrt{f(z)(z_m^{d-1} - z^{d-1})}}. \tag{89}$$

The main contribution of the former integral comes from near $z = z_m$. However the integral remains finite unless the turning point approaches to the bifurcation surface $z = z_H$ of the black brane. Hence if we take the size of the subsystem to be large, the extremal surface eventually gets close to the bifurcation surface. The observation allows us to holographic interpretation of the fact that entanglement entropy of thermal ensembles $\rho = e^{-\beta H}$ reduce to the thermal entropy (plus divergent part) in large subsystem limit. Indeed if we substitute $z_m = z_H$, the area become,

$$S = \frac{L_0^{d-2} l}{z_H^{d-1}} + S_{\text{div}}. \tag{90}$$

The divergent part of the integral comes from the contribution of the region near the boundary of the AdS.

4.6 A proof of the holographic entanglement entropy formula

In this section we would like to consider a proof of Ryu- Takayanagi formula. This section is based on [29].

A Euclidean black hole is associated with a certain thermal ensemble. It's on shell action computes the trace of the density matrix of the ensemble tr ρ_{th}. The Euclidean timelike direction τ is periodic with a periodicity β, $\tau \sim \tau + \beta$. In addition, the geometry has a $U(1)$ isometry which is the translational symmetry along the timelike direction. The event horizon is a fixed point of the $U(1)$ isometry, and the regularity of the metric at the fixed point determines the temperature $1/\beta$ of the black hole.

To prove the Ryu Takaynagi formula, one needs to find a Euclidean geometries whose on shell actions compute traces of the given reduced density matrices tr ρ_A^n. At the conformal boundary of the AdS, the geometries are $\mathcal{R}_n$, whose partition functions are tr ρ_A^n . We seek to find a bulk extension of the $\mathcal{R}_n$. $\mathcal{R}_n$ is periodic along the Euclidean timelike direction with period $2\pi n$, $\tau \sim \tau + 2\pi n$, and it contains a branch cut along the subsystem A. Therefore it only have Z_n symmetry along the Euclidean timelike direction, instead of the $U(1)$ isometry of Euclidean black holes.

To find the geometry which computes $Z_n = \text{tr}\, \rho_A^n$, we assume some properties of it.

- Assumption 1: The uclidean timelike direction is periodic with period $2\pi n$, on the other hand fields on which are 2π periodic, $\phi(\tau + 2\pi) \sim \phi(\tau)$. This means the Z_n symmetry of $\mathcal{R}_n$ is extendable into the bulk.

- Assumption 2: As analogous to Euclidean black holes, the Euclidean time cycle of the geometry shrinks at somewhere in the bulk.

Although when n is an integer, these two assumptions are compatible with each other, when n is a non-integer, they do not seem to be compatible, as the configuration looks singular at the tip of the cigar. We further assume the singularity is relatively harmless, and it does not contributes to the on shell action.

Once we specify the metric of the Euclidean geometry $g[n]$ and its on-shell action Z_n, one can determine the entanglement entropy by the combination,

$$S = -\frac{\partial}{\partial n} \left(\log Z_n - n \log Z_1 \right). \tag{91}$$

The second term in (91) can be regraded as a $2\pi n$ periodic configuration, but without any conical singularity. To compute (91), it is convenient to employ the technique used in section 10, namely,

$$S = -\frac{\partial}{\partial n} \left[(\log Z_n - \log Z_{\text{off}}) + (\log Z_{\text{off}} - n \log Z_1) \right]. \tag{92}$$

where the Z_{off} is the action of the regularized metric, which is regular at the vicinity of the tip,

$$ds^2 = n^2 dr^2 + r^2 d\tau^2 + \cdots, \quad \text{at} \quad r \sim 0. \tag{93}$$

and outside of the region it close the $g[1]$ of Z_1.

When n is close to 1, $n = 1 + \epsilon$, $\epsilon \ll 1$, the first term vanishes since the metric $g[n]$ of Z_n satisfy the equations of motion, hence small variations of the metric around $g[n]$ do not change the on shell action. The second contribution is computed by introducing a specific regularized metric, as in[122] (See also section 10 of this thesis). In the case of Einstein Hilbert action, the result is

$$\log Z_{\text{off}} - n \log Z_1 = (1-n)\frac{\text{Area}(\Sigma)}{4G_N} \tag{94}$$

Where Area(Σ) denotes the area of the surface transverse to the two dimensional cone at the tip of it . Therefore final result is

$$S = -\frac{\partial}{\partial n}\left[0 + (1-n)\frac{\text{Area}(\Sigma)}{4G_N}\right] = \frac{\text{Area}(\Sigma)}{4G_N} \tag{95}$$

In summary the holographic entanglement entropy is given by the area of the codimension two surface at the tip of the cone.

Next task is to find the location where the Euclidean timelike cycle shrinks. The location is determined by demanding the metric $g[n]$ is still on shell when $n = 1 + \epsilon$. To see this let us employ the coordinates near the tip, $(z, \bar{z})$ for the two dimensional cone, and $\{y_i\}$ for the manifold Σ transverse to the cone. The tip is located at the origin $(z, \bar{z}) = (0, 0)$. When $n = 1$, the on shell metric $g[1]$ whose action is $-\log Z[1]$, can be written near the tip as,

$$ds^2 = dzd\bar{z} + g_{ij}(dy^i + b^i_\alpha dx^\alpha)(dy^i + b^i_\alpha dx^\alpha) + O(r^2) \tag{96}$$

$$g_{ij} = h_{ij} + zK^z_{ij} + \bar{z}K^{\bar{z}}_{ij} \tag{97}$$

where $K^z_{ij}, K^{\bar{z}}_{ij}$ is the extrinsic curvature of Σ at the tip. If we slightly change n to be non integer $n = 1 \to 1 + \epsilon$, the metric is expected to become,

$$ds^2 = |z|^\epsilon dzd\bar{z} + (g_{ij} + \delta g_{ij})\left(dy^i + (b^i_\alpha + \delta b^i_\alpha)dx^\alpha)\right)\left(dy^j + (b^j_\alpha + \delta b^j_\alpha)dx^\alpha\right) + O(r^2) \tag{98}$$

The resulting variations of Ricci curvatures contain divergent terms. The dangerous components contain two derivatives in terms of z or $\bar{z}$. Actually δR_{zz} contains a term which diverges as $\frac{1}{z}$ near the tip.,

$$\delta R_{zz} = -\frac{\epsilon}{z}K_z + (regular terms). \tag{99}$$

Hence for metric $g[1 + \epsilon]$ at $n = 1 + \epsilon$ to satisfy the equations of motion, we need $K_z = 0$. By a similar argument one can also show $K_{\bar{z}} = 0$. Therefore the tip is located at the minimal surface, where the extrinsic curvatures vanish. From (95), we see that holographic entanglement entropy is given by the area of the extremal surface.

4.7 holographic entanglement entropy formula for higher curvature gravities

We have mainly considered holographic entanglement entropy when the bulk theory is Einstein gravity. One may wonder how the holographic entanglement entropy formula is modified when the bulk action includes the higher curvature terms. Since we know that Wald formula computes entropy of black holes in the presence of higher curvature terms, it is natural to anticipate that holographic entanglement entropy for general higher curvature gravity is obtained by extremizing the Wald formula. However, there are counterexamples of this naive guess, ie the extrema of t Wald formula does not reproduce the correct form of the entanglement entropy (37) [74].

In this subsection we see that when the subsystem A is a ball B^d ($\partial A = S^{d-1}$), the extrema of Wald formula does compute the entanglement entropy of the dual CFT[30]. This is because when the subsystem A is a ball B^d, the entanglement entropy is equivalent to the thermal entropy of the CFT on $S^1 \times H_{d-1}$, where H_{d-1} denotes the d-1 dimensional hyperbolic space. One can see this statement by a purely CFT argument. The thermal entropy of the CFT on a hyperbollic space is equivalent to certain black hole entropy in the bulk. This implies that the entanglement entropy is computed by Wald formula.

Suppose the CFT we consider is defined on the flat space $\mathbb{R}^d$. Let us begin with the metric of the flat space is

$$ds^2_{\mathbb{R}^d} = dt^2 + dr^2 + r^2 d\Omega^2_{d-2} = dw d\bar{w} + \left(\frac{w+\bar{w}}{2}\right)^2 d\Omega^2_{d-2}, \quad w = r + it \tag{100}$$

where Ω_{d-2} denotes the coordinates of the sphere S^{d-2}. On the other hand, The metric of the $S^1 \times H_{d-1}$ is

$$ds^2_{S^1\times H_d} = d\theta^2 + R^2\left(d\eta^2 + \sinh^2\eta \Omega^2_{d-2}\right) = R^2\left(d\sigma d\bar{\sigma} + \sinh^2\left(\frac{\sigma+\bar{\sigma}}{2}\right) d\Omega^2_{d-2}\right), \quad \sigma = \eta + i\frac{\theta}{R} \tag{101}$$

The θ direction is periodic $\theta \sim \theta + 2\pi R$.

The flat space $\mathbb{R}^d$ and the hyperbolic space $S^1 \times H_d$ are related by the following map,

$$e^{-\sigma} = \frac{R-w}{R+w}. \tag{102}$$

The ball region $r < R$ at $t = 0$ in the flat space $\mathbb{R}^d$ is mapped to the hyperbolic space via the map. One can also check that (102) is a conformal map.

To derive the trace of the reduced density matrix tr ρ_A^n, one needs to compute the path integral on the n-fold covering of the flat space with branch cut along the subsystem A. Since the subsystem A is mapped to the hyperbolic space H_{d-1}, if we take the time direction in the $S^1 \times H_{d-1}$ to be the θ direction, the path integral can be written as a thermal partition

function with temperature $\frac{1}{2\pi Rn}$, ie tr ρ_A^n = tr $e^{-2\pi RnH_\theta}$. H_θ is the Hamiltonian with respect to the θ direction. From the conformal map (102) we see that the Hamiltonian H_θ is related to the component of the stress energy tensor T_{00} in the original flat space $\mathbb{R}^d$ as,

$$H_\theta = 2\pi \int_A \frac{R^2 - r^2}{2R^2} T_{00} dr. \tag{103}$$

The equivalence of the entanglement entropy and the thermal entropy implies that the reduced density matrix ρ_A can be written as a density matrix of a canonical ensemble,

$$\rho_A = e^{-H_A}, \quad H_A = 2\pi R H_\theta. \tag{104}$$

In general, thermal entropy of a dual field theory is holographically related to entropy of a black hole in the bulk. Here we would like to specify this black hole whose entropy is equivalent to the entanglement entropy. Two specific properties of the black hole are (1) The conformal boundary of the black hole is $S^1 \times H_{d-1}$. (2) Since $S^1 \times H_{d-1}$ is conformally mapped to the flat space $\mathbb{R}^d$, the black hole is mapped to Poincare AdS_{d+1} via some coordinate transformations. Actually the black holes satisfying these properties have been known, namely, topological black holes . The metric of the topological black holes are given by

$$ds^2 = -(r^2 - R^2)dt^2 + \frac{dr^2}{(r^2 - R^2)} + r^2(du^2 + \sinh u^2 d\Omega_{d-2}^2). \tag{105}$$

For the precise map between the black holes and Poincare AdS_{d+1}, we refer the original paper [30]. The important point is that via the map the event horizons of these black holes are mapped to the surfaces in the Poincare AdS which satisfy the following equation,

$$z^2 + r^2 = R^2. \tag{106}$$

This is the conjectured extremal surfaces whose areas compute the entanglement entropy for spherical entangling region.

The entropy of the topological black holes can be computed by Wald formula

$$S = \int_{H_{d-1}} dx^{d-1} \sqrt{h} \frac{\partial \mathcal{L}}{\partial R^{ab}{}_{cd}} \epsilon^{ab} \epsilon_{cd}, \tag{107}$$

$\mathcal{L}$ denotes the Lagrangian density, and ϵ_{cd} is the binormal of the horizon, $\epsilon_{cd} = \xi_c \eta_d - \xi_d \eta_c$, where ξ_c is the killing vector which is vanishing on the horizon, and η_d is the normal vector of the horizon, with the normalization $\xi_c \eta^c = 1$. By evaluating the integrand in the pure AdS, we get the following form for the black hole entropy,

$$S = \frac{2\Gamma(d/2) a_d}{\pi^{d/2-1}} \int dx^{d-1} \sqrt{h}. \tag{108}$$

a_d in the expression is equal to the A type central charge of the CFT [30]. Since the event horizons of the topological black holes are hyperbolic spaces, these entropies are diverging,

and we need to regulate them to derive finite answers. The structure of the divergence is same as that of holographic entanglement entropy in Einstein gravity, since the integral (108) computes the area of the minimal surface (106), in Poincare coordinate. Especially, the result reproduces the expected divergence of entanglement entropy (35) (38).

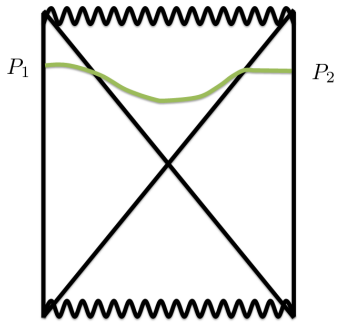

Figure 5: An extremal surface in theAdS eternal black brane

5 Eternal black holes and Global quenches

5.1 A holographic realization of global quenches

In this section, we would like to discuss a way to holographically realize global quenches. Since the entanglement entropy is thermalized in these processes, it is natural to guess that the global quenches are holographically related to gravitational collapses, the whose final states are black branes.

In the works [36, 37, 38, 39, 40, 41, 42] the linear growth and subsequent thermalization of entanglement entropy in these global quenches was reproduced by applying the holographic formula [21, 22] to Vidya spacetime where the Poincare AdS suddenly change into the black brane via null ray propagations from the boundary of the AdS.

Remarkably, in the recent paper [32], it is shown that the linear growth of the entanglement entropy in these quenches is actually intrinsic to black branes which are final states of the gravitational collapses, and related to the growth of the interior region of these black branes in a particular time slice. In other words, their work makes it clear the connection between the linear growth of the entanglement entropy in global quenches and evolution of the interior of black branes.

In the subsection, we would like to review their argument. To illustrate their discussion, let us first compute the length of the extremal surface connecting $P_1 : (t, x_i, z) = (\frac{i\beta}{2} + t_b, 0, a)$ in the left boundary of the eternal black brane and $P_2 : (t, x_i, z) = (t_b, 0, a)$ in the right boundary. See figure 5 . As we have discussed in the section 4.1.4, the eternal black brane is the gravity dual of the thermofield double state (66). The length of the extremal surface computes roughly the entanglement between the left Hilbert space $\mathcal{H}_L$ and the right Hilbert space $\mathcal{H}_R$. We will elaborate the relation between the calculation here and evolutions of entanglement entropy under global quenches in the single Hilbert space $\mathcal{H}_L$.

We employ the following coordinate of the AdS black brane.

$$ds^2 = -g(\rho)^2 dt^2 + d\rho^2 + h(\rho)^2 dx_{d-1}^2. \tag{109}$$

The event horizon is located at $\rho = 0,\ g(0) = 0$. To analytically continue the metric, it is convenient to employ the Kruskal coordinates (U, V) which are defined by

$$U = \rho e^{\frac{2\pi}{\beta}t} \quad V = \rho e^{-\frac{2\pi}{\beta}t}. \tag{110}$$

The outside of the event horizon is correspond to the region $U, V > 0$. The inside of the event horizon is the region $U > 0, V < 0$. A coordinate of the inside of the event horizon is given by $(\kappa, t_I),\ \kappa = i\rho,\ t_I = t + \frac{i\beta}{4}$. There is also a secondary asymptotic region $U, V < 0$. A coordinate of the region is given by $(\rho, t + \frac{i\beta}{2})$.

If we parametrize a surface in the black brane by $t = t(\rho)$ the area functional is given by

$$S = L_0^{d-2} \int d\rho h(\rho)^{d-2} \sqrt{-g(\rho)^2 t'(\rho)^2 + 1}. \tag{111}$$

We assume the extremal surface is symmetric under the flip, $t_I \to -t_I$. Hence its derivative $t'(\rho)$ diverges at somewhere inside of the horizon. Let us denote the location to be $\rho = i\kappa_0$.

The functional (111) does not depend on $t(\rho)$ itself. By solving the conserved equation associated with the symmetry, one finds the boundary time t_b

$$t_b = -\frac{i\beta}{4} + \int_{i\kappa_0}^{a} \frac{d\rho}{g\sqrt{1 - \frac{g^2 h^{2d-4}}{g_0^2 h_0^{2d-4}}}}. \tag{112}$$

where $g_0 = g(\kappa_0), h_0 = h(\kappa_0)$.

One can choose κ_0 to be an appropriate value κ_m so that the derivative of the denominator of the integrand vanishes at $\kappa = \kappa_0 (= \kappa_m)$. When the boundary time t_b becomes large, the κ_0 gets close to the κ_m. In that case the extremal surface gets close to the surface $\kappa = \kappa_m$. At sufficiently large t_I the extremal surface starts to deviate from it. In the large t_b limit one can approximate the integral (111)as,

$$S_A = \frac{L_0^{d-2}}{2G_N} \int dt\ h(\rho)^{d-2} \sqrt{-g(\rho)^2 + \rho'^2} = \sim \frac{L_0^{d-2}}{2G_N} \sqrt{-g(\kappa_m)^2} h(\kappa_m)^{d-2} t_b \tag{113}$$

We see that at sufficiently late time $t_b >> 1$, the length of the extremal surface is proportional to the boundary time t_b. This is quite similar to the linear growth of entanglement entropy in the global quenches. Since the dominant contribution to the integral (113) comes from the inside of the horizon, the linear growth of the length captures information about the inside of the horizon, namely the linear growth of certain time slice.

Figure 6: Left: Hartle Hawking geometry. Right:Hartle Hawking geometry is identified by $t_I \sim -t_I$

5.1.1 Relation to global quenches

Here we argue the eternal black brane provides a simple gravity realization of global quenches. To realize a global quench, one need to prepare an initial state which evolves non-trivially at $t > 0$. In the gravity side, one can prepare such a candidate of the initial state via the Hartle Hawking prescription. Let us consider a Euclidean black brane. The temporal direction of it is a circle with period β. The topology of the Euclidean black brane is two dimensional disk D^2 times $\mathbb{R}^{d-1}$. This $\mathbb{R}^{d-1}$ is the spatial directions of the boundary. We then divide the disc D^2 into half. let us call the half disc as $D^2_{\frac{\beta}{2}}$. See figure 6. A path integral over the half disc $D^2_{\frac{\beta}{2}}$ provides a state on the cross section of the half disc. However note that as we have reviewed in Section 4.1.4, the resulting state in the field theory side is the thermo field double state (66), this is not what we prepare in the global quenches.

We then let the prepared Hartle Hawking state evolve to a black brane. Again, the evolution have simple realization. This is achieved by gluing the cross section of the half disc $D^2_{\frac{\beta}{2}}$ and $t = 0$ spatial surface of the Lorentzian eternal black brane together. let us call the geometry as a Hartle Hawking geometry.

The Hartle Hawking geometry provides a simple toy model of gravitational collapse or thermalization, in that the initial Hartle Hawking state evolve to the final eternal black brane. However the this geometry is has two unsatisfactory point as a candidate of a gravity dual of a CFT global quench. One problem is that the Hartle Hawking geometry contains two conformal boundaries, whereas the global quenches happen in usual single Hilbert space CFT. Second problem is that as we have pointed out, the initial Hartle Hawking state in gravity side is dual to the thermo field double state, which is not the initial state of global quench.

A simple way to resolve the problems is to divide the geometry into two parts by introducing a spacetime boundary at $t_I = 0$ and its trivial extension to the Euclidean regime, and left only one part of them. See figure 6. The prescription make the geometry to contain only one conformal boundary [5]. Furthermore, in the geometry one can put a

[5]To discriminate the AdS boundary between the spacetime boundary we introduced, below we call the

CFT boundary state $|B\rangle$ at the bottom of the Euclidean regime. At the initial timeslice $t = 0$, the state becomes

$$|\psi\rangle = e^{-\frac{\beta}{4}H}|B\rangle \tag{114}$$

which is same as the initial states of the global quenches.

In summary we find a simple holographic dual of global quench, by taking a half of the Hartle Hawking geometry. The linear growth of the entanglement entropy comes from the extremal surface attaching on the spacetime boundary.

5.2 BTZ black holes and two dimensional global quenches

So far, we have discussed a holographic realization of the global quenches in terms of eternal black branes. In the analysis above, the thermalizations of entanglement entropy were invisible because we took the subsystem A to be infinitely large.

In this section, We would like to discuss the evolution of holographic entanglement entropy under global quenches when the subsystem A is finite. To obtain an analytic answer, we consider BTZ black strings which are related to Poincare AdS_3 via coordinate transformations. Although we consider the eternal BTZ strings, we can relate it to the single boundary black strings, by taking the half of the configuration just as we explained.

5.2.1 Coordinate transformation between Poincare AdS_3 and BTZ black string

First we see the detail of the coordinate transformation between a Poincare AdS_3 and a BTZ black string[6] . A three dimensional anti de Sitter space is defined as a surface in $\mathbb{R}^{2,2}$,

$$-Y_{-1}^2 - Y_0^2 + Y_1^2 + Y_2^2 = -1, \tag{115}$$

with the metric,

$$ds^2 = -dY_{-1}^2 - dY_0^2 + dY_1^2 + dY_2^2. \tag{116}$$

A Poincare coordinate is defined by the following parametrization,

$$\begin{aligned} Y_{-1} &= \frac{1}{2z}\left[1 + (z^2 + w^+w^-)\right], \quad Y_2 = \frac{1}{2z}\left[1 - (z^2 + w^+w^-)\right], \\ Y_0 &= \frac{w^+ - w^-}{2z}, \quad Y_1 = \frac{w^+ + w^-}{2z}. \end{aligned} \tag{117}$$

the Poincare metric is

$$ds^2 = \frac{1}{z^2}\left(dw^+dw^- + dz^2\right). \tag{118}$$

AdS boundary as conformal boundary.

[6]In the section we set $l = 1$

The exterior coordinate of a BTZ black string is defined as

$$Y_{-1} = \cosh\frac{2\pi x}{\beta}\cosh\rho, \quad Y_2 = -\sinh\frac{2\pi x}{\beta}\cosh\rho,$$
$$Y_0 = \sinh\frac{2\pi t}{\beta}\sinh\rho, \quad Y_1 = \cosh\frac{2\pi t}{\beta}\sinh\rho. \tag{119}$$

The metric of the outside of the event horizon is

$$ds^2 = -\left(\frac{2\pi}{\beta}\right)^2\sinh^2\rho\, dt^2 + d\rho^2 + \left(\frac{2\pi}{\beta}\right)^2\cosh^2\rho\, dx^2. \tag{120}$$

The exterior region corresponds to $-Y_0^2 + Y_1^2 \geq 0$,$-Y_{-1}^2 + Y_2^2 \leq -1$ of the equation (115) . The metric of Region III is derived by the replacement $t \to t + \frac{i\beta}{2}$

The inside of the event horizon is mapped as

$$Y_{-1} = \cosh\frac{2\pi x}{\beta}\cos\kappa, \quad Y_2 = \sinh\frac{2\pi x}{\beta}\cos\kappa$$
$$Y_0 = \cosh\frac{2\pi t_I}{\beta}\sin\kappa, \quad Y_1 = \cosh\frac{2\pi t_I}{\beta}\sin\kappa. \tag{121}$$

. The metric of the inside of the horizon is hence given by

$$ds^2 = -d\kappa^2 + \left(\frac{2\pi}{\beta}\right)^2\sin^2\kappa\, dt_I^2 + \left(\frac{2\pi}{\beta}\right)^2\cos^2\kappa\, dx^2. \tag{122}$$

The direct map between the Poincare AdS_3 and the BTZ black string is given by solving the relation between (117) and (119) for outside of the event horizon or (121) for inside of the event horizon. The boundary of the Poincare AdS_3 and that of the BTZ black string is related by

$$w^+ = e^{\frac{2\pi}{\beta}(x+t)}, \quad w^- = e^{\frac{2\pi}{\beta}(x-t)}, \quad \frac{1}{z} = \frac{e^\rho}{2}e^{-\frac{2\pi}{\beta}x}, \quad z \sim 0. \tag{123}$$

5.2.2 Length of extremal surfaces in the BTZ string

In the subsection, we would like to compute length of extremal surfaces in the BTZ black string by making use of the coordinate transformation introduced in the previous subsection. The boundary of the subsystem A in the BTZ is given by $P_1 : (t_b + \frac{i\beta}{2}, L)$, $P_2 : (t_b + \frac{i\beta}{2}, 0)$ at the right boundary, and $P_3 : (t_b, L)$, and $P_4 : (t_b, 0)$ at the left boundary. These points are mapped to points in the Poincare AdS_3 by using the near boundary coordinate transformation(boundary conformal map) (123) .

$$P_1 : (w^+, w^-) = (e^{\frac{2\pi}{\beta}(L+t_b)}, e^{\frac{2\pi}{\beta}(L-t_b)}), P_2 : (w^+, w^-) = (e^{\frac{2\pi}{\beta}t_b}, e^{-\frac{2\pi}{\beta}t_b})$$
$$P_3 : (w^+, w^-) = (e^{\frac{2\pi}{\beta}(L+t_b)}, e^{\frac{2\pi}{\beta}(L-t_b)}), \quad P_4 : (w^+, w^-) = (e^{\frac{2\pi}{\beta}t_b}, e^{-\frac{2\pi}{\beta}t_b})$$

There are two extremal surfaces in the Poincare AdS_3. One extremal surface, which we call as disconnected surface is consists of two pieces, one of which connects P_1 and P_3, and the other connects P_2 and P_4. Another extremal surface is the usual extremal surface which connects P_1 and P_2, P_3 and P_4 respectively.

The contribution of the disconnected surface to the holographic entanglement entropy is given by

$$L_{dc} = \frac{c}{6} \log \left(\frac{\beta}{\pi a} \cosh \frac{2\pi t}{\beta} \right) \tag{124}$$

the contribution of the connected surface is

$$L_c = \frac{c}{6} \log \left(\frac{\beta}{\pi a} \sinh \frac{2\pi l}{\beta} \right) \tag{125}$$

The actual value of entanglement entropy is given by the minimal value among then. Hence in the high temperature limit

$$S_A = \begin{cases} \frac{2\pi c t}{3\beta} & (t < \frac{L}{2}) \\ \frac{\pi c l}{3\beta} & (t \geq \frac{L}{2}) \end{cases} \tag{126}$$

In summary we find the thermalization of entanglement entropy.

6 A general construction of holographic quantum quenches

In this section, we would like to discuss a way to systematically construct a gravity dual of general quantum quenches in 2d CFTs. In the 2d CFT side, according to the dictionary we saw in the previous section, a quantum quench is specified by an associated Riemann surface Σ with boundaries. Correlation functions on Σ and the entanglement entropy can be computed by BCFT techniques. The Riemann surface is mapped to the half plane by an appropriate conformal map $f(z)$. By analytically continuing the setup one obtains time evolution.

Below we explain gravity descriptions of these CFT setup. This is achieved by introducing a spacetime boundary to the bulk. We also discuss extremal surfaces in the dual gravity systems. We emphasize that in the system there is an additional extremal surface which ends on the spacetime boundary we introduced (disconnected surface).

6.1 A gravity description of CFT on half plane

It is known that a CFT on a half plane has a dual gravity description [54, 55, 56, 57, 58]. Its concrete system is a Poincare AdS_3 with a codimension one brane which is located at an appropriate AdS_2 submanifold whose boundary coincide with that of half plane. See figure 7. The configuration keeps $SL(2,R)$ symmetry of the original $SL(2,R) \times SL(2,R)$ of the poincare AdS_3. Note that the same symmetry breaking appears in CFTs on the half plane. The prescription passes some nontrivial checks, for example it reproduces correct form of one point function of a operator in the presence of the boundary in CFT side [55, 57].

To begin with , it is convenient to use the AdS_2 foliation of AdS_3

$$ds^2 = d\rho^2 + \cosh^2\rho \left(\frac{-dT^2 + dy^2}{y^2} \right). \tag{127}$$

Via a coordinate transformation

$$Z = \frac{y}{\cosh\rho} \qquad X = y \tanh\rho, \tag{128}$$

we obtain a Poincare metric,

$$ds^2 = \frac{-dT^2 + dX^2 + dZ^2}{Z^2}. \tag{129}$$

Since the brane we introduced is a codimension one object, its back reaction can be treated via following junction condition[56, 57]

$$K_{\mu\nu} - K h_{\mu\nu} = \mathcal{T} h_{\mu\nu}, \tag{130}$$

with a boundary condition that demand the brane end at the boundary of the half plane on the conformal boundary of the AdS_3. The equation determines the location of the brane.

In the equation, $h_{\mu\nu}$ denotes the induced metric on the spacetime boundary, $K_{\mu\nu}$ is its extrinsic curvature, and $K = K^{\mu}_{\mu}$. $\mathcal{T}$ is the tension of the brane. In the back reacted description, this brane can be regarded as a spacetime boundary. The bulk region enclosed by the spacetime boundary and conformal AdS_3 boundary is proposed to be the holographic duals of BCFTs.

The solution of (130) which satisfies the boundary condition is given by $\rho = \rho_*$(constant) plane with

$$\mathcal{T} = \tanh \rho_*. \tag{131}$$

By changing $\mathcal{T}$, one can change boundary state of dual BCFT. In the corresponding entanglement entropy, this only changes a constant term that does not depend on subsystem we take.[7] Therefore below we set $\mathcal{T} = 0$, then the spacetime boundary in the Poincare AdS_3 is located at $X = 0$.

6.2 The bulk extension of Lorentzian conformal maps

The bulk extension of a boundary Lorentzian conformal map $f_{\pm}(x^{\pm})$ has also been known [46]. The explicit map is

$$W_{\pm} = f_{\pm}(x^{\pm}) + \frac{2z^2 f_{\pm}'^2 f_{\mp}''}{8f_{\pm}' f_{\mp}' - z^2 f_{\pm}'' f_{\mp}''} \qquad Z = z\frac{(4f_{+}' f_{-}')^{\frac{3}{2}}}{8f_{+}' f_{-}' - z^2 f_{+}'' f_{-}''}, \tag{132}$$

where $W^{\pm} = X \pm T$. The map transforms the Poincare metric (129) to the metric,

$$ds^2 = L_{+}dx_{+}^2 + L_{-}dx_{-}^2 + \left(\frac{2}{z^2} + \frac{z^2}{2}L_{+}L_{-}\right)dx_{+}dx_{-} + \frac{dz^2}{z^2}. \tag{133}$$

where the $L_{\pm}$ are Schwarzian derivatives of the boundary conformal map

$$L_{\pm} = \frac{3f_{\pm}''^2 - 2f_{\pm}' f_{\pm}'''}{4f_{\pm}'^2}. \tag{134}$$

The holographic stress tensor [47] of the metric is given by

$$T_{\pm\pm} = \frac{1}{8\pi G_N}L_{\pm} \qquad T_{\pm\mp} = 0, \tag{135}$$

which are expected from the boundary point of view.

Combining these two ingredients, a gravity dual of a quantum quench is given by pulling back the Lorenzian AdS_3 with a spacetime boundary at $X = 0$ by the bulk extension of the Lorentzian conformal map associated with the quench.

[7] This quantity is called as boundary entropy [61]. See [60] for a holographic calculation.

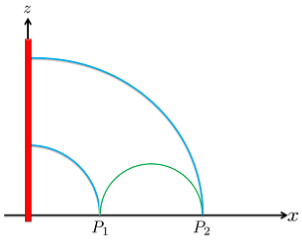

Figure 7: Sketch of the spacetime boundary in the Poincare AdS_3 (thick red line) at $X = 0$ and extremal surfaces in the system.

6.3 Extremal surfaces in holographic systems

The time evolution of entanglement entropy for a subsystem A under a quench is holographically derived by finding extremal surfaces in the dual gravity configuration which are anchored to the boundaries of of the subsystem A. In the Poincare AdS_3 with the spacetime boundary at $X = 0$, one finds two extremal surfaces which satisfy the boundary condition. Suppose the boundary of the subsystem A is given by $P_1(X_1, T_1)$ and $P_2(X_2, T_2)$.

One extremal surface is connecting between P_1 and P_2, the length of which is given by

$$L_c = \log \frac{\sqrt{(X_1 - X_2)^2 - (T_1 - T_2)^2}}{a_{AdS_3}}, \tag{136}$$

where a_{AdS_3} denote the UV cut off. Below we call it as a connected surface. The other surface consist of two pieces of disconnected surfaces, one of which is connecting between P_1 and the spacetime boundary at $X = 0$ the other of which is connecting between P_2 and the boundary. The total length of the geodesics is

$$L_{dc} = \frac{1}{2} \log \frac{X_1}{a_{AdS_3}} + \frac{1}{2} \log \frac{X_2}{a_{AdS_3}}, \tag{137}$$

below we call it as a disconnected surface. See figure 7. Extremal surfaces in a gravity dual of a quantum quench are obtained by pulling back extremal surfaces in the Poincare AdS_3 via (132) . Holographic entanglement entropy is given in terms of actual minimum of area [21, 22, 24],

$$S_{HEE} = \frac{1}{4G_N} \min\{L_c, L_{dc}\}, \tag{138}$$

where G_N is the Newton constant in three dimensions. As we will see below, there are phase transitions between these two surfaces in general.

6.4 Entanglement entropy for infinite interval

When the subsystem A is an infinite interval $[-\infty, l]$, time evolutions of entanglement entropy in the CFT side precisely agree with the holographic entanglement entropy computed from the disconnected surface for arbitrary quantum quench. Entanglement entropy of the CFT side is

$$S_{\rm CFT} = \frac{c}{6}\log\frac{W^+(l+t)+W^-(l-t)}{a_Q^2\sqrt{\frac{dW^+}{dx^+}(l+t)\frac{dW^-}{dx^-}(l-t)}}. \tag{139}$$

Holographic entanglement entropy computed form the disconnected surface is

$$S_{\rm HEE} = \frac{c}{6}\log\frac{W^+(l+t)+W^-(l-t)}{a_{AdS_3}}, \quad c = \frac{3}{2G_N}. \tag{140}$$

Since a_{AdS_3} and the location of the UV cut off of the gravity dual of the quantum quench a_Q is related via

$$a_{AdS_3}^2 = a_Q^2\sqrt{\frac{dW^+}{dx^+}(l+t)\frac{dW^-}{dx^-}(l-t)}, \tag{141}$$

therefore they precisely agree. Note that the introduction of the spacetime boundary and the disconnected surface attaching on it is essential to get the correct behavior of entanglement entropy holographically. Below we consider holographic entanglement entropy for finite intervals.

7 Application of the construction to various quenches

7.1 Global quenches

As a check, we apply the construction to global quenches.The analytic continuation of the associated conformal map are

$$W^+ = e^{\frac{2\pi}{\beta}(x+t)} \qquad W^- = e^{\frac{2\pi}{\beta}(x-t)} \tag{142}$$

where β denotes twice of the width of the strip. One find the gravity dual of the quench via the prescription mentioned in the previous section. The resulting geometry is nothing but a ordinary BTZ black string with inverse temperature β.

Next we summarize the time evolution of holographic entanglement entropy. The contribution of the disconnected surface to holographic entanglement entropy is

$$S_{dc} = \frac{c}{3} \log \frac{\beta}{\pi a_Q} \cosh \frac{2\pi}{\beta} t. \tag{143}$$

The contribution of the connected surface is

$$Sc = \frac{c}{3} \log \frac{\beta}{\pi a_Q} \sinh \frac{\pi}{\beta} l, \tag{144}$$

hence there is a phase transition when $t = \frac{L}{2}$ in the high temperature limit $\beta \to 0$.

For global quenches our setup precisely agree with the prescription introduced in section 5.

7.2 Infinitesimally inhomogeneous quenches

Here we would like to discuss a holographic realization of infinitesimally inhomogeneous quenches [53] which we reviewed in section 2. The metric of the gravity dual is derived by substituting the $\langle T_{\pm\pm} \rangle$ of the inhomogeneous quench (53) into the general metric (133). The spacetime can be regarded as BTZ black string with a small perturbation added. The boundary of the spacetime $x^\pm$ and that of a Poincare AdS_3 $W^\pm$ is related by the conformal map

$$W^+ = e^{\frac{2\pi}{\beta}(x^+ - f(x^+))} \qquad W^- = e^{\frac{2\pi}{\beta}(x^- - f(x^-))}. \tag{145}$$

From the map one can compute the length of both extremal surfaces in the spacetime. The contribution of the connected surface (136) to holographic entanglement entropy is

$$\begin{aligned} S_c(l_1,l_2,t) = &\frac{c}{3}\log\left[\frac{\beta}{2\pi a_Q}\sinh\frac{\pi(l_2-l_1)}{\beta}\right] \\ &-\frac{c\pi}{6\beta}\left[(f(l_2+t)-f(l_1+t))+(f(l_2-t)-f(l_1-t))\right] \\ &+\frac{c}{12}\left[f'(l_1+t)+f'(l_2+t)+f'(l_1-t)+f'(l_2-t)\right] \end{aligned} \tag{146}$$

To derive the expression, we assume that inhomogeneity is small $h(x) << \beta$. The contribution of the disconnected surface is

$$\begin{aligned} S_{dc}(l_1,l_2,t) = &\frac{c}{3}\log\left[\frac{\beta}{2\pi a_Q}\cosh\frac{2\pi t}{\beta}\right] \\ &-\frac{c\pi}{6\beta}\left[(f(l_1+t)-f(l_1-t))+(f(l_2+t)-f(l_2-t))\right] \\ &+\frac{c}{12}\left[f'(l_1+t)+f'(l_2+t)+f'(l_1-t)+f'(l_2-t)\right] \end{aligned} \tag{147}$$

Since we are assuming the fluctuation is infinitesimal $h(x) << \beta$, the critical time when the phase transition of both surface happen does not change. By using (50), we find an agreement between the CFT result (51) and the holograhic result.

One can rewrite the expression of entanglement entropy (51) into a suggestive form by making use of (53). When inhomogeneity is small, one can neglect $f'''(x\pm t)$ terms in (53). Then the variation of energy density is

$$\delta\langle T_{tt}(x,t)\rangle = \frac{c\pi}{6\beta^3}\left[h(x+t)+h(x-t)\right]. \tag{148}$$

Since the last terms in (146), (147) can be neglected in high temperature limit $\beta\to 0$, The variation of entanglement entropy can be recast into the form,

$$\begin{aligned} \delta S(l_1,l_2,t) = &\theta\left(\frac{l_2-l_1}{2}-t\right)\beta\int_0^t\left(\delta\langle T_{tt}(l_1,s)\rangle+\delta\langle T_{tt}(l_2,s)\rangle\right)ds \\ &+\theta\left(t-\frac{l_2-l_1}{2}\right)\beta\int_{l_1}^{l_2}\delta\langle T_{tt}(s,t)\rangle ds. \end{aligned} \tag{149}$$

The second term of the expression comes from the first law of thermodynamics, since at late time entanglement entropy is reduced to thermal entropy in high temperature limit. The first term is specific to the quench. Holographically, this term comes from the fluctuation of the inside of the horizon.

7.3 A finite inhomogeneous quench

In the previous subsection, we consider quenches where the inhomogeneity of energy density is infinitesimal. In this section we consider a quench whose inhomogeneity is finite. We find for example following conformal map is interesting.

$$W^{\pm} = \left(\frac{-1 + \sqrt{1 + 4e^{\frac{2x^{\pm}}{\lambda}}}}{2} \right)^{\frac{\pi\lambda}{\beta}} . \tag{150}$$

In the region $\frac{x^{\pm}}{\lambda} \gg 1$, one can approximate the map as $W^{\pm} \sim e^{\frac{\pi x^{\pm}}{\beta}}$, thus the corresponding bulk geometry is a black string metric with temperature $T = \frac{1}{2\beta}$. On the other hand, the region $\frac{x^{\pm}}{\lambda} \ll -1$ corresponds to a black string geometry with $T = \frac{1}{\beta}$.

In figure 8 we plot the time evolution of the energy density $\langle T_{tt}(t,x) \rangle$ under the quench. In the figure one can see the third plateau in $|x| < |t|$. Below we will confirm that the region is described by a black string with $T = \frac{3}{4\beta}$ which is the average of temperature of two black strings on both sides. Thus in the bulk a black string with temperature $T_1 = \frac{1}{\beta}$ (below we call it black string 1) and a black string with temperature $T_3 = \frac{1}{2\beta}$(black string 3) are colliding at $x = 0$ and $t = 0$, and a new black string with temperature $T_2 = \frac{3}{4\beta}$ is emerging (black string 2). The emergent black string expands in the speed of light form the origin. The final state of the process is a thermal equilibrium in terms of the emergent black string 2. The parameter λ is interpreted as the size of the intermediate regions between each of two black strings.

One can compute the contribution of both connected and disconnected surface $S_c(l_1, l_2, t)$, $S_{dc}(l_1, l_2, t)$ to the holographic entanglement entropy by using general formulas (331), (332) in the Appendix and the conformal map (150). Since exact expressions are complicated and do not illuminating, we do not depict them. The late time limit of the $S_c(l_1, l_2, t)$ is,

$$\begin{aligned} S_c(l_1, l_2, t) &\to \frac{c}{6} \log \left[(\frac{\beta}{2\pi a})^2 \sinh \frac{\pi}{\beta}(l_2 - l_1) \sinh \frac{\pi}{2\beta}(l_2 - l_1) \right] \quad t \to \infty \\ &\sim \frac{c\pi}{4\beta}(l_2 - l_1), \end{aligned} \tag{151}$$

which is equal to thermal entropy with temperature $T = \frac{3}{4\beta}$. On the other hand, the final state of the process is the emergent black string (black string 2). Thus as we have advertised, the temperature of the emergent black string is determined to be $T_2 = \frac{3}{4\beta}$.

In figure (10) we plot $S_c(l_1, l_2, t)$ and $S_{dc}(l_1, l_2, t)$ with $l_1 < 0 < l_2$. Let us first discuss the time dependence of $S_c(l_1, l_2, t)$ of the connected surface. When $t < \min\{|l_1|, l_2\}$, $S_c(l_1, l_2, t)$ remains constant. Then in $\min\{|l_1|, l_2\} \leq t < \max\{|l_1|, l_2\}$ it increases linearly in time. When $t \geq \max\{|l_1|, l_2\}$, it again becomes constant. This behavior can be interpreted in terms of the following bulk picture. In the high temperature limit $\frac{\lambda}{\beta} \ll 1$, each intermediate

regions which connects between black strings with different temperature can be ignored. In the limit, if we take a time slice $t = t_0$, each black string is extending between $-\infty < x < t_0$ (string 1), $-t_0 < x < t_0$ (string 2), $t_0 < x < \infty$ respectively. Apart from junction points black strings are in local equilibrium with their own temperature.

When $t < \min\{|l_1|, l_2\}$, two end points of the emergent black string (string 2) are located inside of the interval $[l_1, l_2]$, see figure 4. $S_c(l_1, l_2, t)$ of a BTZ black string with inverse temperature β is given by

$$S_c(l_1, l_2, t)_{BTZ} = \frac{c\pi}{3\beta}(l_2 - l_1), \tag{152}$$

in the high temperature limit $\beta \ll (l_2 - l_1)$. Hence $S_c(l_1, l_2, t)$ in $t < \min\{|l_1|, l_2\}$ is thus obtained by summing contributions form three black strings.

$$\begin{aligned} S_c(l_1, l_2, t) &= \frac{c\pi}{3}\left[\frac{|l_1| - t}{\beta} + \frac{3}{4\beta}2t + \frac{l_2 - t}{2\beta}\right] \\ &= \frac{c\pi}{3}\left(\frac{|l_1| + l_2}{2\beta}\right). \end{aligned} \tag{153}$$

This explains the time independence of $S_c(l_1, l_2, t)$ in $t < \min\{|l_1|, l_2\}$. From the plot one can also confirm that the value of the constant is actually given by (153).

When $\min\{|l_1|, l_2\} \leq t < \max\{|l_1|, l_2\}$, one of the end point of the emergent black string is located at outside of the interval $[l_1, l_2]$ due to the expansion. Therefore $S_c(l_1, l_2, t)$ is

$$S_c(l_1, l_2, t) = \frac{c\pi}{3}\left[\frac{t}{4\beta} + \frac{1}{4\beta}(2l_2 + 3|l_1|)\right]. \tag{154}$$

Therefore it grows linearly in time with coefficient $\frac{c\pi}{12\beta}$. We check can this in figure 10.

When $t \geq \max\{|l_1|, l_2\}$, both of the end points of string 2 are located out side of the interval $[l_1, l_2]$, thus $S_c(l_1, l_2, t)$ is thermalized by the black string.

$$S_c(l_1, l_2, t) = \frac{c\pi}{4\beta}(l_2 - l_1). \tag{155}$$

Next we consider the behavior of $S_{dc}(l_1, l_2, t)$ of the disconnected surface. Although it increases linearly in time, its coefficient $\frac{\partial S_{dc}}{\partial t}$ jumps at $t = \min\{|l_1|, l_2\}$ and $t = \max\{|l_1|, l_2\}$, see Figure 10. The behavior can be understood again in terms of the expansion of the emergent black string .

We know that in a BTZ black string the disconnected surface is consist of two part, and each part is located at $x = l_1$or $x = l_2$. Each of them contribute to holographic entanglement entropy as

$$S_{dc}(l_1, l_2, t)_{BTZ} = \frac{\pi c}{3\beta}t. \tag{156}$$

When $t < \min\{|l_2|, l_1\}$, one part of the disconnected surfaces probes the string 1 and the other probe the string 3 respectively. Thus the total contribution is

$$S_{dc}(l_1, l_2, t) = \frac{\pi c}{2\beta} t. \tag{157}$$

When $\min\{|l_1|, l_2\} \leq t < \max\{|l_1|, l_2\}$, we have two cases. When $|l_1| < l_2$, since one part of the surface probes the string 2 and another probes the string 3, the total contribution is

$$S_{dc}(l_1, l_2, t) = \frac{\pi c}{12\beta} \left(5t + |l_1|\right). \tag{158}$$

In the expression, we add a constant term for continuity of S_{dc} at $t = \min\{|l_2|, l_1\}$. When $|l_1| \geq l_2$ they probe the string 2 and the string 1, thus

$$S_{dc}(l_1, l_2, t) = \frac{\pi c}{12\beta} \left(7t - l_2\right). \tag{159}$$

comparing them with (157) we conclude there is a jump in $\frac{\partial S_c}{\partial t}$ at $t = \min\{|l_1|, l_2\}$.

After $t = \max\{|l_1|, l_2\}$ both part probe the black string 2, then

$$S_{dc}(l_1, l_2, t) = \begin{cases} \frac{\pi c}{12\beta} \left(6t + 5l_2 + |l_1|\right) & (|l_1| < l_2) \\ \frac{\pi c}{12\beta} \left(6t + 7|l_1| - l_2\right) & (l_2 < |l_1|) \end{cases} \tag{160}$$

again we find a jump at $t = \max\{|l_1|, l_2\}$.

Next we consider the phase transition between two surfaces. When $|l_1| < l_2$, from Figure 11 we see this happens when (154) and (158) become equal. Thus we find the critical time is

$$t_c = \frac{l_2 - l_1}{2}, \tag{161}$$

which is the half of the size of the subsystem. We can check that this is also true when $l_2 < |l_1|$. The expression agrees with that of derived from BTZ black string dual to the global quench. In the CFT quasiparticle picture, the result is anticipated. We also compare the gravity result for the quench and CFT result in figure 6, finding a nice agreement.

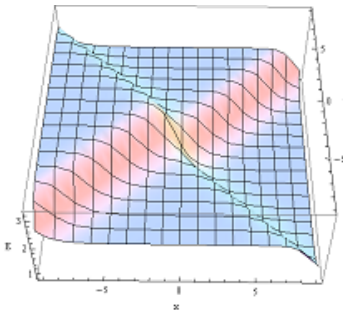

Figure 8: The time volution of energy density $\langle T_{tt}(t,x)\rangle$ in the finite inhomogeneous quench.

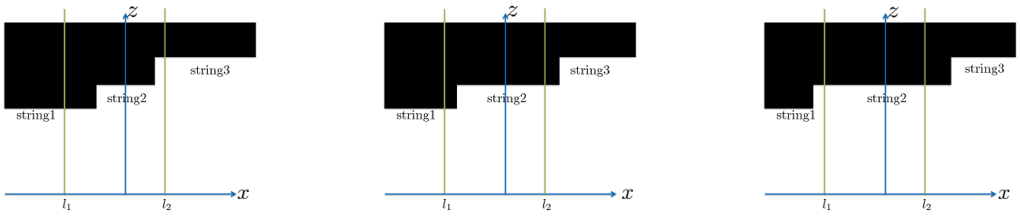

Figure 9: Sketch of the fusion of two black strings (string1 and string3) into string 2. Left: When $t < \min\{|l_1|, l_2\}$, the string 2 is contained in the bulk extension of the subsystem $[l_1, l_2]$. Middle:When $\min\{|l_1|, l_2\} \leq t < \max\{|l_1|, l_2\}$, one end point of the string 2 is located outside of the subsystem and the other is in the bulk extension of the subsystem. Right: When $t \geq \max\{|l_1|, l_2\}$ both end points are located out side the bulk extension of the subsystem.

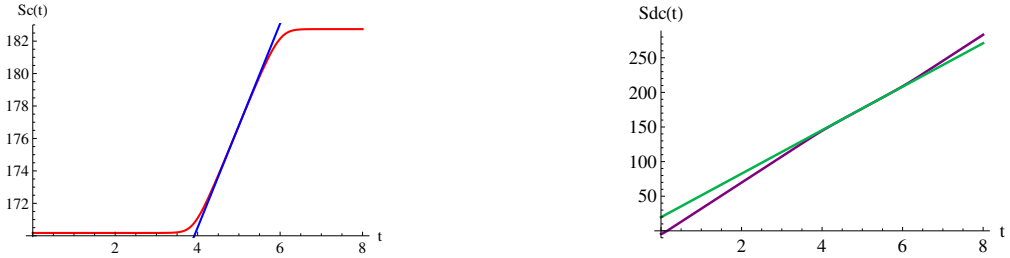

Figure 10: Left: Plot of the length of the connected surface as a function of time in the finite inhomogeneous quench (red). We also plot (154) (blue). Right:Plot of the length of the connected surface as a function of time in the finite inhomogeneous quench(green). We also plot (158) (purple) We take $l_1 = -4, l_2 = 6, \lambda = \frac{1}{4}, \beta = \frac{1}{4}$.

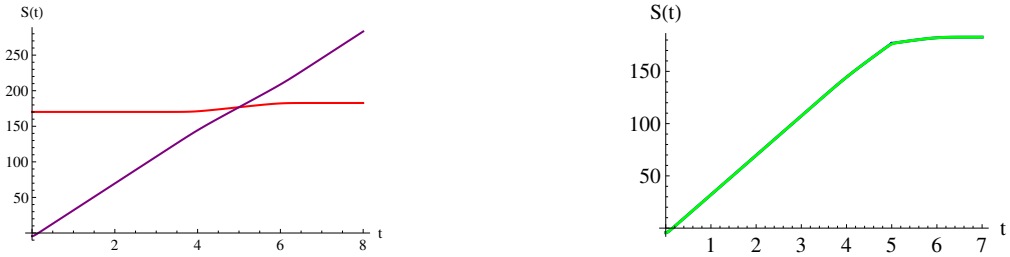

Figure 11: Left: We compare the contribution of the disconnected surface (purple) and connected surface (red) to holographic entanglement entropy. Right: We compare the CFT result (green) and holographic result (blue), finding a nice agreement. We take $l_1 = -4, l_2 = 6, \lambda = \frac{1}{4}, \beta = \frac{1}{4}$.

7.4 holographic dual of local quench

In local quenches we heat up one point of the initial time slice. By these quenches an entangled pair of quasi particles are emitted from the point we heated up. We can see the behavior from the one point functions of the stress energy tensor.

$$\langle T_{++}\rangle = \frac{c\epsilon^2}{8(x_+^2+\epsilon^2)^2} \qquad \langle T_{--}\rangle = \frac{c\epsilon^2}{8(x_-^2+\epsilon^2)^2}. \tag{162}$$

The component of the stress tensor $\langle T_{++}\rangle$ have a peak at $x_+ = 0$ which is the world line of the emitted leftmoving quasiparticle In the high energy limit $\epsilon \to 0$ the stress tensor localizes on the world line. One can also extract the world line of the rightmoving quasiparticle from $\langle T_{--}\rangle$.

Now we consider the time evolution of holographic entanglement entropy under the local quench. An attempt has been made in [45]. We take subsystem A to be $[l_1, l_2]$ and assume $l_2 > 0$.

The contribution from the disconnected surface to holographic entanglement entropy is derived by substituting the analytic continuation of the conformal map (54) into the general formula (331) in the Appendix. The result is

$$S_{dc} = \log \frac{\left(2l_1 + \sqrt{(l_1+t)^2+\epsilon^2} + \sqrt{(l_1-t)^2+\epsilon^2}\right)\left(2l_2 + \sqrt{(l_2+t)^2+\epsilon^2} + \sqrt{(l_2-t)^2+\epsilon^2}\right)}{a_{LQ}^2\sqrt{\left(1+\frac{l_1+t}{\sqrt{(l_1+t)^2+\epsilon^2}}\right)\left(1+\frac{l_2+t}{\sqrt{(l_2+t)^2+\epsilon^2}}\right)\left(1+\frac{l_1-t}{\sqrt{(l_1-t)^2+\epsilon^2}}\right)\left(1+\frac{l_2-t}{\sqrt{(l_2-t)^2+\epsilon^2}}\right)}}. \tag{163}$$

In figure 13 we plot the behavior of $S_{dc}(t)$.When $t < \min\{|l_1|, l_2\}$, $S_{dc}(t)$ remains constant with the value

$$S_{dc}(0) = \frac{c}{6}\log\frac{4|l_1|l_2}{a_{LQ}^2}, \tag{164}$$

in the high energy limit $\epsilon \to 0$. We can also see at $t = l_1$ and $t = l_2$, the derivative $S'_{dc}(t)$ suddenly jumps. At late time $t >> 1$, $S_{dc}(t)$ keeps increasing.

$$S_{dc} \to \frac{c}{3}\log\frac{t^2}{\epsilon a_{LQ}} \quad t \to \infty. \tag{165}$$

The contribution of the connected surface is

$$S_c(t) = \frac{c}{6}\log\frac{\left(l_2 - l_1 + \sqrt{(l_2+t)^2+\epsilon^2} - \sqrt{(l_1+t)^2+\epsilon^2}\right)\left(l_2 - l_1 + \sqrt{(l_2-t)^2+\epsilon^2} - \sqrt{(l_1-t)^2+\epsilon^2}\right)}{a_{LQ}^2\sqrt{\left(1+\frac{l_1+t}{\sqrt{(l_1+t)^2+\epsilon^2}}\right)\left(1+\frac{l_2+t}{\sqrt{(l_2+t)^2+\epsilon^2}}\right)\left(1+\frac{l_1-t}{\sqrt{(l_1-t)^2+\epsilon^2}}\right)\left(1+\frac{l_2-t}{\sqrt{(l_2-t)^2+\epsilon^2}}\right)}} \tag{166}$$

We also plot the time dependence of $S_c(t)$ in figure 13. At late time $t \to \infty$, it reduces to the usual Poincare AdS_3 value,

$$S_c \to \frac{c}{3} \log \frac{|l_1 - l_2|}{a_{LQ}} \quad t \to \infty. \tag{167}$$

The early time behavior of $S_c(l_1, l_2, t)$ depends on the sign of l_1. When $l_1 > 0$ it reduces to the Poincare AdS_3 value,

$$S_c(0) = \frac{c}{3} \log \frac{|l_1 - l_2|}{a_{LQ}}. \tag{168}$$

When $l_1 < 0$, it becomes

$$S_c(0) = \frac{c}{3} \log \frac{2|l_1|l_2}{a_{LQ}\epsilon}. \tag{169}$$

There is an intuitive interpretation of the time dependence of $S_c(t)$ and $S_{dc}(t)$. In the high energy limit $\epsilon \to 0$, the expectation value of the stress tensor localizes near the pulse $x_+ = 0$, $x_- = 0$ ie, $\langle T_{++} \rangle \propto \delta(x_+)$ and $\langle T_{--} \rangle \propto \delta(x_-)$. From (133), we see that the metric of the bulk is modified from that of the Poincare AdS_3 only near the pulse. Note that the Poincare AdS_3 is different from the one (129) where the spacetime boundary is located at $X = 0$. The pulse can be regarded as a bulk extension of the quasi particle pair. Extremal surfaces in the bulk can be regarded as extremal surfaces in the Poincare AdS_3 with slight modification in the vicinity of the pulse. As an intersection of an extremal surface and the pulse occurs deeper and deeper in the bulk, the change of the length of the surface become larger and larger because while the pulse significantly changes the IR metric of the bulk. However it doesn't change the UV metric which is fixed to be asymptotically AdS_3. We notice the change of the length is positive from the explicit result. The figure 12 shows the location of two extremal surfaces in the Poincare AdS_3 together with the pulse at various time. Let us discuss the $l_1 < 0 < l_2$ case as a specific example. When $0 < t < \min\{|l_1|, l_2\}$, both of leftmoving and rightmoving pulse intersect with the connected surface. Since locations of intersections gradually get close to the boundary, the length of the connected surface is decreasing as time increases. At $\min\{|l_1|, l_2\} \leq t < \max\{|l_1|, l_2\}$, one part of the pulse intersects with the connected surface and the other with the disconnected surface. Since the intersection of the part of the pulse and the disconnected surface gradually leaves the boundary, the length of the disconnected surface is increasing. At $t \geq \max\{|l_1|, l_2\}$, both part of the pulse intersect with the disconnected surface, thus the length of the disconnected surface is increasing but the length of the connected surface remains constant. Sudden changes of the length of both surfaces at $t = l_1$ and $t = l_2$ in the figure also support our intuitive picture. In $0 < l_1 < l_2$ case, one can also make a similar argument for the behavior of the both surfaces.

When $l_1 \leq 0 < l_2$, since the length of the disconnected surface is monotonically increasing in time, and the length of the connected surface is monotonically decreasing, there is a phase transition between two surfaces in general. Because of inhomogeneity of the

quench, The critical time t_c when the phase transition happens depends on how we take a subsystem A. For example, when the subsystem A is given by $[0, l]$, $t_c = l/4$ in high energy limit $\epsilon \to 0$. Note that the phase transition is crucial to the get correct early time behavior of entanglement entropy holographically. In figure 13 we compare the CFT result and the holographic result for $l_1 < 0 < l_2$ case. By comparing expressions (164),(167) and (56),(58) we find both early time and late time behavior agree. However near the critical time t_c, two results are different. The reason of the difference come from the fact that in CFT side, we approximate the two point function on the upper half plane by (44) to get a universal result.

In figure 13 we plot the time dependence of the both length of surfaces for $0 < l_1 < l_2$ case. In the case, the area of the connected surface is always smaller, and there is no phase transition. By comparing it to the CFT result, we find that although the late time behavior agree (167) (56) , but early time does not (168) (57). The reason of the difference is similar as the previous case.

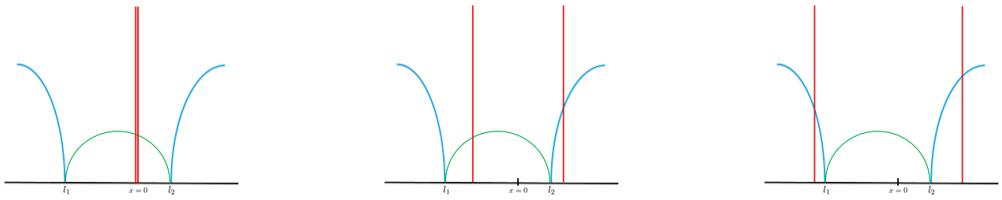

Figure 12: Sketch of the extremal surfaces in AdS_3 (green:connected,blue:disconnected) and pulse (red line). Left: When $t < \min\{|l_1|, l_2\}$, both pulse intersect with the connected surface. Middle:When $\min\{|l_1|, l_2\} \leq t < \max\{|l_1|, l_2\}$ one of the pulse intersect with the connected surface and the other intersect with the disconnected surface. Right: $t \geq \max\{|l_1|, l_2\}$ both pulse intersect with the disconnected surface.

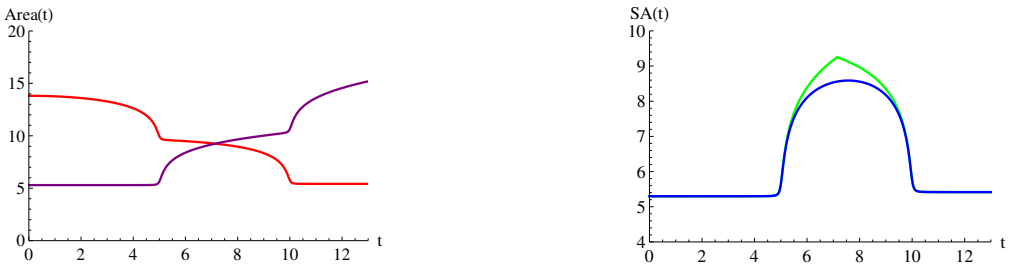

Figure 13: Left: a plot of the length of the both surface as a function of time(red:connected, purple:disconnected). We take $l_1 = -5, l_2 = 10, \epsilon = \frac{1}{10}$. Right:comparison with CFT result(green: bulk, blue:CFT).

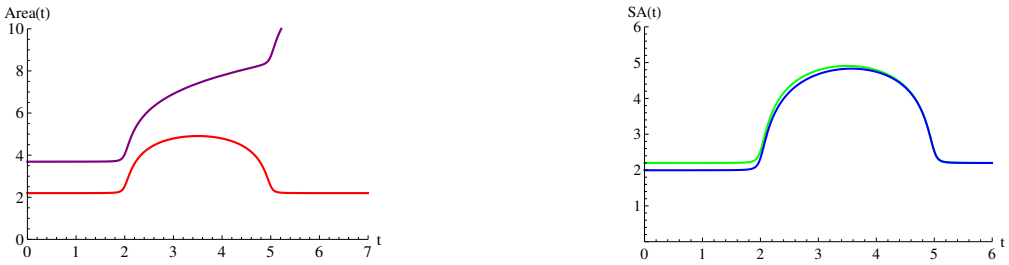

Figure 14: Left:a plot of the length of the both surface as a function of time(red:connected, purple:disconnected). We take $l_1 = 2, l_2 = 5, \epsilon = \frac{1}{10}$. Right: comparison with CFT result(green: bulk, blue:CFT).

8 Global quenches with finite size effects and their holographic interpretations

So far we have studied quantum quenches in two dimensional conformal field theories and their holographic duals when the spatial directionof CFT is non-compact. In global quenches, the non-compactness of the spatial direction means that the temperature introduced by the quench is sufficiently high, and the dual black hole formed by the quench (gravitational collapse) is stable against Hawking radiations. Therefore we would like to know what happens when the induced effective temperature is not so much high, where the effects of Hawking radiations become significant.

To deal with the setup, in this section we consider global quenches on finite size spatial manifold, especially circles. Again for free fermion theory the calculation is possible because explicit correlation functions with boundary conditions are known.

8.1 An Entropy Puzzle about Time-dependent Holography

In this subsection we address an entropy puzzle about time dependent entropy and consider the way to resolve it. Consider holography in time-dependent backgrounds, especially the ones in AdS/CFT. We are particularly interested in a situation where a black hole horizon is created by a gravitational collapse. Such a time-dependent process has been considered to be dual to thermalizations and indeed we can construct explicit examples in AdS/CFT setups [63, 64], where non-normalizable perturbations lead to a creation [38] This is partly because there are two different notions of horizons: event horizon and apparent horizon. Currently, there are several evidences that the latter will be more appropriate to define entropy [22, 23]. However, still we need to specify the choice of time slices to calculate the apparent horizon and thus there are infinitely many different definitions. Remember that in static spacetimes, the time slice is uniquely chosen and there is no ambiguity.

A closely related issue in the dual CFT side is that we can define a non-vanishing entropy even for a pure state if we perform a coarse-graining of the given total system. If the total system consists of a gas and a heat bath, then the entropy of gap is obtained by tracing out the heat bath and by the required coarse-graining due the fact that our observables are quite restricted compared with the microscopic degrees of freedom. Again this leads to infinitely many different definitions of (coarse-grained) entropy. Below we would like to resolve the above puzzle by paying attention to this coarse-graining procedure.

The resolution of this puzzle is also closely related to that of the black hole information loss problem. This problem occurs since a massive object described by a pure state collapses into a black hole and finally ends up with a thermal gas generated by Hawking radiations, which looks like a mixed state. If this is true, a pure system has to evolve into a mixed state after enough time and clearly contradicts with the principle of quantum mechanics.

8.2 Entanglement Entropy as Coarse-grained Entropy

Typically the coarse-graining is done by cutting out higher energy modes or higher order multi-particle interactions. However, this does not seem to allow straightforward calculations in AdS/CFT setup. Therefore, here we would like to perform a coarse-graining by cutting out a spacial part of the total system. In this case, the obtained entropy coincides with the quantity called entanglement entropy.

We can calculate $S_A(t)$ via AdS/CFT by applying the holographic formula proposed in [22], which generalizes the holographic formula in static spacetime found in [21]. It is simply given by

$$S_A(t) = \frac{\text{Area}\,(\gamma_A(t))}{4G_N}, \tag{170}$$

where G_N is the Newton constant of the AdS space. The surface $\gamma_A(t)$ is a codimension two surface in the AdS space which is defined by the extremal surface whose boundary coincides with the boundary of $A(t)$. We require that $\gamma_A(t)$ is homotopic to $A(t)$. If there are more than one such extremal surfaces, we pick up the one with the lowest area, as is required by the strong subadditivity of entanglement entropy [27]. Note that here we need to directly deal with Lorentzian spacetime without its Euclidean counterpart because it is time-dependent. Indeed, in [22], it was confirmed that such extremal surfaces are well-defined in important examples. Recently, this formula is applied to the AdS_3 Vaidya background and the conformal field theory results in [75] have been remarkably reproduced in the work [37]. Moreover, this calculation has been extended to the higher dimensional cases in [38].

For our purpose, it is convenient to study a $d+1$ dimensional time-dependent background which is asymptotically global AdS_{d+1} space, which includes a finite size effect because its boundary is $R \times S^{d-1}$. We assume that a black hole is produced at a certain time via a gravitational collapse and this process lasts only for a finite time. Our argument below is heuristic and does not depend on the detailed form of the time-dependent solution.

We calculate S_A at a time t when the black hole formation has been ended and when the spacetime is well approximated by a static AdS black hole. First we assume the length size of A (denoted by $|A|$ below) is smaller than the inverse temperature β_{BH} of the AdS black hole temperature. In this case, the extremal surface $\gamma_A(t)$ is localized near the boundary and surrounds the region $A(t)$ [21]. S_A essentially consists of the area law divergent piece

$$S_A \sim \frac{\text{Area}(\partial A)}{a^{d-2}} + ..., \tag{171}$$

which are independent of the temperature. Notice that the condition $|A| << |B|$ assumed here physically means that the system is heavily coarse-grained. As $|A|$ exceeds β_{BH}, S_A gains a finite and extensive contribution, which is essentially the thermal entropy for the subsystem A, in addition to the divergent part S_{div} given by (171). This thermal contribution comes from the part of the surface $\gamma_A(t)$ which is wrapped on a part of the

apparent horizon of the AdS black hole and thus is proportional to $|A|$ as in Fig.15; see [22, 37, 38, 65] for explicit confirmations. An important fact is that though the apparent horizon requires the choice of the time slice, our extremal surface $\gamma_A(t)$ is uniquely determined by the boundary condition.

When this reaches the point $|A| = |B|$, the situation begins to change importantly. If we naively speculate the surface $\gamma_A(t)$ in a continuous way until $|A|$ exceed $|B|$, we may think that it will wrap on a more than half of the apparent horizon as in the right-up figure of Fig.15. However, since the horizon disappears at an earlier time, we can smoothly deform this surface into the one which wraps the opposite part of the horizon. Therefore the result of S_A as a function of $|A|$ becomes symmetric with respect to the point $|A| = |B|$ as in the right-down figure of Fig.15. In other words, we can conclude that in this time-dependent background the entanglement entropy satisfies

$$S_A = S_B, \tag{172}$$

which is indeed known to be true when the total system is a pure state and thus agrees with our holographic setup. This sudden decreasing of the entanglement entropy occurs because the subsystem B which we are tracing out gets smaller than the half of the total system and the information lost by the coarse-graining starts recovering[8].

In the end, we can holographically calculate the von-Neumann entropy for the total system as follows

$$S_{tot} = \lim_{|B|\to 0} (S_A - S_B) = 0. \tag{173}$$

Thus, in the gravity side, we confirmed that the total entropy is always vanishing in spite of the black hole formation. As is clear from the previous argument, the essential point is that the horizon is time-dependent and gets vanishing at earlier time and the minimal area principle (among extremal surfaces) prefers the minimum i.e. $S_{tot} = 0$ at any time. In summary, in the time-dependent background which describes a thermalization of a pure state, the von-Neumann entropy of the total system is indeed vanishing also in the gravity side. This contrasts strikingly with the setup of an eternal AdS black hole [79] as it is dual to a mixed state in a thermal CFT and has a non-vanishing thermal entropy, which precisely coincides with the value $\lim_{|B|\to 0} (S_A - S_B)$ [80].

The non-zero entropy is obtained only after a certain coarse-graining. Among various such entropies defined in the dual CFT, only the entanglement entropy has its clear holographic dual in time-dependent backgrounds at present. From this viewpoint, we can define a coarse-grained effective entropy S_{eff} which looks analogous to the thermal entropy by

$$S_{eff} = 2\left(S_A - S_A^{(0)}\right)\Big|_{|A|=|B|}. \tag{174}$$

[8]A similar behavior has been known in the analysis of quantum information in evaporating black holes [78]. This has been considered to be crucial to resolve the information paradox of quantum black holes because the information may be recovered after more than half of a black hole has been evaporated.

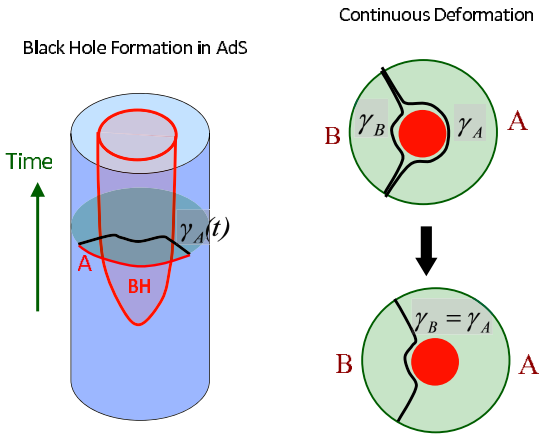

Figure 15: The minimal surface γ_A for the holographic calculation of entanglement entropy in the AdS black formation (left). Though for an eternal AdS black hole we have $\gamma_A \neq \gamma_B$ (upper right), in our case of black hole formation, we actually find that $\gamma_A = \gamma_B$ (lower right). This is because the horizon vanishes at early time.

We subtracted the entanglement entropy $S_A^{(0)}$ before the thermalization. This clearly includes the divergent part S_{div} given by (171) and therefore S_{eff} is finite. The reason why we put the factor two is A covers only a half of the total system. We would like to argue that (174) is a definition of coarse-grained entropy which is uniquely calculable both in gravity and CFT side of the AdS/CFT. Notice that though the calculation of entropy from an apparent horizon requires the choice of time slice and is ambiguous, our entropy S_{eff} has no ambiguity as the extremal surface condition of $\gamma_A(t)$ determined where the surface wraps the apparent horizon.

Finally, we would like to come back to the relation to the black hole information problem [62]. From the above argument, it is clear that there is no information loss in the gravitational collapsing process because $S_{tot} = 0$ is always satisfied. However, we cannot study the most important process of the decay due to Hawking radiations because the absence of the holographic formula of entanglement entropy beyond the supergravity approximation. Therefore, for this purpose, it is a better idea instead to study its CFT dual, directly. We will analytically investigate such an example in the next section.

8.3 Global quenches with finite size effects

In this subsection we compute the evolution of entanglement entropy under the global quench when the spatial manifold is a circle S^1 for the free Dirac fermion theory

The calculation of the entanglement entropy is quite similar to that of the torus entanglement entropy which we have reviewed in 2.4. One difference is that here we need to evaluate correlation functions of the twisted operator for the initial state of the quench $|\psi\rangle = e^{-\frac{\beta}{4}}|B\rangle$. If we take the subsystem A to be a segment $[\sigma_1, \sigma_2]$, the trace of the reduced density matrix is given by

$$\begin{aligned}\mathrm{Tr}[\rho_A(t)^N] &= \prod_{a=-\frac{N-1}{2}}^{\frac{N-1}{2}} \langle \sigma^{(a)}(y_1, \bar{y}_1)\sigma^{(-a)}(y_2, \bar{y}_2)\rangle_{cylinder} \\ &= \prod_{a=-\frac{N-1}{2}}^{\frac{N-1}{2}} \frac{\langle B|e^{-\frac{\beta}{2}H}\sigma^{(a)}(y_1,\bar{y}_1)\sigma^{(-a)}(y_2,\bar{y}_2)|B\rangle}{\langle B|e^{-\frac{\beta}{2}H}|B\rangle}. \end{aligned} \tag{175}$$

Here we normalized the two point functions such that $\mathrm{Tr}[\rho_A(t)] = 1$.

As we reviewed in2.4 . massless Dirac fermion $(\psi, \bar{\psi})$ can be bosonized into a free scalar X via the standard formula

$$\psi_L(y) = e^{iX_L(y)}, \quad \bar{\psi}_L(y) = e^{-iX_L(y)}, \quad \psi_R(\bar{y}) = e^{iX_R(\bar{y})}, \quad \bar{\psi}_R(\bar{y}) = e^{-iX_R(\bar{y})}. \tag{176}$$

Our normalization of the two dimensional CFT in this paper is $\alpha' = 2$ in string theory world-sheet [82] and the free Dirac fermion is equivalent to the compact boson X at the radius $R = 1$. If we write the primary fields as $V_{(k_L,k_R)}(y, \bar{y}) = e^{ik_L X_L(y) + ik_R X_R(\bar{y})}$, then there are two candidates of the twisted vertex operators, which lead to the twisted boundary conditions (23),

$$\sigma_1^{(a)}(y, \bar{y}) = V_{(\frac{a}{N}, -\frac{a}{N})}(y, \bar{y}) = e^{i\frac{a}{N}(X_L(y) - X_R(\bar{y}))}, \tag{177}$$

$$\sigma_2^{(a)}(y, \bar{y}) = V_{(\frac{a}{N}, \frac{a}{N})}(y, \bar{y}) = e^{i\frac{a}{N}(X_L(y) + X_R(\bar{y}))}, \tag{178}$$

which have the lowest dimensions if a runs $a = -\frac{N-1}{2}, -\frac{N-3}{2}, \cdots, \frac{N-1}{2}$ [80].

What we need to calculate to obtain the entanglement entropy are the two point functions of (177) or (178) on the cylinder. This can be found by performing calculations using the explicit form the boundary state $|B\rangle$ (see e.g. [89]) as summarized in the appendix A. One may think that there are two choices i.e. the Neumann and Dirichlet boundary condition in the free scalar theory. If we returns to the Dirac fermion theory, the Neunmann boundary condition relates ψ_L and $\bar{\psi}_L$ to ψ_R and $\bar{\psi}_R$ at the boundary, while the Dirichlet one does $\psi_{L,R}$ to $\bar{\psi}_{R,L}$, respectively. We can see that the discrete Fourier transformation, employed to map the replicated fermions into the new ones which satisfy (23), is consistent only when we choose $\sigma_1^{(a)}$ or $\sigma_2^{(a)}$ for the Neumann or Dirichlet boundary condition, respectively.

We define the subsystem $A(t)$ as an interval in the Imy direction at time $\epsilon + it$. We can parameterize the location of the two ends points of this interval as

$$(y_1, \bar{y}_1) = (\frac{\beta}{4} + it + i\sigma_1, \frac{\beta}{4} + it - i\sigma_1), \quad \text{and} \quad (y_2, \bar{y}_2) = (\frac{\beta}{4} + it + i\sigma_2, \frac{\beta}{4} + it - i\sigma_2). \tag{179}$$

The final result of the normalized two point functions in both Neumann and Dirichlet is given by the same expression

$$\langle\sigma^{(a)}(y_1,\bar{y}_1)\sigma^{(-a)}(y_2,\bar{y}_2)\rangle = \left(\frac{\eta(\frac{i\beta}{2\pi})^6\cdot|\theta_1(\frac{\frac{\beta}{4}+it}{\pi i}+\frac{\sigma}{2\pi}|\frac{i\beta}{2\pi})||\theta_1(\frac{\frac{\beta}{4}+it}{\pi i}-\frac{\sigma}{2\pi}|\frac{i\beta}{2\pi})|}{|\theta_1(\frac{\sigma}{2\pi}|\frac{i\beta}{2\pi})|^2\cdot|\theta_1(\frac{\frac{\beta}{4}+it}{\pi i}|\frac{i\beta}{2\pi})|^2}\right)^{\frac{a^2}{N^2}}, \quad (180)$$

where we defined $\sigma\equiv\sigma_2-\sigma_1$. Refer to appendix A for a derivation of this result (180).

By substituting the two point functions (180) into (175) , we obtain the entanglement entropy,

$$S_A(t,\sigma)=\frac{1}{6}\log\frac{|\theta_1(\frac{\sigma}{2\pi}|\frac{i\beta}{2\pi})|^2\cdot|\theta_1(\frac{\frac{\beta}{4}+it}{\pi i}|\frac{i\beta}{2\pi})|^2}{\eta(\frac{i\beta}{2\pi})^6\cdot|\theta_1(\frac{\frac{\beta}{4}+it}{\pi i}+\frac{\sigma}{2\pi}|\frac{i\beta}{2\pi})||\theta_1(\frac{\frac{\beta}{4}+it}{\pi i}-\frac{\sigma}{2\pi}|\frac{i\beta}{2\pi})|\cdot a_{UV}^2}, \quad (181)$$

where we recovered the cut off a_{UV} dependence in an obvious way. Notice that this is independent from the choice of the boundary condition (Neumann or Dirichlet one). From this it is clear that $S_A(t)$ satisfies

$$S_A(t,\sigma)=S_A(t,2\pi-\sigma)=S_B(t,\sigma). \quad (182)$$

This is consistent with the assumption that the total system is a pure state and the von-Neumann entropy for the total system is vanishing.

After the modular transformation, we can rewrite (181) as follows[9]

$$S_A(t,\sigma)=\frac{1}{3}\log\frac{2\epsilon}{\pi a_{UV}}+\frac{1}{6}\log\frac{|\theta_1(\frac{i\sigma}{4\epsilon}|\frac{\pi i}{2\epsilon})|^2\cdot|\theta_1(\frac{\epsilon+it}{2\epsilon}|\frac{\pi i}{2\epsilon})|^2}{\eta(\frac{\pi i}{2\epsilon})^6\cdot|\theta_1(\frac{\epsilon+it}{2\epsilon}+\frac{i\sigma}{4\epsilon}|\frac{\pi i}{2\epsilon})||\theta_1(\frac{\epsilon+it}{2\epsilon}-\frac{i\sigma}{4\epsilon}|\frac{\pi i}{2\epsilon})|}, \quad \epsilon=\frac{\beta}{4}. \quad (183)$$

The explicit form of $S_A(t,\pi)$ is plotted in Fig.16 as a function of t. In the limit $\beta\to\infty$, where the quench disappears, we reproduce the standard result [83, 84]

$$S_A=\frac{1}{3}\log\left(\frac{2}{a_{UV}}\sin\frac{\sigma}{2}\right). \quad (184)$$

In the opposite limit $\beta\to 0$, which corresponds to the infinitely extended space, we can easily reproduce the result (46) at the central charge $c=1$

$$\begin{aligned} S_A &= S_{div}+\tfrac{2\pi t}{3\beta} \quad (0<t<\tfrac{\sigma}{2}) \\ &= S_{div}+\tfrac{\pi\sigma}{3\beta} \quad (t>\tfrac{\sigma}{2}), \end{aligned} \quad (185)$$

where we separate the divergent part $S_{div}\equiv\frac{1}{3}\log\frac{\beta}{2\pi a_{UV}}$.

[9] Actually, in this expression, the values of $\theta_1(\frac{\epsilon+it}{\epsilon}|\frac{\pi i}{2\epsilon})$, $\theta_1(\frac{\epsilon+it}{2\epsilon}+\frac{i\sigma}{4\epsilon}|\frac{\pi i}{2\epsilon})$, where $\epsilon=\frac{\beta}{4}$ and $\theta_1(\frac{\epsilon+it}{2\epsilon}-\frac{i\sigma}{4\epsilon}|\frac{\pi i}{2\epsilon})$ are always all real even before we take their absolute values. This justify our analytical continuation $\mathrm{Re}[y]\to\epsilon+it$.

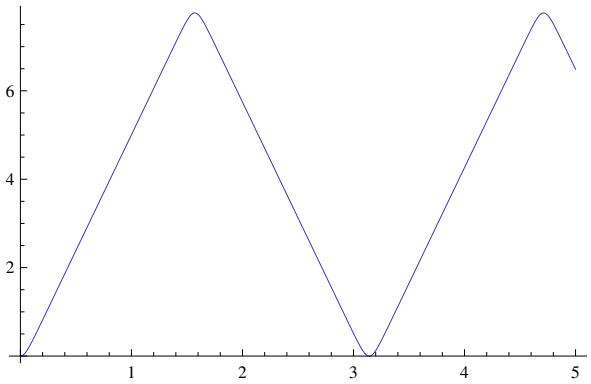

Figure 16: The plot of $S_{eff}(t) \equiv 2\left(S_A(t,\pi) - S_A(0,\pi)\right)$ as a function of t at $\epsilon = 0.2$.

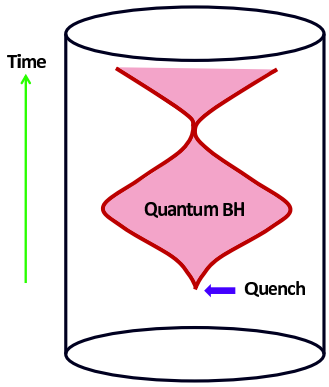

Figure 17: Quantum black hole creations and annihilations in AdS space by the quantum quench as obtained from Fig.16.

8.4 Holographic interpretation of the result

Let us discuss the holographic interpretation of the result, although since we are considering free CFT, corresponding bulk gravity is highly quantum. In figure 16 ,one can easily see the resulting entanglement entropy $S_A(t,\pi)$ is linearly growing in $t < \frac{\pi}{2}$, and linearly decreasing $t > \frac{\pi}{2}$. One can also observe the the entanglement entropy is periodic in time.

$$S_A(t,\sigma) = S_A(t+\pi,\sigma) \tag{186}$$

Despite its highly quantum nature, one can imagine an effective classical description qualitatively. Let us prepare two eternal black holes with temperature β, and consider the region $-\frac{\pi}{2} < t < \frac{\pi}{2}$ of them. We then glue the $t = -\frac{\pi}{2}$ slice of the one of the black holes with $t = \frac{\pi}{2}$ slice of the another black hole. The resulting geometry can be seen as a black hole is continued at $t = \frac{\pi}{2}$ to a white hole. The white hole at $t > \frac{\pi}{2}$ can be regarded as a model of quantum black hole emitting huge amounts of Hawking radiations.

As we have seen previously, the linear growth of the entanglement entropy in $t < \frac{\pi}{2}$ can be interpreted by the growth of interior region of the dual black hole. The decrease of entanglement entropy $t > \frac{\pi}{2}$ also can be interpreted by the reduce of the interior region of the white hole. The behavior in $t > \frac{\pi}{2}$ of (181) can be interpreted by referring $t < 0$ behavior of (124) in the eternal black hole, where the entanglement entropy is linearly decreasing. In the region $t < 0$ in the eternal black hole, the disconnected surface, the area of which is given by (124) probes inside of the white hole. Since the interior region of the white hole is gradually reducing, the area of the disconnected surface is decreasing. Hence we see the geometry in the above paragraph provides a bulk interpretation of the CFT result, namely the black hole creation and subsequent evaporation of via the Hawking radiations. After the evaporation of the black hole, the emitted Hawking radiations are reflected at the time like boundary of the AdS. Then they again concentrate at the center of AdS to recreate a black hole. Successive recursions of the creation and the evaporation of the black hole explain the time periodic nature of the entanglement entropy $S_A(t,\pi)$.

8.5 Time evolutions of correlation functions

In this section we would like to consider time evolutions of correlation functions. We also interpret these results by the bulk picture discussed in the previous section.

8.5.1 One Point Functions

Assume that an operator O in CFT is dual to a field O in AdS. The bulk to boundary relation in AdS/CFT [88] argues that the one point function $\langle O(x)\rangle$ in the CFT is proportional to the value of the field Ø near the AdS boundary. Since we are not deforming the CFT itself, the profile of O is supposed to be normalizable.

The most important one point function in time-dependent backgrounds will be that of the energy stress tensor. Due to its conservation law, this clearly becomes time-independent.

It is straightforward to calculate the energy density $\mathcal{E}_n$ of the left-moving oscillator α_n as follows

$$\mathcal{E}_n = \frac{1}{2\pi}\langle \alpha_{-n}\alpha_n\rangle = \frac{n}{2\pi(e^{\beta n}-1)}. \tag{187}$$

This indeed obeys the Bose-Einstein distribution with the effective temperature. This temperature can also be seen in the reduced density matrix when we trace out the right-moving oscillators $\tilde{\alpha}_n$ (or equally left-moving ones)

$$\rho_L = \mathrm{Tr}_R e^{-\frac{\beta}{4}H}|B\rangle\langle B|e^{-\frac{\beta}{4}H} = \prod_{m=0}^{\infty}\sum_{n=0}^{\infty} e^{-\beta mn}\frac{(\alpha_{-m})^n}{\sqrt{n!}}|0\rangle\langle 0|\frac{(\alpha_m)^n}{\sqrt{n!}}, \tag{188}$$

where we omit the zero modes. The total energy density in the $\beta \to 0$ limit can be found as usual $\mathcal{E}_{tot} \simeq 2\sum_{n=1}^{\infty}\mathcal{E}_n \simeq \frac{\pi}{6}T_{eff}^2$.

Even though we confirmed that our system is thermalized, we cannot find signals of black hole creation and annihilation from the time-independent one point function (187). Motivated by this we would like to calculate another one point function which is not dual to any conserved quantities. Especially we consider the one point function $\langle e^{ikX(t,\sigma)}\rangle$ for the Dirichlet boundary state for the initial state $|\Psi_0\rangle$, where k can take only integer values as we set $R = 1$. After a calculation similar to the appendix D, we finally obtain (we set $\sigma = 0$)

$$\langle e^{ikX(t,0)}\rangle = \frac{\theta_3\left(\frac{k(\epsilon+it)}{\pi i}|\frac{2\epsilon i}{\pi}\right)}{\theta_3\left(0|\frac{2\epsilon i}{\pi}\right)}\cdot\frac{|\eta\left(\frac{2\epsilon i}{\pi}\right)|^{3k^2}}{|\theta_1\left(\frac{\epsilon+it}{\pi i}|\frac{2\epsilon i}{\pi}\right)|^{k^2}}, \qquad \epsilon = \frac{\beta}{4}. \tag{189}$$

As is clear from the plot in Fig.18, it has peaks at $t = 0, \pi, 2\pi, \cdots$. This behavior is actually natural from our interpretation in terms of black hole creations and annihilations. As the result of the entanglement entropy suggests, a black hole is created at $t = 0$ and reaches its maximal size at $t = \frac{\pi}{2}$. Therefore, we expect that the radiations from the black hole will be the most strong at $t = \frac{\pi}{2}, \frac{3\pi}{2}, \cdots$, remembering the periodicity π. They will reach at the AdS boundary after the propagation time[10] $\Delta t = \pi/2$. This explains the peaks of $\langle e^{ikX(t,0)}\rangle$ since the one point function is dual to the value of bulk scalar field near the AdS boundary and its square should be proportional to the strength of radiations. Notice that this non-vanishing one point function is peculiar to time-dependent black holes. This is because the one point function, which is holographically dual to a classical radiation, is vanishing in the static thermal CFT.

[10]This can be found from the metric of the global AdS_3: $ds^2 = -\cosh^2\rho dt^2 + d\rho^2 + \sinh^2\rho d\theta^2$ as $\Delta t = \int_0^{\infty}\frac{d\rho}{\cosh\rho} = \frac{\pi}{2}$. In the presence of black holes one may think that the propagation time of a massless particle will be changed. Indeed, in a semiclassical black hole, this happens and affects the structures of singularities of two point functions [81]. However, we do not consider this modification as we are interested in a region in gravity where quantum corrections are so large that the even horizon does not seem to be defined using a metric.

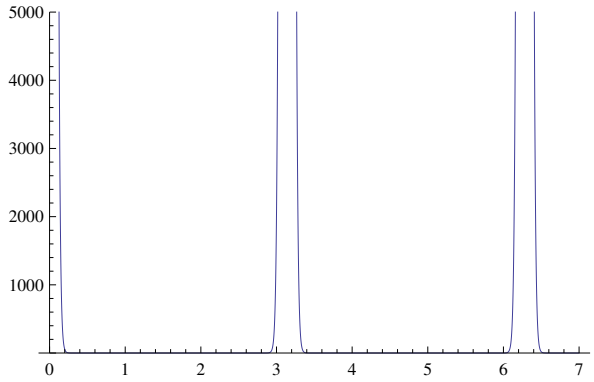

Figure 18: The plot of the one point function $e^{ikX(t,0)}$ as a function of t at $\epsilon = 0.2$ and $k = 3$.

8.5.2 Evolution of two point function in the quench

We would like to elaborate on time dependent correlation functions in the quench to discuss the information loss problem of black holes [62]. In [79, 85, 87], it has been argued that information loss problem is dual to the quasinormal behavior (exponential decay) of time dependent two point functions in a large N gauge theory at finite temperature:

$$\langle O(t_1)O(t_2)\rangle \sim \exp[-c|t_1 - t_2|]. \tag{190}$$

where c is a positive real constant. These behavior breaks the unitarity of the theory because this shows that any fluctuations that we add to the initial state will eventually vanish. In the same papers, it has also been conjectured in a finite N gauge theory, the decay of the correlation stops at the value of order $\exp[-O(N^2)]$, then correlation grows, and repeats this behavior because of the Poincare recurrence of the theory.

Indeed, this quasinormal behavior can be seen in our model. If we set $y_1 = \frac{\beta}{4} + it$, $y_2 = \frac{\beta}{4}$ and $k_L = k_R = k$ in the two point functions (340) for the Neumann boundary condition, we find

$$\begin{aligned} G(t) &= \langle \exp ikX(t,0) \exp -ikX(0,0)\rangle_N \\ &= \eta\left(\frac{i\beta}{2\pi}\right)^{6k^2} \cdot \left|\frac{\theta_1\left(\frac{(\frac{\beta}{4}+it)}{\pi i}|\frac{i\beta}{2\pi}\right)}{\theta_1\left(\frac{t}{2\pi}|\frac{i\beta}{2\pi}\right)^2}\right|^{k^2} \cdot \left|\frac{\theta_1\left(\frac{\beta}{4\pi i}|\frac{i\beta}{2\pi}\right)}{\theta_1\left(\frac{\frac{\beta}{2}+it}{2\pi i}|\frac{i\beta}{2\pi}\right)^2}\right|^{k^2} . \end{aligned} \tag{191}$$

In Fig.19, we show the plot of $G(t)$. It has the periodicity 2π as a signal propagates from $\sigma = 0$ and it has to go back to the same point. The divergences at $t \in 2\pi\mathrm{Z}$ come from the usual short distance behavior of the operator product. If $\beta \ll t \ll 1$, we can find the

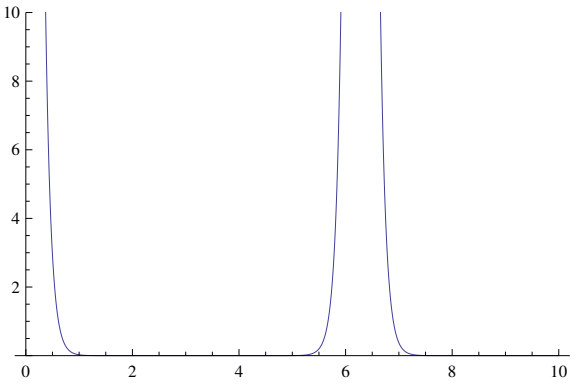

Figure 19: The plot of $G(t)$ as a function of t at $\epsilon = 0.2$.

following exponential behavior of $G(t)$

$$G(t) \simeq f(\beta) \exp\left[-\frac{2\pi k^2 t}{\beta}\right], \tag{192}$$

for a certain time-independent function $f(\beta)$. Due to the 2π periodicity, after $G(t)$ gets decreased exponentially, it reaches its (non-zero) minimum at $t = \pi$ and then again begins to increase.

Finally, it is also intriguing to study the time evolution of the two point function with separated points $\langle \exp ikX(t,\sigma) \exp -ikX(t,0)\rangle$ for Neumann boundary condition. If we use the formula (340) of Appendix A, and set $y_1 = \frac{\beta}{4} + it + i\sigma$ and $y_2 = \frac{\beta}{4} + it$, we have

$$\begin{aligned} F(t,\sigma) &= \langle \exp ikX(t,\sigma) \exp -ikX(t,0)\rangle_N \\ &= \eta\left(\tfrac{i\beta}{2\pi}\right)^{6k^2} \cdot \frac{\left|\theta_1\left(\frac{\frac{\beta}{4}+it}{\pi i}|\frac{i\beta}{2\pi}\right)\right|^{2k^2}}{\left|\theta_1\left(\frac{\sigma}{2\pi}|\frac{i\beta}{2\pi}\right)\right|^{2k^2}\left|\theta_1\left(\frac{2(\frac{\beta}{4}+it)+i\sigma}{2\pi i}|\frac{i\beta}{2\pi}\right)\right|^{k^2}\left|\theta_1\left(\frac{2(\frac{\beta}{4}+it)-i\sigma}{2\pi i}|\frac{i\beta}{2\pi}\right)\right|^{k^2}}. \end{aligned}$$

In Fig.20, we plot $F(t,\sigma)$. The graph shows that the correlation becomes strong when S_{eff} is large (compare with Fig.16). This can be regarded as a further evidence of the successive productions and annihilations of quantum black holes in our system.

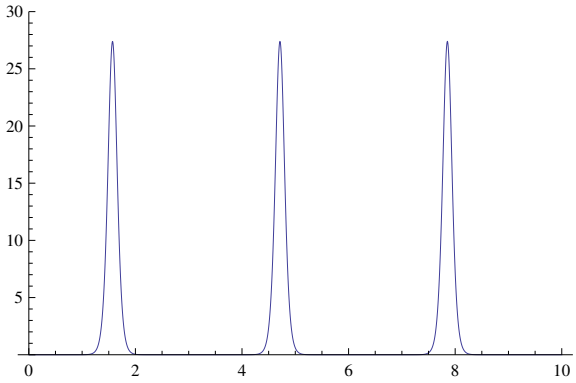

Figure 20: The plot of $F(t, \sigma)$ as a function of t at $\epsilon = 0.2$.

9 Higher spin theory

9.1 Why higher spin ??

A higher spin field is a massless field with spin larger than two. Gravitational field can couple to these higher spin fields. In this section, we would like to consider generalizations of ordinary theories of gravity where these higher spin fields are coupled (higher spin theories). The primary motivation to consider higher spin theories is the fact that string theory contains massive higher spin states. Their mass in the Minkowski space is given by

$$m_s^2 = \frac{s}{l_s^2}, \tag{193}$$

where l_s is the string scale. If we consider curved spacetimes, these excitations are expected to be massless when the curvature of the background spacetime is large compared to the string scale. To explore classical dynamics of string theory in this regime we need to take these fields into account. A spin s field is described by a rank s fully symmetric tensor $\varphi_{\mu_1\cdots\mu_s}$. The linearized equation of motion of the spin s field $\varphi_{\mu_1\cdots\mu_s}$ around a flat space has been written down by Fronsdal [98]

$$\Box\varphi_{\mu_1\cdots\mu_s} - \partial_{(\mu_1}\partial^{\lambda}\varphi_{|\mu_2\cdots\mu_s)\lambda} + \partial_{(\mu_1}\partial_{\mu_2}\varphi^{\lambda}_{\mu_3\cdots\mu_s\lambda} = 0, \tag{194}$$

The equation is invariant under the gauge transformation of the spin s field.

$$\delta\varphi_{\mu_1\cdots\mu_s} = \partial_{(\mu_1}\xi_{\mu_2\cdots\mu_s)}, \tag{195}$$

where $\xi_{\mu_1\cdots\mu_s}$ satisfies the following traceless conditions

$$\xi^{\lambda}_{\mu_1\cdots\mu_{s-3}\lambda} = 0. \tag{196}$$

Although in the Minkowski space it is difficult to construct interacting higher spin theories due to Coleman Maudula theorem, however one can construct these theories in spacetime with cosmological constants. Thanks to Vasiliev and his collaborators, the nonlinear equations of motion for higher spin fields have been known [91, 92]. To write down these equations in general we need to consider multiplets which are containing infinitely many higher spin fields, hence their expressions are highly complicated. However in three dimension dramatical simplifications occur, because all these higher spin fields become topological. Blencowe [107] found that Chern Simon theories with gauge groups $G \supset \mathrm{SL}(2,\mathbb{R})$ describe higher spin theories.

In the context of AdS/CFT correspondence, The necessity to include the effects of higher spin fields has been already pointed out few years after the discovery of the correspondence. The basic observation is that there are additional higher spin conserved currents in the free limit $\lambda_{\mathrm{t'Hooft}} \to 0$ of the gauge theory side, which is related to the higher curvature limit of gravity side. To see this, for example consider a free scalar boson ϕ, and the current operator,

$$J_{\mu_1\cdots\mu_s} = \phi\partial_{(\mu_1}\cdots\partial_{\mu_s)}\phi. \tag{197}$$

The current is conserved $\partial^\lambda J_{\lambda\cdots\mu_s} = 0$ because of the equation of motion of the free boson $\partial^2\phi = 0$. This is what we anticipated also in gravity side (emergence of higher spin fields.) Klebanov and Polyakov conjectured the concrete duality between a higher spin theory in AdS_4 and (singlet sector of) three dimensional $O(N)$ model [93].

Quite recently, Gaberdiel and Gopakumar conjectured similar holographic duality between a higher spin theory in AdS_3 and a large N limit of a $\mathcal{W}_N$ minimal model [97] .

The simplicity of three dimensional gravities makes more elaborated studies of quantum gravity as well as black holes possible. There are two main achievements in this direction. First, Brown and Henneaux found that the asymptotically symmetry algebra of AdS_3 which is a subalgebra of general coordinate transformations that keep the given boundary conditions of the configuration at the conformal boundary of AdS_3 is a pair of Virasoro algebra with central charge $c = \frac{3l}{2G}$[28]. This does imply that quantum theories of gravity on AdS_3 has same symmetry with two dimensional conformal field theories. This can be regarded as an important precursor of AdS/CFT correspondence. In two dimensional CFTs on a torus, Cardy's formula counts the number of operators with sufficiently large scaling dimensions. Strominger found that the entropy of BTZ black holes can be explained microscopically in the CFT side, by using the Cardy's formula together with the Brown and Henneaux's central charge [100]. Hence we know what kind of chiral primary operators are dual to microstates of BTZ black holes in principle. The situation is very much different to understanding of microstates of usual four dimensional asymptotically flat schwarzchild black holes.

The quantum gravity in two dimension is also actually tractable. However it turned out that formation of quantum black holes in these theories are highly unlikely [109]. In summary, to have a model of quantum gravity with enough complexity to contain black holes nevertheless tractable, working in three dimensions is most easy and promising way, compared with working on other dimensions.

9.2 Higher spin theory in three dimensions

In this section we see how higher spin theories in three dimensions can be described by Chern Simons actions with gauge group $G \supset \mathrm{SL}(2,\mathbb{R})$.

9.2.1 $\mathrm{SL}(2,\mathbb{R})$ Chern Simons theory and Einstein gravity

First of all, we see that a pair of $\mathrm{SL}(2,\mathbb{R})$ Chern Simons theory is classically equivalent to Einstein gravity with negative cosmological constant ([105, 106]). The action is given by

$$I = S_{cs}[A] - S_{CS}[\bar{A}] \quad S_{cs}[A] = \frac{k}{4\pi}\int \mathrm{tr}\,\left(dA\wedge A + \frac{2}{3}A\wedge A\wedge A\right), \tag{198}$$

the Chern Simons level k is given $k = \frac{l}{4G_N}$ [11]. The equations of motion are nothing but flatness conditions of these Chern Simons conenctions.

$$F = dA + A \wedge A = 0 \quad \bar{F} = d\bar{A} + \bar{A} \wedge \bar{A} = 0. \tag{199}$$

If we introduce new variables ω, e,

$$A = \omega + e, \quad \bar{A} = \omega - e, \tag{200}$$

the equations of motion are rewritten as

$$d\omega + \omega \wedge \omega + e \wedge e = 0 \quad de + e \wedge \omega + \omega \wedge e = 0 \tag{201}$$

If we interpret the new variable e to be the tetrad of the spacetime, and ω to be the spin connection, the second equation is nothing but the torsion free condition of the spin connection. In addition, $d\omega + \omega \wedge \omega$ term appearing in the first equation is the curvature two form of the spacetime. By contracting it by the tetrad we obtain Einstein equation with negative cosmological constant. Hence Three dimensional Einstein gravity is at least classically equivalent to a pair of Chern Simons theory with the non compact gauge group $\mathrm{SL}(2, \mathbb{R})$.

Let us remark how symmetry of both theories are related. Einstein gravity is invariant under general coordinate transformations $x^\mu \to x^\mu + \xi^\mu$, and the Chern Simons theory is invariant under gauge transformations of the connections,

$$A \to A + d\lambda + [A, \lambda] \quad \bar{A} \to \bar{A} + d\bar{\lambda} + [\bar{A}, \bar{\lambda}]. \tag{202}$$

By introducing a set of generators $\{T_a\}$ of $\mathrm{SL}(2, \mathbb{R})$, $A_\mu = A^a_\mu T_a$, $[T_a, T_b] = \epsilon^c_{ab} T_c$, we find the change of the tetrad δe^a_μ via the gauge transformation,

$$\delta e^a_\mu = \partial_\mu(\lambda^a - \bar{\lambda^a}) + \epsilon^a_{bc}(\lambda^b - \bar{\lambda^b})\omega^c_\mu + \epsilon^a_{bc}(\lambda^b + \bar{\lambda^b})e^c_\mu. \tag{203}$$

Therefore if we choose the gauge functions $\lambda^a, \bar{\lambda}^a$ to be

$$\lambda^a = \frac{1}{2} e^a_\mu \, \xi^\mu \qquad \bar{\lambda^a} = -\frac{1}{2} e^a_\mu \, \xi^\mu, \tag{204}$$

we get

$$\delta e^a_\mu = e^a_\mu \partial_\nu \xi_\mu + \xi^\nu \partial_\nu e^a_\mu + \epsilon^a_{bc} e^b_\mu \xi^\mu \omega_\nu. \tag{205}$$

On the other hand the variation of the tetrad in terms of the coordinate transformation is $x^\mu \to \xi^\mu$,

$$\delta e^a_\mu = e^a_\mu \partial_\nu \xi_\mu + \xi^\nu \partial_\nu e^a_\mu \tag{206}$$

hence they are related up to the local Lorentz transformation.

Since we have identified e^a_μ to be the tetrad of the spacetime, one can recover the spacetime metric from the tetrad as

$$g_{\mu\nu} = \mathrm{tr}\ \mathrm{e}_{(\mu}\mathrm{e}_{\nu)}. \tag{207}$$

[11] The Chern Simons level of A and that of $\bar{A}$ need not to be equal. If these are different, the theory is classically equivalent to topologically massive gravity

9.2.2 Chern Simons theory with $G \supset \mathrm{SL}(2,\mathbb{R})$ anh higher spin theories

When the gauge group G of the Chern Simons theory contains $\mathrm{SL}(2,\mathbb{R})$, it is naturally identified as a higher spin theory in three dimension [107]. These higher spin fields are given by a product of tetrads. For example, the spin three field is given by

$$\varphi_{\mu\nu\rho} = \ e_{(\mu}e_{\nu}e_{\rho)} \tag{208}$$

Actually, one can recover the linearized equations of motion pf higher spin fields in anti de Sitter space from the flatness conditions of the Chern Simons connection [98].

9.3 Asymptotically symmetry algebra

In this subsection we derive asymptotically symmetry algebras (below we call them as "ASG" in short) of three dimensional higher spin theories. In particular, we consider $\mathrm{SL}(3,\mathbb{R})$ Chern Simon theory which is the simplest higher spin theory, as we have reviewed. The goal of the section is to see the ASG of the $\mathrm{SL}(3,\mathbb{R})$ Chern Simon theory is so called W_3 algebra which is a generalization of Virasoro algebra. An ASG is the algebra of a set of symmetry transformations which maps a state in the phase space of the theory into an another state in the phase space. In classical theories of gravity such a phase space is defined by specifying certain boundary conditions at the infinity of the spacetime in question.. First we define a phase space of $\mathrm{SL}(3,\mathbb{R})$ Chern Simons theory by specifying appropriate boundary conditions of the Chern Simons connections so that the action is gauge invariant even in the presence of the conformal boundary. We then specify a set of gauge transformations which map an element of the phase space into the another element. We denote our spacetime manifold $\mathcal{M}$, and assume its time slice have topology of a disk D, $\mathcal{M} \sim \mathbb{R}_t \times D$. We use $(\rho, x^{\pm})$ as a coordinate of the spacetime, where the ρ is the radial coordinate, and $x^{\pm}$ are light cone coordinates of the boundary cylinder at $\rho = \infty$.

First we employ a gauge where the radial dependence of connections becomes trivial. To do this we fix the radial components of the connections to be

$$A_\rho = b^{-1}(\rho)db(\rho) \qquad \bar{A}_\rho = b(\rho)db^{-1}(\rho). \tag{209}$$

Then by the flatness conditions of the connections we gauge away the radial dependences of the other components

$$A_{\pm}(\rho, x^{\pm}) = b(\rho)\ a_{\pm}(x^{\pm})\ b(\rho)^{-1}, \qquad \bar{A}_{\pm}(\rho, x^{\pm}) = b(\rho)\ \bar{a}_{+}(x^{\pm})\ b(\rho)^{-1}, \tag{210}$$

the remaining degrees of freedom are connections at the boundary cylinder $a_{\pm}(x^{\pm})$.

Next we impose boundary conditions for the connections so that the Chern Simons action on $\mathcal{M}$ is gauge invariant. If we slightly vary the connections $A_{\pm} \to A_{\pm} + \delta A_{\pm}$ the action is varied by

$$\delta S = \int_{\partial\mathcal{M}} dx^{+} \wedge dx^{-} \mathrm{tr}\ \left(A_{+}\delta A_{-} - A_{-}\delta A_{+}\right). \tag{211}$$

this motivates the boundary condition $A_- = 0$ at the boundary cylinder. We also have a similar boundary condition for the barred connection, namely $\bar{A}_+ = 0$.

Since we are interested in spacetimes with negative cosmological constant, we also would like to impose asymptotic AdS conditions to the connections. To do this, let us introduce a explicit generator of $\mathrm{sl}(3,\mathbb{R})$, namely $\{L_i, W_m\}$ with $i = -1 \cdots 1, m = -2 \cdots 2$. L_i generate a $\mathrm{sl}(2,\mathbb{R})$ subalgebra,

$$[L_i, L_j] = L_{i+j}. \tag{212}$$

and remaining generators transform as spin 2 operators of the $\mathrm{sl}(2,\mathbb{R})$ (principal embedding),

$$[L_i, W_m] = W_{i+m}. \tag{213}$$

For specific generators, see Appendix A. The connections which are corresponding to the global AdS_3 is given by

$$A = \left(e^{\rho} L_1 + \frac{1}{4} e^{-\rho} L_{-1}\right) dx^+ + L_0 \, d\rho, \quad \bar{A} = -\left(e^{\rho} L_{-1} + \frac{1}{4} e^{-\rho} L_1\right) dx^- - L_0 \, d\rho. \tag{214}$$

It is convenient to use $a_\pm$ by choosing $b(\rho) = e^{\rho L_0}$,

$$a = \left(L_1 + \frac{1}{4} L_{-1}\right) dx^+ \qquad \bar{a} = -\left(L_{-1} + \frac{1}{4} L_{-1}\right) dx^-. \tag{215}$$

By using the relation between metric and connection (207) we obtain global AdS_3 metric.

We then propose the following asymptotic AdS boundary conditions for connections.

$$A - A_{\mathrm{AdS}_3}\big|_{\rho=\infty} = O(1) \quad \bar{A} - \bar{A}_{\mathrm{AdS}_3}\big|_{\rho=\infty} = O(1). \tag{216}$$

From the commutation relations of the generators, one can specify the form of the connections which keep the boundary conditions

$$a = \left(L_1 - \frac{2\pi \mathcal{L}(x^+)}{k} L_{-1} - \frac{\pi}{2k} \mathcal{W}(x^+) W_{-2}\right) dx^+ \quad A = e^{\rho L_0} a e^{-\rho L_0} + L_0 d\rho. \tag{217}$$

In summary, we define our phase space $\mathcal{C}$ for connections A as follows

$$\mathcal{C} = \{A |\ A - A_{\mathrm{AdS}_3} = O(1),\ A_- = 0,\ A_\rho = L_0\}. \tag{218}$$

As we have seen the configuration space is spanned by two arbitrary functions $\{\mathcal{L}(x^+), \mathcal{W}(x^+)\}$ we also define a similar configuration space for $\bar{A}$.

Next we would like to find a set of gauge transformations $\delta A = d\Lambda + [A, \Lambda]$ which are closed in $\mathcal{C}$. Two conditions $\{A_- = 0,\ A_\rho = L_0\}$ constrain the $\Lambda(\rho, x^\pm)$ to following form

$$\delta A_\rho = 0 \to \lambda(\rho x^\pm) = e^{\rho L_0} \lambda(x^\pm) e^{-\rho L_0}, \qquad \delta A_- = 0 \to \partial_- \lambda(x^\pm) = 0. \tag{219}$$

To discuss constraints of the gauge function $\lambda(x^+)$ which comes from the asymptotic AdS conditions, let us expand the function by the generators of $\mathrm{SL}(3,\mathbb{R})$

$$\lambda(x^+) = \sum_{i=-1}^{1} \epsilon^i(x^+) L_i + \sum_{m=-2}^{2} \chi^m(x^+) W_m. \tag{220}$$

If we denote ϵ^1 and χ^2 to be ϵ and χ respectively, the other functions are written in terms of ϵ and χ because of the asymptotic AdS conditions.

$$\epsilon^0 = -\epsilon', \quad \epsilon^{-1} = \frac{1}{2}\epsilon'' + \frac{2\pi}{k}\epsilon\mathcal{L} + \frac{4\pi}{k}\chi\mathcal{W}. \tag{221}$$

$$\begin{aligned}
\chi^1 &= -\chi', \\
\chi^0 &= \frac{1}{2}\chi'' + \frac{4\pi}{k}\chi\mathcal{L}, \\
\chi^{-1} &= -\frac{1}{6}\chi''' - \frac{10\pi}{3k}\chi'\mathcal{L} - \frac{4\pi}{3k}\chi\mathcal{L}', \\
\chi^{-2} &= -\frac{1}{24}\chi''' + \frac{4\pi}{3k}\chi''\mathcal{L} + \frac{7\pi}{6k}\chi'\mathcal{L}' + \frac{\pi}{3k}\chi\mathcal{L}'' + \frac{4\pi^2}{k^2}\chi\mathcal{L} - \frac{\pi}{2k}\epsilon\mathcal{W}.
\end{aligned} \tag{222}$$

by the gauge transformation which satisfy the conditions the functions changes as follows

$$\begin{aligned}
\delta_\epsilon\mathcal{L} &= \epsilon + 2\epsilon'\mathcal{L} + \frac{k}{4\pi}\epsilon''', \\
\delta_\epsilon\mathcal{W} &= \epsilon\mathcal{W}' + 3\epsilon'\mathcal{W},
\end{aligned} \tag{223}$$

$$\begin{aligned}
\delta_\chi\mathcal{W} &= 2\chi\mathcal{W}' + 3\chi'\mathcal{W}, \\
\delta_\chi\mathcal{W} &= -\frac{1}{3}\left(2\chi\mathcal{L}''' + 9\chi'\mathcal{L}'' + 10\chi'''\mathcal{L} + \frac{k}{4\pi}\chi^{(5)}\right) \\
&\quad - \frac{64\pi}{3k}\left(\chi\mathcal{L}\mathcal{L}' + \chi'\mathcal{L}^2\right).
\end{aligned} \tag{224}$$

Here we would like to find the algebra of the conserved charges which are associated with these gauge transformations. For a given gauge transformation Λ, associated charge of the Chern Simons theory is

$$G[\Lambda] = \int_{\mathcal{M}} \mathrm{tr}\Lambda F_{ij} dx^i \wedge dx^j + Q[\Lambda], \quad Q[\Lambda] = \int_{\partial\mathcal{M}} \mathrm{tr}\Lambda A_i dx^i. \tag{225}$$

In the presence of boundary, the variation of the first term does not only proportional to δA_μ in the bulk , but also depend on their boundary value. The last term is added so that

the total charge have well defined functional derivative. Due to the second term, the total charge $G[\Lambda]$ does not always vanish. A transformation Λ whose generating charge $G[\Lambda]$ is non vanishing is not a gauge transformation but rather a global transformation. The transformation does changes a state into a physically inequivalent state.

Since the bulk contribution of the charge (224) vanishes on shell $F_{ij} = 0$, The variation of a function F of the Chern Simons connections by a global transformation Λ can be written as

$$\delta_\Lambda F = \{Q[\Lambda], F\} \tag{226}$$

Substituting the change of dynamical variables $(\mathcal{L}, \mathcal{W})$, (224) and the definition of the $Q[\Lambda]$ into the formula, we find the following Poisson structure,

$$\begin{aligned}
\{\mathcal{L}_p, \mathcal{L}_q\} &= (p-q)\mathcal{L}_{p+q} + \frac{c}{12}(p^3 - p)\delta_{p+q,0}, \quad c = 6k \\
\{\mathcal{L}_p, \mathcal{W}_q\} &= (2p-q)\mathcal{W}_{p+q}, \\
\{\mathcal{L}_p, \mathcal{W}_q\} &= \frac{(p-q)}{3}(2p^2 + 2q^2 - pq - 8)\mathcal{L}_{p+q} + \frac{32}{c}(p-q)\Lambda_{p+q} \\
&\quad + \frac{c}{36}p(p^2-1)(p^2-4)\delta_{p+q},
\end{aligned} \tag{227}$$

where $\mathcal{L}_p, \mathcal{W}_p$ denotes Fourier coefficients of $\mathcal{L}(x^+), \mathcal{W}(x^+)$,

$$\mathcal{L}(x^+) = -\frac{1}{2\pi}\sum_{p=-\infty}^{\infty} \tilde{\mathcal{L}}_p e^{ipx^+}, \quad \mathcal{L}_p = \tilde{\mathcal{L}}_p - \frac{k}{4}\delta_{p,0}, \quad \mathcal{W}(x^+) = \frac{1}{2\pi}\sum_{p=-\infty}^{\infty} \mathcal{W}_p e^{ipx^+} \tag{228}$$

and Λ_{p+q} appearing in the last equation in (227) is defined as

$$\Lambda_p = \sum_{q=-\infty}^{\infty} \mathcal{L}_{q+p}\mathcal{L}_q \tag{229}$$

The algebra is known as $\mathcal{W}_3$ algebra, which is a nonlinear generalization of Virasoro algebra, and containing spin three generators $\{\mathcal{W}_m\}$. The same algebra is also realized as the asymptotic symmetry of the barred connections $\bar{A}$.

In conclusion, we find that asymptotic symmetry algebra of the higher spin theory in terms of $\mathrm{SL}(3, \mathbb{R})$ Chern Simons theory.

9.4 Gaberdiel Gopakumar duality

We see that the CFT dual of a higher spin theory in AdS_3 has $\mathcal{W}$ symmetry. Indeed, Gaberdiel and Gopakumar [97] conjectured a precise holographic duality between a higher spin theory and a large N limit of CFT with $\mathcal{W}$ symmetry. Let us briefly see the content of the duality. For details, we refer the review [104].

The bulk theory contains higher spin fields and a scalar field. Gauge group of the theory is the infinite dimensional Lie algebra $hs[\lambda]$, the generators of which are again labeled by $\mathrm{sl}(2,\mathbb{R})$ spin, $\{V_n^s\}, |n| < 2s-1, n = 1, \cdots \infty$. The commutators of the generators depend on the real parameter λ.

The boundary CFT is given by a large N limit of $\mathcal{W}_\mathcal{N}$ minimal model. More precisely, This is given by a WZW model of the coset,

$$\frac{SU(N)_k \times SU(N)_1}{SU(N)_{k+1}} \tag{230}$$

with the large N limit

$$N \to \infty, N \to \infty \quad \lambda = \frac{N}{N+k}; \text{fixed} \tag{231}$$

This CFT turned out to have infinite dimensional symmetry $\mathcal{W}_\infty[\lambda]$. In bulk higher spin side, we also find $\mathcal{W}_\infty[\lambda]$ as the asymptotic symmetry algebra of $hs[\lambda]$ [101]. This can be viewed as a nontrivial evidence of the duality. There are several other evidences in favor of the duality, including matching of three point functions, [102], and perturbative partition function [103].

$hs[\lambda]$, $\mathcal{W}[\lambda]$

9.5 higher spin black holes

So far we see that the asymptotic symmetry algebra of $\mathrm{SL}(3,\mathbb{R})$ Chern Simons theory is a pair of $\mathcal{W}_3$ algebra. This implies that dual CFT_2 states are labeled by both the scaling dimension L_0 and the spin 3 charge W_0. In the presence of the additional charge W_0, one can consider a grand canonical ensemble with the spin 3 chemical potential μ_3, which is the canonical conjugate of the spin 3 charge W_0.

When we consider a partition function $Z(\beta)$ of a usual canonical ensemble of the dual CFT_2, its saddle point which is dominant at high temperature limit $\beta \to 0$ have a natural gravitational interpretation, namely a BTZ black hole. Actually Cardy's formula enumerates the degeneracy of primary operators with sufficiently high scaling dimensions $(L_0, \bar{L_0})$, and its logarithm does match with the entropy of BTZ black hole with $(L_0, \bar{L_0})$.

Hence we anticipate that the saddle point of a grand canonical partition function with spin 3 charge W_0 has a gravity interpretation in terms of a black hole with a nontrivial spin 3 field configuration (higher spin black hole). Following the intuition, in this subsection we construct a black hole solution in $\mathrm{SL}(3,\mathbb{R})$ Chern Simons theory with spin 3 charge.

To begin with, recall that the connections of the form (217) have a natural CFT interpretation, namely states $|\psi\rangle$ with fixed expectation value of spin 2 and 3 currents $\hat{\mathcal{L}}, \hat{\mathcal{W}}$, $\mathcal{L} = \langle\psi|\hat{\mathcal{L}}|\psi\rangle, \mathcal{W} = \langle\psi|\hat{\mathcal{W}}|\psi\rangle$. For example if we take $\mathcal{W} = 0$ and $\mathcal{L} = \bar{\mathcal{L}} > 0$, the connection corresponds to a static BTZ black hole. The associated metric is

$$ds^2 = -\left(e^\rho - \frac{2\pi\mathcal{L}}{k}e^{-\rho}\right)^2 dt^2 + d\rho^2 + \left(e^\rho + \frac{2\pi\mathcal{L}}{k}e^{-\rho}\right)^2 d\theta^2. \tag{232}$$

The horizon of the black hole is located at $\rho = \rho_+$, satisfying

$$e^{\rho_+} = \sqrt{\frac{2\pi\mathcal{L}}{k}}, \tag{233}$$

To construct higher spin black holes which are dual to the saddles of the grand canonical partition functions, we need to perturb the connection by adding a spin 3 chemical potential. To do this let us consider the following ansatz of the connections,

$$\begin{aligned} a &= \left(L_1 - \frac{2\pi\mathcal{L}}{k}L_{-1} - \frac{\pi}{2k}\mathcal{W}W_{-2}\right)dx^+ \\ &\quad + \left(\mu W_2 + w_1 W_1 + w_0 W_0 + w_{-1}W_{-1} + w_{-2}W_2 + lL_{-1}\right)dx^-. \\ \bar{a} &= -\left(L_{-1} - \frac{2\pi\bar{\mathcal{L}}}{k}L_1 - \frac{\pi}{2k}\bar{\mathcal{W}}W_2\right)dx^- \\ &\quad - \left(\bar{\mu}W_{-2} + \bar{w_{-1}}W_{-1} + \bar{w_0}W_0 + \bar{w_1}W_1 + \bar{w_2}W_2 + \bar{l}L_1\right)dx^+. \end{aligned} \tag{234}$$

We assume that all the coefficient of generators depends on both $x^\pm$.

Substituting the ansatz to flatness conditions of the connections, we find,

$$\begin{aligned} l &= \frac{4\pi}{k}\mathcal{W}\mu, \\ w_1 &= -\partial_+\mu, \\ w_0 &= \frac{1}{2}\partial_+^2\mu - \frac{4\pi}{k}\mathcal{L}\mu, \\ w_{-1} &= -\frac{1}{6}\partial_+^3\mu + \frac{4\pi}{3k}\partial_+\mathcal{L}\mu + \frac{10\pi}{3k}\mathcal{L}\partial_+\mu, \\ w_{-2} &= \frac{1}{24}\partial_+^4\mu - \frac{4\pi}{3k}\partial_+^2\mathcal{L} - \frac{7\pi}{6k}\partial_+\mathcal{L}\partial_+\mu - \frac{\pi}{3k}\partial_+^2\mathcal{L}\mu + \frac{4\pi^2}{k^2}\mathcal{L}^2\mu. \end{aligned} \tag{235}$$

Furthermore, there are additional constraints involving $\mathcal{L}, \mathcal{W}$,

$$\partial_-\mathcal{L} = -3\mathcal{W}\partial_+\mu - 2\partial_+\mathcal{W}\mu, \tag{236}$$

$$\partial_-\mathcal{W} = -\frac{k}{12\pi}\partial_+^5\mu + \frac{2}{3}\partial_+^3\mathcal{L}\mu + 3\partial_+^2\mathcal{L}\partial_+\mu + 5\partial_+\mathcal{L}\partial_+^2\mu + \frac{10}{3}\mathcal{L}\partial_+^3\mu - \frac{64\pi}{3k}\mathcal{L}\partial_+\mathcal{L}\mu - \frac{64\pi}{3k}\partial_+\mu. \tag{237}$$

The last two equations have a natural CFT_2 interpretation. Let us begin with the first equation (236). Let $\langle T(z)\rangle_\mu$ be the one point function of the holomorphic part of the stress tensor in the presence of the spin 3 chemical potential μ. If we evaluate it in the linear order in μ, we get,

$$\langle T(z)\rangle_\mu = \langle T(z)\rangle_0 + \int dw^2 \mu(w)\langle T(z)\mathcal{W}(w)\rangle + O(\mu^2), \tag{238}$$

where $\langle T(z)\rangle_0$ denotes the expectation value of the stress tensor in the absence of the chemical potential. In this case the field theory has exact conformal symmetry, ie, $\partial_z\langle T(z)\rangle_0 = 0$.

The integral appearing in (238) can be calculated by considering the OPE for the stress tensor and the spin 3 current $\mathcal{W}(w)$,

$$T(z)\mathcal{W}(w) = \frac{3}{(z-w)^2}\mathcal{W}(0) + \frac{1}{z-w}\partial\mathcal{W}(0) + \cdots. \tag{239}$$

Due to the OPE, $\langle T(z)\rangle_\mu$ have nontrivial $\bar{z}$ dependence. Sustituting the OPE (239) into the integral (238), and taking derivatives of both sides with $\bar{z}$, we get

$$\frac{1}{2\pi}\partial_{\bar{z}}\langle T(z)\rangle_\mu = -3\langle\mathcal{W}(z,\bar{z})\rangle\partial_{\bar{z}}\mu(z,\bar{z}) + 2\partial_z\mathcal{W}(z,\bar{z})\rangle\mu(z,\bar{z}). \tag{240}$$

By using the identification similar to (228) $\langle T\rangle = \frac{1}{2\pi}\mathcal{L}$, we get the (236).

One can make a similar interpretation for (237), by making use of the OPE of spin 3 currents

$$\begin{aligned}\mathcal{W}(z)\mathcal{W}(w) = &-\frac{5k}{\pi^2}\frac{1}{(z-w)^6} + \frac{10}{\pi}\frac{1}{(z-w)^4}\mathcal{L} + \frac{5}{\pi}\frac{1}{(z-w)^3}\partial\mathcal{L} + \frac{3}{2\pi}\frac{1}{(z-w)^2}\partial^2\mathcal{L}\\ &- \frac{1}{3\pi}\frac{1}{z-w}\partial^3\mathcal{L} - \frac{32}{3k}\frac{1}{z-w}\mathcal{L}\partial\mathcal{L} - \frac{32}{3k}\frac{1}{(z-w)^2}\mathcal{L}^2.\end{aligned} \tag{241}$$

In summary we find that a dictionary between μ appearing in the Chern Simons connections and the spin 3 chemical potential in the dual CFT_2. We confirm this by showing the flatness conditions of the Chern Simons connections (234) correctly predicts anti holomorphic part of stress energy tensor in the presence spin 3 chenical potential.

We are interested in the case of constant spin 3 chemical potential. In that case the connections are given by

$$\begin{aligned}a = &\left(L_1 - \frac{2\pi\mathcal{L}}{k}L_{-1} - \frac{\pi}{2k}\mathcal{W}W_{-2}\right)dx^+\\ &+ \mu\left(W_2 - \frac{4\pi\mathcal{L}}{k}W_0 + \frac{4\pi^2\mathcal{L}^2}{k^2}W_{-2} + \frac{4\pi\mathcal{W}}{k}L_{-1}\right)dx^-,\\ \bar{a} = &-\left(L_{-1} - \frac{2\pi\bar{\mathcal{L}}}{k}L_1 - \frac{\pi}{2k}\bar{\mathcal{W}}W_2\right)dx^-\\ &- \bar{\mu}\left(W_{-2} - \frac{4\pi\bar{\mathcal{L}}}{k}W_0 + \frac{4\pi^2\bar{\mathcal{L}}^2}{k^2}W_2 + \frac{4\pi\bar{\mathcal{W}}}{k}L_1\right)dx^+.\end{aligned} \tag{242}$$

Since the connection reduces to the usual BTZ black hole if we set $\mu = 0, \mathcal{W} = 0$, we can identify the solution as a black hole solution with spin 3 charge which describe the saddle point of the dual CFT_2 partition function with spin three chemical potential.

9.6 More general higher spin black holes

Here we briefly mention how to systematically derive higher spin black hole solutions in $\mathrm{sl}(N,\mathbb{R})$ or more generally $hs[\lambda]$ Chern Simons theory. To do this we employ the so called principal embedding of $\mathrm{sl}(2,\mathbb{R})$, where the generators of G constitute some representations of the $\mathrm{sl}(2,\mathbb{R})$ subalgebra. For example generators $\mathrm{sl}(N,\mathbb{R})$ can be divided into $\mathrm{sl}(2,\mathbb{R})$ generators $\{L_i\}$, and remaining generators are labeled by two integers as $\{V^s_m\}$ $s=3,\cdots N, m=-2s+1\cdots 2s-1$ and each generators with fixed s behave as spin $s-1$ states of the subalgebra $\mathrm{sl}(2,\mathbb{R})$.

One can fix the gauge so that only the highest weight of $\mathrm{sl}(2,\mathbb{R})$, L_{-1}, V^s_{-s+1} appears in the holomorphic (or anti holomorphic) part of the connection a (or $\bar{a}$).

$$
\begin{aligned}
a_+ &= L_1 - \frac{2\pi\mathcal{L}}{k}L_{-1} + \sum_{s=3}^{N}\mathcal{W}_s V^s_{-s+1} \\
\bar{a}_- &= -\left(L_{-1} - \frac{2\pi\bar{\mathcal{L}}}{k}L_1 + \sum_{s=3}^{N}\bar{\mathcal{W}}_s V^s_{s-1}\right)
\end{aligned}
\tag{243}
$$

From the analysis of asymptotically symmetry algebras that is similar to the analysis of the previous section, the coefficients in front of the generators V^s_{-s+1} turned out to be spin s charge of dual CFT_2. (We assume appropriate normalizations of the generators)

The remaining parts of the connections (a_- and $\bar{a}_+$) are determined by the flatness conditions. Since the connections are constant, the equations imply that a_+ and a_- are commute (similarly, $\bar{a}_-$ and $\bar{a}_+$ are commute). Hence these part can be written as

$$
a_- = \sum_{s=3}^{N}\mu_s\left(a_+^{s-1} - \frac{1}{N}\mathrm{tr}\ a_+^{s-1}I\right) \quad a_- = \sum_{s=3}^{N}\mu_s\left(\bar{a}_-^{s-1} - \frac{1}{N}\mathrm{tr}\ \bar{a}_-^{s-1}I\right). \tag{244}
$$

Here we add second terms in each connections so that they are traceless (we denote I to be a N $\times$N unit matrix). The coefficients appearing in the connections μ_s turn out to be the spin s chemical potentials. This is proved by OPE analysis as we did in the previous section.

9.7 Thermodynamics of higher spin black holes

9.7.1 The regularity condition of Euclidean higher spin black holes

In this section we would like to explore thermodynamics of higher spin black holes. To do this let us recall the way to derive thermodynamical quantities of usual black holes with event horizons in general relativity in the semi classical limit. First, we make the black hole Euclidean by the analytic continuation, $t \to i\tau$, then identify the Euclidean timelike

direction with period β (inverse temperature). The metric of the Euclidean black hole have a tip at the event horizon. The near horizon metric can be written as

$$ds^2 = a^2\rho^2 dt_E^2 + d\rho^2 \quad \tau \sim \tau + \beta, \tag{245}$$

where ρ in the metric denotes the coordinate of the radial direction, and the horizon is located at $\rho = 0$. a is some constant. The inverse temperature can not be independent with other parameters of the black hole, for example mass of the black hole, ie $M = M(\beta)$. This is because we need to avoid the conical singularity at the tip, or we have a delta functional divergence of Ricci curvature $R \sim \delta(\rho)$ which can not appear in a saddle point configuration. The free energy of the black hole is derived by integrating the temperature dependent mass $M(\beta)$ by β. below we call the prescription as Gibbons Hawking prescription.

However the Gibbons Hawking prescription does not work for higher spin black holes. The reason is that it is not a gauge invariant prescription in a higher spin theory, since gauge transformations of higher spin fields can change a metric non trivially. In general the gauge transformations can change a black metric with an event horizon into a metric *without* event horizons. For instance, the metric of static spin 3 black hole in the highest weight gauge does not have an event horizon.

$$\begin{aligned} ds^2 = d\rho^2 - dt^2 \left[\left(2\mu e^{2\rho} + \frac{\pi}{k}\mathcal{W}e^{-2\rho} - \frac{8\pi^2}{k^2}\mu\mathcal{L}^2 e^{-2\rho} \right)^2 + \left(e^{\rho} - \frac{2\pi}{k}\mathcal{L}e^{-\rho} + \frac{4\pi}{k}\mu\mathcal{W}e^{-\rho} \right)^2 \right] \\ + d\theta^2 \left[\left(e^{\rho} + \frac{2\pi}{k}\mathcal{L}e^{-\rho} + \frac{4\pi}{k}\mu\mathcal{W}e^{-\rho} \right)^2 + \left(2\mu e^{2\rho} + \frac{\pi}{k}\mathcal{W}e^{-2\rho} - \frac{8\pi^2}{k^2}\mu\mathcal{L}^2 e^{-2\rho} \right)^2 + \frac{64\pi^2}{3k^2}\mu^2\mathcal{L}^2 \right]. \end{aligned} \tag{246}$$

One can check $g_{tt}(\rho) > 0$ for generic values of parameters appearing in the metric. However in [110], it was found that the metric of the spin 3 black hole in the highest weight gauge can be mapped to a metric with an event horizon via some gauge transformation. [12]

The break down of the Gibbons Hawking prescription is a generic feature of black holes in higher spin theories, we need to find alternative regularity conditions of Euclidean black holes.

For three dimensional higher spin theory, this is possible by using the holonomy of the Chern Simons connection along the Euclidean timelike cycle. Let us consider a BTZ black hole where the usual Gibbons Hawking prescription is safely applied, and rephrase the regularity condition of the metric by the condition of Chern Simons connection. If the Euclidean black hole is regular at the tip, the holonomy of the connection along the

[12]Here a gauge transformation mean a transformation with vanishing charge.

Euclidean timelike cycle C_T has to be trivial[13] .

$$1 = \exp\left[i\int_{C_T} A\right] = b(\rho)\, e^{\omega}\, b(\rho)^{-1}, \quad \omega = 2\pi(\tau a_+ - \bar{\tau} a_-). \tag{247}$$

$$1 = \exp\left[i\int_{C_T} \bar{A}\right] = b(\rho)^{-1}\, e^{\bar{\omega}}\, b(\rho) \quad \bar{\omega} = 2\pi(\tau \bar{a_+} - \bar{\tau} \bar{a_-}). \tag{248}$$

$$\tag{249}$$

In the expression we introduced the moduli parameter τ of the boundary torus. In static black holes this is related to the inverse temperature β as $\tau = \frac{i\beta}{2\pi}$, but it can have a real part in general, when the black hole is stationary $\mathcal{L} \neq \bar{\mathcal{L}}$. The regularity condition tell us following relations,

$$\tau = \frac{ik}{2}\frac{1}{\sqrt{2\pi k\mathcal{L}}}, \quad \bar{\tau} = \frac{ik}{2}\frac{1}{\sqrt{2\pi k\mathcal{L}}} \tag{250}$$

One can check the conditions (247) (248) are indeed satisfied by Euclidean BTZ black holes, the metric of which satisfy the regularity condition. Actually by substituting the temperature of the black holes derived by the metric regularity condition into their connections, and using the basis of the generators in Appendix A we have

$$\omega_{BTZ} = \begin{pmatrix} 2\pi i & 0 & 0 \\ 0 & -2\pi i & 0 \\ 0 & 0 & 0 \end{pmatrix} \quad \bar{\omega}_{BTZ} = \begin{pmatrix} 2\pi i & 0 & 0 \\ 0 & -2\pi i & 0 \\ 0 & 0 & 0 \end{pmatrix}, \tag{251}$$

hence the holonomies are trivial.

Next we would like to consider the partition function of the black hole. Since logarithm of the partition function $\log Z(\tau)$ and stress tensor $\mathcal{L}(\tau), \bar{\mathcal{L}}(\tau)$ is related by

$$\mathcal{L} = \frac{-i}{4\pi^2}\frac{\partial}{\partial\tau}\log Z, \quad \bar{\mathcal{L}} = \frac{i}{4\pi^2}\frac{\partial}{\partial\bar{\tau}}\log Z. \tag{252}$$

By integrating these relation, we have,

$$\log Z_{BTZ} = \frac{i\pi k}{2\tau} - \frac{i\pi k}{2\bar{\tau}} \tag{253}$$

Entropy of the black hole is derived by the Legendre transformation of it.

$$S_{BTZ} = -4\pi^2 i\left(\tau\mathcal{L} + \bar{\tau}\bar{\mathcal{L}}\right) + \log Z = \frac{i\pi k}{\tau} - \frac{i\pi k}{\bar{\tau}} \tag{254}$$

One can check that the entropy actually coincide with the Bekenstein Hawking entropy . Hence the entropy can be microscopically derived by using Cardy's formula, which counts the number of primary operators with sufficiently high scaling dimensions $(L_0, \bar{L_0})$.

[13]More generally, the holonomy has to be a center of the complexified gauge group.

9.7.2 Thermodynamics of higher spin black holes

In the previous section, we argued that thermodynamics of BTZ black holes in the Chern Simons theory point of view. The argument was divided by two parts. First we discussed a way to impose the regularity condition to the Chern Simons connections of the black holes in terms of the holonomy of the Euclidean time like cycle. Form the condition one could find the relation between stress tensor of the black holes $\mathcal{L}, \bar{\mathcal{L}}$ and the modular parameter of the boundary torus (temperature). In the second part of the argument we derived the entropy or partition function of the black holes by integrating the first law of thermodynamics.

In this section we would like to apply the argument for spin 3 black holes (242). First we need to impose regularity conditions. For this purpose, we *assume* that the regularity condition of higher spin black holes is same as that of BTZ black holes. Namely, we demand that the holonomies of higher spin black holes for Euclidean time like cycle $\omega_{HS}, \bar{\omega}_{HS}$ satisfy

$$\omega_{HS} = \omega_{BTZ} \quad \bar{\omega}_{HS} = \bar{\omega}_{BTZ} \tag{255}$$

One can check the validity of the prescription from various point of view. Here we summarize the evidences of it.

- At the linearized level of spin 3 chemical potential, one can check that the condition is equivalent to the regularity condition of the metric $g_{\mu\nu}$ and spin 3 field $\phi_{\mu\nu\rho}$ [108]
- As we will see, the spin 2 $\mathcal{L}$ and spin 3 $\mathcal{W}$ charge derived from the condition satisfy the integrability conditions, hence we can derive the partition function consistently. For certain gauge group $hs[\lambda]$ one can reproduce the derived partition function from the dual CFT_2 computation[115, 116].

The holonomy conditions (255) in $\mathrm{sl}(3,\mathbb{R})$ are equivalent to the following equations.

$$8\pi^2 + \mathrm{tr}\ \omega_{HS}^2 = 0, \qquad \det \omega_{HS} = 0 \tag{256}$$
$$8\pi^2 + \mathrm{tr}\ \bar{\omega}_{HS}^2 = 0, \qquad \det \bar{\omega}_{HS} = 0 \tag{257}$$

These equaitons can be solved order by order in μ expansion. For the latter convenience we instead use $\alpha = \bar{\tau}\mu$ as the expansion parameter. Then the resulting charges $\mathcal{L}(\tau,\alpha), \mathcal{W}(\tau,\alpha)$

$$\mathcal{L}(\tau,\alpha) = -\frac{k}{8\pi\tau^2} + \frac{5k\alpha^2}{6\pi\tau^6} - \frac{20k\alpha^4}{3\pi\tau^{10}} + \frac{1768k\alpha^6}{27\pi\tau^{14}} - \frac{57664k\alpha^8}{81\pi\tau^{18}}\cdots \tag{258}$$
$$\mathcal{W}(\tau,\alpha) = -\frac{k\alpha}{3\pi\tau^5} + \frac{80k\alpha^3}{27\pi\tau^9} - \frac{272k\alpha^5}{9\partial i\tau^{13}} + \frac{27136k\alpha^7}{81\pi\tau^{17}} - \frac{954880k\alpha^9}{243\pi\tau^{21}}\cdots . \tag{259}$$

As we have advertised, he resulting charges satisfy the integrability condition

$$\frac{\partial\mathcal{L}}{\partial\alpha} = \frac{\partial\mathcal{W}}{\partial\tau} \tag{260}$$

Hence there exists the partition function of the black hole consistently. The logarithm of the partition function of the spin 3 black hole is related to charges via first law of thermodynamics,

$$\mathcal{L} = -\frac{i}{4\pi^2}\frac{\partial \log Z}{\partial \tau} \quad \mathcal{W} = -\frac{i}{4\pi^2}\frac{\partial \log Z}{\partial \alpha} \tag{261}$$

therefore the holomorphic part of the partition funciton is given by

$$\log Z_{hol}(\tau,\alpha) = \frac{ik\pi}{2\tau} - \frac{2ik\pi\alpha^2}{3\tau^5} + \frac{80ik\pi\alpha^4}{27\tau^9} - \frac{544ik\pi\alpha^6}{27\tau^{13}}\frac{13568ik\pi\alpha^8}{81\tau^{17}} + \cdots \tag{262}$$

One can obtain the anti holomorphic part of the partition function by integrating the first law.

Finally the entropy of the black hole is obtained by taking the Legendre transformation of the logarithm of the partition function. It's holomorphic part is

$$S_{hol} = \frac{ik\pi}{\tau} - \frac{4ik\pi\alpha^2}{\tau^5} + \frac{800ik\pi\alpha^4}{27\tau^9} - \frac{7616ik\pi\alpha^6}{27\tau^{13}} + \frac{27136ik\pi\alpha^8}{9\tau^{17}}\cdots \tag{263}$$

In this way, we derive the entropy of the higher spin black holes. One can compare the entropy of higher spin black holes in $hs[\lambda]$ and the dual CFT entropy, finding nice agreement.

10 An entropy formula for higher spin black holes via conical singularity

In previous section we introduced higher spin black holes in three dimensional higher spin theory. We then discussed thermodynamics of the black holes. This is achieved by demanding the holonomy condition of the black hole connections, which is the natural generalization of Gibbons-Hawking regularity condition. By integrating first law of thermodynamics we derived entropy of higher spin black holes.

One may complain the procedure to derive the black hole entropy is quite indirect. It would be nice if there is a kind of Wald formula, which directly computes entropy of higher spin black holes from their connections. In thenext section we derive the entropy formula by using conical singularity approach which was developed by Fursaev and Solodukhin[FS]. The resulting entropy formula turned out to satisfy the correct first law of thermodynamics.

10.1 Review of the derivation of the Wald formula via conical singularity

In this section, we review the derivation of the Wald formula by evaluating the gravitational action of a conical singularity. In subsection 10.1.1, we evaluate the Einstein-Hilbert action of a conical singularity in two dimensions by taking the limit of a regularized metric. Since a Euclidean black hole with deficit angle on the bifurcation surface looks like a direct product of a two dimensional cone and the bifurcation surface near the tip, we can use the result of 10.1.1 to evaluate the action of the singular black hole. We then discuss its relation to the Wald formula in subsection 10.1.2.

10.1.1 Evaluation of the action of a conical singularity in 2 dimension

In this section, we review the evaluation of the Einstein-Hilbert action of a metric with a conical singularity on a two dimensional manifold [119, 120, 121, 122]. As an example, consider the metric:

$$ds^2 = e^{\Phi(r)}(dr^2 + r^2 d\theta^2). \tag{264}$$

Let us assume $\theta \sim \theta + 2\pi\alpha,\ \alpha \neq 1$. The metric has a conical singularity at the tip when the period of the θ direction is not 2π. It is convenient to embed the cone into $\mathbb{R}^3$ by the map:

$$x = r\alpha \sin\frac{\theta}{\alpha} \qquad y = r\alpha\cos\frac{\theta}{\alpha} \qquad z = \sqrt{1-\alpha^2}r, \tag{265}$$

so the cone is mapped to the surface

$$\frac{1-\alpha^2}{\alpha^2}(x^2+y^2) - z^2 = 0 \tag{266}$$

with metric $ds^2 = e^{\Phi(r)}(dx^2 + dy^2 + dz^2)$, the pull back of which gives the metric (264) on the 2d plane. In this form, the singularity is manifest because $\frac{\partial z}{\partial x}, \frac{\partial z}{\partial y}$ are indeterminate at the tip of the cone $z = 0$.

Since the metric (264) has a conical singularity, the curvature of the metric contains a delta functional divergence at the tip in addition to the ordinary regular part, $R \sim R_{reg} + (1-\alpha)\delta(r)$. The coefficient in front of the delta function is attached so that for a regular $\alpha = 1$ metric, only R_{reg} appears in R.

To see this, we would like to evaluate the contribution of the singularity to the Einstein Hilbert action $\int \sqrt{g}R$. Two steps are needed. First we construct a family of smooth metrics $g_{\mu\nu}(a)$, each labeled by a real positive number a, and demand that they approach to the original singular one in the limit $a \to 0$. We call the family the "regularization" of the singular metric. One way to construct a regularization is by modifying the surface (265) by a function $f(r, a)$ as

$$z = \sqrt{1-\alpha^2} f(r, a), \qquad \partial_r f(r, a)|_{r=0} = 0, \qquad \lim_{r\to\infty} f(r, a) \to r, \tag{267}$$

with the ambient metric $ds^2 = e^{\Phi(r)}(dx^2+dy^2+dz^2)$ held fixed. We also assume $f(r, 0) = r$. For example, if we take

$$z = \sqrt{a^2 + \frac{1-\alpha^2}{\alpha^2} r^2}, \tag{268}$$

then the surface is replaced by a smooth hyperboloid when $a \neq 0$. For general $f(r, a)$, the pull back of the metric on the 2D plane is modified as

$$ds^2 = e^{\Phi(r)}(u(r)dr^2 + r^2 d\theta^2) \qquad u(r) = \alpha^2 + (1-\alpha^2)(\partial_r f(r, a))^2. \tag{269}$$

We can see these metrics are regular at the tip $r = 0$. Second, we evaluate the Einstein Hilbert actions $I(a)$ of the regularized metrics for general non zero a. Since these metrics are regular, we can safely evaluate $I(a)$,

$$\begin{aligned} I(a) &= 2\pi\alpha \int_0^\infty dr \frac{u'(r)}{u^{\frac{3}{2}}} - \int_0^\infty dr \int_0^{2\pi\alpha} r d\theta \sqrt{u(r)} \Delta\Phi(r) \\ &= 4\pi(1-\alpha) - \int_0^\infty dr \int_0^{2\pi\alpha} r d\theta \sqrt{u(r)} \Delta\Phi(r), \end{aligned} \tag{270}$$

where Δ is the Laplacian of the metric without conformal factor (depending on $u(r)$). The $a \to 0$ limit correspond to the action of the original metric with a conical singularity.

$$\lim_{a\to 0} I(a) = 4\pi(1-\alpha) - \int_0^\infty dr \int_0^{2\pi\alpha} r d\theta \Delta\Phi(r). \tag{271}$$

Since the second term of the expression can be derived by directly substituting the metric (264) into the action, it describes the contribution from the regular part of the curvature

to the action. However, there is an additional term. The first term in (271) is interpreted as the contribution of the conical singularity at the tip, because it vanishes when $\alpha = 1$. The result show that the scalar curvature of the metric (264) is given by

$$\sqrt{g}R = \sqrt{g}R_{reg} + \frac{2(1-\alpha)}{\alpha}\delta(r), \tag{272}$$

as we expected. It is important to note that the contribution of the singularity to the action does not depend on the regularization function $f(r, a)$ we use. This assures us that the value $4\pi(1-\alpha)$ is intrinsic to the conical singularity.

10.1.2 Relation to black hole entropy

We can generalize the result to higher dimensions if the manifold we consider is the direct product of a 2 dimensional cone $C_\alpha = S^1_\alpha \times \mathbb{R}$ and a smooth manifold Σ. In the case of the metric of the form

$$ds^2 = e^{\Phi(r)}(r^2 d\theta^2 + dr^2) + ds^2_\Sigma, \tag{273}$$

we are assuming $\theta \sim \theta + 2\pi\alpha,\ \alpha \neq 1$. Demanding that the volume of the $S^1_\alpha \times \Sigma$ located at $r = r_0$ is held fixed, the general regularization of the metric can be written

$$ds^2 = e^{\Phi(r)}(r^2 d\theta^2 + u(r)dr^2) + ds^2_\Sigma, \quad u(0) = \alpha^2, \quad u(\infty) = 1 \tag{274}$$

Note that only g_{rr} is allowed to change. This turn out to be the correct regularization and from this one can compute various geometric invariants in the presence of the conical deficit. The results turn out to be equivalent to the statement that the Riemann tensor contains a delta functional singularity on Σ,

$$R^{\mu\nu}_{\alpha\beta} = (R_{reg})^{\mu\nu}_{\alpha\beta} + 2\pi(1-\alpha)(n^\mu_\alpha n^\nu_\beta - n^\mu_\beta n^\nu_\alpha)\delta_\Sigma, \tag{275}$$

where δ_Σ is delta function on Σ which satisfie

$$\int_{C_\alpha \times \Sigma} \delta_\Sigma \sqrt{g} = \int_\Sigma \sqrt{h}, \tag{276}$$

and $n^\mu_\alpha = n^\mu_1 n_{\alpha 1} + n^\mu_2 n_{\alpha 2}$, where n_1, n_2 denotes the vector fields normal to Σ .

Euclidean black holes with temperature different from the Hawking temperature are examples of these geometries. In this case Σ is the bifurcation surface of the black hole.

Suppose $Z(\beta)$ is the quantum gravity partition function with fixed temperature β, evaluated semiclassically as

$$Z(\beta) = \int [Dg] e^{-I^E[\beta, g]} \simeq e^{-I^E_c[\beta, g_c(\beta)]} \qquad \frac{\delta I^E[\beta, g]}{\delta g}\Big|_{g=g_c(\beta)} = 0, \tag{277}$$

where I^E denotes the Euclidean action. Then the entropy $S(\beta)$ of the system is given by

$$S(\beta) = \left(\beta\frac{\partial}{\partial\beta} - 1\right) I^E[\beta, g_c(\beta)]. \tag{278}$$

Note that semiclassical metric depends on β because of regularity.

There is an alternative way of computing $S(\beta)$,

$$S(\beta) = \left(\alpha\frac{\partial}{\partial\alpha} - 1\right)\Big|_{\alpha=1} I_c^E[\alpha\beta, g_c(\beta)]. \tag{279}$$

This expression instructs to first evaluate the Euclidean action for the fixed metric $g_c(\beta)$ but with varying time periodicity $\alpha\beta$. Such geometries with $\alpha \neq 1$ have conical singularities, and their action can be calculated by the method reviewed in the previous section. By substituting (275) into (279) one immediately obtains the Wald formula [121, 122].

$$S = 4\pi \int_\Sigma \sqrt{h}\frac{\partial\mathcal{L}}{\partial R_{\mu\nu\alpha\beta}} n_{\mu\alpha} n_{\nu\beta}. \tag{280}$$

Note that if we divide the action into the regular part and the singular part, $I_c^E[\alpha, g_c(\beta)] = I_{reg}^E + I_{sing}^E$, the former does not contribute to the entropy,

$$\left(\alpha\frac{\partial}{\partial\alpha} - 1\right) I_{reg}^E = 0, \tag{281}$$

because I_{reg}^E is proportional α as we saw in (271).

10.2 Entropy of black holes via conical singularities in the Chern-Simons formulation

In this section we adapt the discussion of the previous section to the Chern-Simons formulation. We focus on BTZ black holes for our explicit computations, but then propose that the resulting entropy formula holds in general. The validity of this proposal will be confirmed in the next section.

10.2.1 Entropy of the BTZ black hole

It is well known that 3d Einstein gravity with negative cosmological constant can be formulated in terms of Chern Simons theory with the gauge group $SL(2,R) \times SL(2,R)$,

$$I[A, \bar{A}] = I_{CS}[A] - I_{CS}[\bar{A}], \tag{282}$$

$$I_{CS}[A] = \frac{k}{4\pi}\int \mathrm{Tr}\left(A \wedge dA + \frac{2}{3} A \wedge A \wedge A\right), \tag{283}$$

with $k = 1/4G$. For definiteness, in this section we consider the 2×2 matrix representation for SL(2,R) (although the final formulas will not end up depending on that choice) with generators obeying

$$[L_i, L_j] = (i-j)L_{i+j} \ , \quad \mathrm{Tr}(\mathrm{L_1 L_{-1}}) = -1 \ , \quad \mathrm{Tr}(\mathrm{L_0 L_0}) = \frac{1}{2} \ . \tag{284}$$

The connections are related to the vielbein e and spin connection ω as

$$A = \omega + e, \qquad \bar{A} = \omega - e, \tag{285}$$

and the metric is given by

$$g_{\mu\nu} = 2\mathrm{Tr}[\mathrm{e}_\mu \mathrm{e}_\nu]. \tag{286}$$

The connections for the nonrotating BTZ black hole can be taken as

$$A = e^{\rho_+} \left(e^r L_1 - e^{-r} L_{-1} \right) dx^+ + L_0 dr \tag{287}$$

$$\bar{A} = -e^{\rho_+} \left(e^r L_{-1} - e^{-r} L_1 \right) dx^- - L_0 dr, \tag{288}$$

where the horizon is at $r = 0$ and $e^{\rho_+} = \sqrt{\frac{2\pi\mathcal{L}}{k}}$, where $\mathcal{L}$ is proportional to the mass.

The metric of the black hole is

$$ds^2 = 4e^{2\rho_+} \left(-\sinh r^2 dt^2 + \cosh r^2 d\theta^2 \right) + dr^2. \tag{289}$$

The value of the entropy of the black hole is obtained by the Bekenstein-Hawking formula

$$S = \frac{A}{4G} = \frac{4k\pi^2}{\beta}, \tag{290}$$

where β is the inverse Hawking temperature $\beta = \pi e^{-\rho_+}$.

We now show how to derive this by the conical singularity method. If we keep the connections fixed but identify the time coordinate as $t \cong t + i\alpha\beta$ then we introduce a conical singularity in the metric for $\alpha \neq 1$. This can be seen at the level of the connections by evaluating the holonomies around the imaginary time circle,

$$e^{\oint A} = \begin{pmatrix} \cos\pi\alpha & -ie^{-r}\sin\pi\alpha \\ -ie^{r}\sin\pi\alpha & \cos\pi\alpha \end{pmatrix} \ , \tag{291}$$

$$e^{\oint \bar{A}} = \begin{pmatrix} \cos\pi\alpha & -ie^{r}\sin\pi\alpha \\ -ie^{-r}\sin\pi\alpha & \cos\pi\alpha \end{pmatrix} \ . \tag{292}$$

For a nonsingular metric we need the holonomies to be in the center of SL(2,R), which requires α to be an integer.

Now we would like to evaluate $I_{CS}[A]$ for this connection. We proceed by regularizing the connection, evaluating its action, and then removing the regulator.

It is convenient to use a rescaled Euclidean time coordinate T, $t = i\alpha\beta T$, so that the coordinate periodicity is fixed as $T \cong T + 1$. In this coordinate the singular connection is written

$$A = i\alpha\beta A_t dT + A_\theta d\theta + L_0 d\rho \qquad \bar{A} = i\alpha\beta \bar{A}_t dT + \bar{A}_\theta d\theta - L_0 d\rho, \tag{293}$$

and the corresponding singular metric is

$$g_{TT}(S) = -\frac{1}{2}(\alpha\beta)^2 \mathrm{Tr}\left(A_t - \bar{A}_t\right)^2 \tag{294}$$

$$g_{\theta\theta}(S) = \frac{1}{2}\mathrm{Tr}\left(A_\theta - \bar{A}_\theta\right)^2. \tag{295}$$

There are various way to regularize the connection. For example, consider

$$\begin{aligned}\tilde{A} &= \frac{A_t}{u(r)}\left(i\beta\alpha dT - c d\theta\right) + \left(cA_t + A_\theta\right) d\theta + L_0 d\rho \\ \tilde{\bar{A}} &= \frac{\bar{A}_t}{u(r)}\left(i\beta\alpha dT + c d\theta\right) + \left(-c\bar{A}_t + \bar{A}_\theta\right) d\theta - L_0 d\rho,\end{aligned} \tag{296}$$

where c is some constant. The connections (296) are regular provided $u(0) = \alpha$. We also demand $u(\infty) = 1$ so that we go back to the original one at the boundary. A_ρ and $\bar{A}_\rho$ are unchanged because we are working on the gauge where $A_\rho = L_0, \bar{A}_\rho = -L_0$.

Below we fix the value of c that appears in the connections so that the regularization is consistent with the regularization of the metric (274). The metric components $g_{TT}(R)$ and $g_{\theta\theta}(R)$ of these regularized connection near the tip $r \sim 0$ look like

$$g_{TT}(R) = -\frac{1}{2}\beta^2 \mathrm{Tr}\left(A_t - \bar{A}_t\right)^2 \tag{297}$$

$$g_{\theta\theta}(R) = \frac{1}{2}\mathrm{Tr}\left[c\left(A_t + \bar{A}_t\right)\left(1 - \frac{1}{\alpha}\right) + \left(A_\theta - \bar{A}_\theta\right)\right]^2. \tag{298}$$

From these expressions one notices how the metric components change by the regularization. In particular, in the BTZ case,

$$\delta g_{TT} = g_{TT}(R) - g_{TT}(S) = 2(1-\alpha) g_{TT}(S), \qquad \delta g_{\theta\theta} = -2c(1-\alpha) g_{\theta\theta}(S). \tag{299}$$

We used the property of the BTZ connection at $r = 0$, namely, $A_t + \bar{A}_t = A_\theta - \bar{A}_\theta$. As in the metric case (274), we demand that the volume of the torus located at $r = r_0, r_0 << 1$ be held fixed. In this case, c appearing in the regularization (296) has to be 1.

Now that we have specified the regularization, we can compute the action $I_{CS}[A]$ of the singular configuration via regularization. As we are only interested in terms which are proportional to $(1-\alpha)$, we only have to calculate the $\int \mathrm{Tr} A \wedge dA$ term, since the A^3 term

is proportional to α and vanishes in (279)

$$\begin{aligned}\frac{k}{4\pi}\int \mathrm{Tr}A\wedge dA &= \frac{k}{4\pi}\int \mathrm{Tr}\left[(A_t+A_\theta)A_t\right]\wedge\left(-\frac{u'(r)}{u(r)^2}dr\right)\wedge i\alpha\beta dT\wedge d\theta + I_{reg}\\ &= -\frac{ik\beta}{2}(1-\alpha)\mathrm{Tr}\left[(A_t+A_\theta)A_t\right]+I_{reg},\end{aligned} \tag{300}$$

where I_{reg} denotes the terms which are proportional to α. Similarly,

$$\frac{k}{4\pi}\int \mathrm{Tr}\bar{A}\wedge d\bar{A} = -\frac{ik\beta}{2}(1-\alpha)\mathrm{Tr}\left[(-\bar{A}_t+\bar{A}_\theta)\bar{A}_t\right]+\bar{I}_{reg}. \tag{301}$$

Since the Euclidean action is related to the Chern Simons actions via $iI_E = I_{CS}[A]-I_{CS}[\bar{A}]$, we derive the expression for the entropy of the BTZ black hole by using (279),

$$\begin{aligned}S &= \frac{k\beta}{2}\mathrm{Tr}\left[(A_t+A_\theta)A_t\right]+\frac{k\beta}{2}\mathrm{Tr}\left[(\bar{A}_t-\bar{A}_\theta)\bar{A}_t\right]\\ &= \frac{4k\pi^2}{\beta}.\end{aligned} \tag{302}$$

The result reproduces the Bekenstein Hawking formula (290).

This result can be generalized to the rotating BTZ black hole. In this case we have both an inverse temperature β and the angular velocity of the horizon Ω. These can be combined to form $\tau = \frac{i\beta}{2\pi}(1+\Omega)$ and $\overline{\tau} = -\frac{i\beta}{2\pi}(1-\Omega)$. For the Euclidean black hole, τ plays the role of the modular parameter of the boundary torus. Repeating the above analysis for this case we find the result (see Appendix B)

$$S = -2\pi ik\mathrm{Tr}\left[A_+\left(\tau A_+ - \bar{\tau}A_-\right)\right] - 2\pi ik\mathrm{Tr}\left[\bar{A}_-\left(\tau\bar{A}_+ - \bar{\tau}\bar{A}_-\right)\right], \tag{303}$$

which indeed yields the correct entropy of the rotating BTZ black hole.

Although this result was derived for the BTZ black hole, since the formula does not make any specific reference to this solution we propose that it holds more generally. It is not obvious that this is a correct assumption. In particular, in the above argument we didn't consider all possible regularizations of the singular connection, and the argument for setting the constant $c = 1$ is not entirely compelling. Furthermore, the connection representing BTZ is not of the most general form. Fortunately, we can check that the result is correct by verifying that it obeys the correct first law variation. We carry this out in the next section.

10.3 Derivation from the first law

In the preceding section we have motivated a simple expression for the entropy of a higher spin black hole. In this section we wish to verify that the result is indeed correct, and can be

applied to general higher spin black holes. Our main tool is the first law of thermodynamics: in the thermodynamic limit the entropy is defined to be the object whose variation satisfies the first law, and so if we can establish this property then we are done.

To keep the discussion as general as possible, we consider a theory with an infinite tower of higher spin charges, $(W_2, W_3, \ldots)$, where W_s denotes a spin-s charge. Here we focus on just the "holomorphic" or "leftmoving" charges, but everything we say has an obvious parallel on the anti-holomorphic or rightmoving side. Each conserved charge has a corresponding conjugate potential, and we denote these as $(\alpha_2, \alpha_3, \ldots)$. We will interchangeably use a different notation for the spin-2 versions: $W_2 \leftrightarrow \mathcal{L}$ and $\alpha_2 \leftrightarrow \tau$, which are identified as the holomorphic stress tensor and modular parameter.

Following [108] we think in terms of an underlying partition function of the form

$$Z = \mathrm{Tr}\left[e^{4\pi^2 i \sum_{s=2}^{\infty} \alpha_s W_s}\right] . \tag{304}$$

The right hand side has a precise meaning on the CFT side of the AdS/CFT correspondence, but here is just being used as a mnemonic for motivating the form of the first law. Namely, we have

$$\delta S = -4\pi^2 i \sum_{s=2}^{\infty} \alpha_s \delta W_s \ . \tag{305}$$

Next, let us recall the general rules for constructing higher spin black holes, and identifying their charges and potentials. We work in the context of hs[λ]$\times$ hs[λ] Chern-Simons theory, and recall that upon setting $\lambda = \pm N$ this theory reduces to SL(N,R)$\times$SL(N,R) Chern-Simons theory. In fact, it will become clear that our derivation will apply to any Lie algebra with an SL(2,R) subalgebra, which includes hs[λ] as a special case.

The Lie algebra hs[λ] has generators V_m^s, with $s = 2, 3, \ldots$ and $m = -(s-1), \ldots s-1$. An SL(2,R) subalgebra is furnished by $V^2_{\pm 1,0}$. The trace operation obeys

$$\mathrm{Tr}(V_m^s V_n^t) \propto \delta_{s,t}\delta_{m,-n} \tag{306}$$

and in particular we write

$$\mathrm{Tr}(V^s_{s-1} V^s_{-(s-1)}) = t_s \ . \tag{307}$$

Another useful fact is that $V_1^2 V^s_{s-1} = V^s_{s-1} V_1^2 = V_s^{s+1}$.

As is standard we write the connection as

$$A = b^{-1}ab + b^{-1}db \ , \quad b = e^{\rho V_0^2} \tag{308}$$

with

$$a = a_z dz + a_{\bar{z}} d\bar{z} \ . \tag{309}$$

Note that we are working in Euclidean signature. The component a_z is taken to be in highest weight gauge [98]

$$a_z = V_1^2 + \sum_{s=2}^{\infty} c_s W_s V_{-(s-1)}^s \ . \tag{310}$$

The constants c_s are fixed by demanding that the charges W_s obey the algebra of $\mathrm{W}_\infty[\lambda]$. In particular, c_2 is fixed to be

$$c_2 = \frac{2\pi}{t_2 k} \ . \tag{311}$$

Next we need to specify $a_{\overline{z}}$. To define a flat connection it has to commute with a_z, which can be satisfied by taking $a_{\overline{z}}$ to depend on powers of a_z,

$$a_{\overline{z}} = \sum_{s=2}^{\infty} f_{s+1}(a_z)^s \Big|_{\text{traceless}} \tag{312}$$

where f_s are coefficients. The $s = 1$ term is absent, since it can be removed by redefining the coordinates $(z, \overline{z})$. Noting the property $(V_1^2)^s = V_s^{s+1}$ we can write

$$a_{\overline{z}} = \sum_{s=2}^{\infty} f_{s+1}(V_s^{s+1} + \ldots) \tag{313}$$

where $\ldots$ denote generators with small value of the lower mode index. Restoring the ρ dependence, the leading terms displayed above give the leading large ρ behavior.

The coefficients f_s are fixed by the holonomy conditions. The Euclidean black hole has coordinates identified as $(z, \overline{z}) \cong (z + 2\pi, \overline{z} + 2\pi) \cong (z + 2\pi\tau, \overline{z} + 2\pi\overline{\tau})$. Assuming constant a, the holonomy around the τ cycle is

$$H = e^{\omega} \ , \quad \omega = 2\pi(\tau a_z + \overline{\tau} a_{\overline{z}}) \ . \tag{314}$$

A smooth solution is obtained provided H lies in the center of the gauge group, which requires that ω has certain fixed eigenvalues. We can impose these conditions by requiring the $\mathrm{Tr}(\omega^n)$, $n = 2, 3, \ldots$, take fixed values; for instance, for black holes smoothly connected to BTZ, we demand that these traces coincide with their BTZ values. These equations are in one-to-one correspondence to the free parameters f_s, and can be used to fix their values.

The constants f_s are proportional to the potentials α_s appearing in the first law. This was originally shown by a Ward identity analysis [108]. As will become clear momentarily, the relation is

$$f_s = -\frac{2\pi}{k c_s t_s} \frac{\alpha_s}{\overline{\tau}} \tag{315}$$

so that we have

$$a_{\overline{z}} = -\frac{2\pi}{k}\sum_{s=2}^{\infty}\frac{\alpha_s}{c_s t_s \overline{\tau}}(V_s^{s+1} + \ldots) \ . \tag{316}$$

The holonomy relations can now be used to express the potentials α_s in terms of the charges W_s, or vice versa.

Written in terms of the holonomy, the candidate entropy formula is

$$S = -ik\mathrm{Tr}(a_z\omega) \tag{317}$$

together with its anti-holomorphic partner. We now verify that this obeys the correct first law of thermodynamics. We have

$$\delta S = -ik\mathrm{Tr}(\delta a_z\omega) - ik\mathrm{Tr}(a_z\delta\omega) \ . \tag{318}$$

However, it is easy to see that the second contribution vanishes. The condition that the traces of ω take fixed values implies that $\delta\omega = [\omega, X]$ for some X. Using this, along with $[a_z, \omega] = 0$, which follows from the fact that ω is built out of powers of a_z, we readily verify $\mathrm{Tr}(a_z\delta\omega) = 0$. The variation of a_z is

$$\delta a_z = \sum_{s=2}^{\infty} c_s \delta W_s V^s_{-(s-1)} \ . \tag{319}$$

Inserting this and taking the trace yields

$$\delta S = -4\pi^2 i\sum_{s=2}^{\infty}\alpha_s\delta W_s \ . \tag{320}$$

as desired.

Without doing any computations, we can establish that our entropy formula will agree with the results obtained in [108, 111, 112, 113, 115]. This is because those computations were based on solving the holonomy conditions and then integrating the first law variation. Here we have shown that if the holonomy conditions are imposed then our entropy formula obeys the correct first law variation. Therefore, it must agree with previous results.

Let us make some further comments. In the original work [108] it appeared somewhat miraculous that that the first law variation could be consistently integrated; this required verifying the integrability constraints, which turned out to follow rather non-transparently from the holonomy condition. Our discussion here removes the mystery surrounding this procedure. In particular in (318) we see very explicitly that if the holonomy is not kept fixed then δS will acquire an additional unwanted term. This makes it clear that one should fix the holonomy in order to obtain the desired first law. Note also that any fixed holonomy will do, in terms of satisfying the first law.

Another notable point is that our derivation extends essentially automatically to to an arbitrary gauge group containing an SL(2,R) subgroup. Simply decompose the the generators into irreducible representations of SL(2,R), and denote the generators in a given representation as $V_{(i)}{}^{s}_{m}$, $m = -(s-1), \ldots s-1$, where the i label takes into account the multiplicity of a given representation. Note though that in our discussion we took the index s to obey $s > 2$, which leaves out the singlet; including the $s = 1$ case is straightforward. For some gauge groups, such as SL(N,R) with $N > 2$, there are multiple inequivalent choices of SL(2,R) subgroups, and these lead to the existence of black holes with different asymptotics [110]. From the CFT point of view, these correspond to thermal states in CFT with different W-algebra symmetries. Since nowhere in our computation did we assume a particular SL(2,R) subgroup, it should be clear that our entropy formula applies to all such cases.

11 Conclusions

In this thesis we studied various dynamics of black holes in anti de Sitter spaces by using holography.

In the first original part of this thesis we discussed a systematic gravity realization of quantum quenches of 2d CFTs. In the construction we introduced a spacetime boundary into bulk geometries. The spacetime boundary is the gravity counterpart of a boundary state in CFTs[56, 54, 55], which represents the initial condition of the quantum quench we consider. The location of the spacetime boundary in the bulk geometry is determined by pulling back the spacetime boundary in the Poincare AdS_3 by the bulk extension of the associated Lorentzian conformal map.

The introduction of a spacetime boundary means that when we compute holographic entanglement entropy, we need to consider an extremal surface which ends on the spacetime boundary as well as boundary of the subsystem, in addition to a conventional connected surface which only ends on the boundary of the subsystem. We called the surface as disconnected surface. We saw phase transitions between the connected surface and the disconnected surface explain the whole time evolution of entanglement entropy in a quantum quench holographically. Especially the length of the disconnected surface captures the early time behavior of entanglement entropy in most of all cases. We also found that when subsystem is an infinite interval, the time evolution of entanglement entropy is entirely explained by the length of the disconnected surface in all quantum quenches.

We consider several examples as applications of the construction. We saw that a particular inhomogeneous quench is dual to a spacetime in which two black strings merge into the third black string. Except junction points, they are in local equilibrium and the temperature of these strings explain the behavior of entanglement entropy. We address the relation between the local quench in 2d CFTs and shock wave geometry. We saw that the location of the shock wave determines the area of both surfaces.

In the second part, we considered a two dimensional global quench of a Dirac fermion on a cylinder. The result shows that the von-Neumann entropy is always vanishing and the coarse-grained entropy S_{eff} is oscillating as a function of time. This offers us a clear toy holographic dual of a formation and decay of black holes, which is free from the information loss problem. We interpreted this fact as the successive productions and annihilations of quantum black holes. We also studied the behavior of two point functions and confirmed that they support this interpretation. We found that the two point functions cannot be zero and is periodic in time which shows some recurrence of our free system.

In the final section we obtained a formula that computes the entropy of a general stationary higher spin black hole in 2+1 dimensions. Although the notion of an event horizon is somewhat vague for black holes in higher spin theories, we do have a definite notion of a conical singularity in terms of holonomy. A Euclidean black hole with the period of the timelike cycle different from the inverse of the Hawking temperature is an example of a configuration with a conical singularity. Then the field strength of the configuration is

delta functionally divergent at the singularity. It was recognized [119, 120, 121, 122] that only the contribution from the conical singularity to the action is necessary to reproduce the entropy of the black hole.

With this point of view in mind, in this part we developed a method to calculate the contribution of the conical singularity to the Chern Simons action, by carefully regularizing the connection. We used this result to compute the black hole entropy. In the end we find a general formula 303 An advantage of this method is that since only terms with radial derivatives in the action have a chance to produce a delta function like divergence, it is sufficient to evaluate the $\int A \wedge dA$ term in the Chern Simons action. We don't need to care about other terms, such as boundary terms, which should be taken ito account when evaluating the total free energy of the black hole. More precisely, since these terms are all proportional to α (deficit parameter), they vanish in (279).

This statement is equally true in the metric formulation of Einstein gravity. When we evaluate the free energy of the asymptotically flat Schwarzchild black hole, the bulk Einstein-Hilbert action vanishes and we have to take into account the Gibbons-Hawking boundary term. On the other hand, when we compute the entropy of the black hole by the conical singularity method, we only have to evaluate the contribution of the conical singularity at the tip to the Einstein-Hilbert action. Since the entropy only depends on the local geometry of the horizon, it is efficient to use a computational scheme that makes this fact manifest.

There are several outlook for future study. As we have seen, an AdS eternal black brane corresponds to the thermofield double state $|\phi\rangle = \sum_n e^{-\beta E_n}|n\rangle|n\rangle$ of boundary theory. In the $\mathcal{W}_N$ minimal model one can consider thermofield double states perturbed by higher spin chemical potentials, $|\phi\rangle = \sum_n e^{-\beta E_n - \mu W_n}|n\rangle|n\rangle$, where W_n denote higher spin charges of the state $|n\rangle$. It would be interesting to consider the gravity dual of thes states. Since the event horizon of higher spin black holes are gauge dependent, usual analytic continuation of black holes do not work. One need to develop a gauge invariant way of the continuations. A related problem is calculations of boundary retarded green's functions from higher spin black holes. Euclidean two point functions in the presence of higher spin chemical potential were holographically computed in [114]. Again the problem is to find appropriate boundary conditions for scalar fields in the absence of event horizons.

There are interesting time dependent black holes, which have peculiar Penrose diagrams [129, 130]. It would be interesting to consider time evolution of entanglement entropy.

Acknowledgements

The author is grateful to the colleagues in our theoretical high energy physics group of Yukawa institute as well Kavli IPMU. He mostly thanks to his advisor Prof. T. Takayanagi for encouragement , discussions, supports, as well as always correcting the author's terrible English found in his drafts as far as possible. He also thanks J. Bhattacharya, P. Kraus, M. Nozaki, N.Ogawa, S.Ryu for collaboration. He is also thanks UCLA theoretical high energy group for hospitality during his stay after the submission of the paper[3].

A Basis of $SL(3,\mathbb{R})$ generators

We use following basis of $SL(3,R)$ generators

$$L_1 = \begin{pmatrix} 0 & 0 & 0 \\ 1 & 0 & 0 \\ 0 & 1 & 0 \end{pmatrix}, \quad L_0 = \begin{pmatrix} 1 & 0 & 0 \\ 0 & 0 & 0 \\ 0 & 0 & -1 \end{pmatrix}, \quad L_{-1} = \begin{pmatrix} 0 & -2 & 0 \\ 0 & 0 & -2 \\ 0 & 0 & 0 \end{pmatrix}$$

$$W_2 = \begin{pmatrix} 0 & 0 & 0 \\ 0 & 0 & 0 \\ 2 & 0 & 0 \end{pmatrix}, \quad W_1 = \begin{pmatrix} 0 & 0 & 0 \\ 1 & 0 & 0 \\ 0 & -1 & 0 \end{pmatrix}, \quad W_0 = \frac{2}{3}\begin{pmatrix} 1 & 0 & 0 \\ 0 & -2 & 0 \\ 0 & 0 & 1 \end{pmatrix}$$

$$W_{-1} = \begin{pmatrix} 0 & -2 & 0 \\ 0 & 0 & 2 \\ 0 & 0 & 0 \end{pmatrix}, \quad W_{-2} = \begin{pmatrix} 0 & 0 & 8 \\ 0 & 0 & 0 \\ 0 & 0 & 0 \end{pmatrix} \tag{321}$$

The trace of these matrices are

$$\mathrm{tr}(L_0^2) = 2, \qquad \mathrm{tr}(L_1 L_{-1}) = -4, \qquad \mathrm{tr}(W_0 W_0) = \frac{8}{3} \qquad \mathrm{tr}(W_1 W_{-1}) = -4, \qquad \mathrm{tr}(W_2 W_{-2}) = 16 \tag{322}$$

We also use "tr*" which is the quarter of the matrix trace when evaluating Chern Simons action[98].

B Entropy formula for general stationary black holes

In this appendix we derive an entropy formula for general stationary higher spin black holes. An example of a stationary black hole is a rotating BTZ black hole. The connection of the black hole is given by

$$\begin{aligned} A &= \left(e^{\rho} L_1 - e^{-\rho} \frac{2\pi \mathcal{L}}{k} L_{-1} \right) dx^+ + L_0 d\rho \\ \bar{A} &= -\left(e^{\rho} L_{-1} - e^{-\rho} \frac{2\pi \bar{\mathcal{L}}}{k} L_1 \right) dx^+ - L_0 d\rho \end{aligned} \tag{323}$$

with $\mathcal{L} \neq \bar{\mathcal{L}}$. The event horizon is located at

$$e^{2\rho_+} = \frac{2\pi}{k} \sqrt{\mathcal{L}\bar{\mathcal{L}}}. \tag{324}$$

The entropy of the black hole is given by

$$S = \frac{A}{4G} = 2\pi \left(\sqrt{2\pi \mathcal{L} k} + \sqrt{2\pi \bar{\mathcal{L}} k} \right). \tag{325}$$

In the corresponding Euclidean configuration, the modular parameter τ of the boundary torus contains non vanishing real part,

$$\tau = \frac{i\beta}{2\pi} (1 + \Omega) = \frac{ik}{2} \frac{1}{\sqrt{2\pi k \mathcal{L}}}, \tag{326}$$

where Ω is the complex angular velocity. Since lines $\Theta = \theta - \Omega t = const$ are contractible cycles, it is convenient to write the connection as

$$\begin{aligned} A_t dt + A_\theta d\theta &= i\beta \left(A_t + \Omega A_\theta \right) dT + A_\theta d\Theta \\ &= 2\pi \left(\tau A_+ - \bar{\tau} A_- \right) dT + A_\theta d\Theta. \end{aligned} \tag{327}$$

We introduced a rescaled Euclidean time coordinate T which satisfies $t = i\beta T$ and $T \cong T+1$.

The holonomy around the contractible cycle is derived by integrating the connection along the line $\Theta = 0$. When (326) is satisfied the holonomy lies in the center of the gauge group. Suppose we replace $\beta \to \alpha\beta$ appearing in the connection and vary α away from 1 while the relation $T \sim T+1$ is kept fixed. Then the connection develops a conical singularity and the holonomy becomes nontrivial. To evaluate the action, we have to regularize the connections. It turns out that the connections

$$\begin{aligned} \tilde{A} &= \frac{1}{u(r)} \left(2\pi \left(\tau A_+ - \bar{\tau} A_- \right) dT - A_t d\Theta \right) + \left(A_t + A_\theta \right) d\Theta \\ \tilde{\bar{A}} &= \frac{1}{u(r)} \left(2\pi \left(\tau \bar{A}_+ - \bar{\tau} \bar{A}_- \right) dT + \bar{A}_t d\Theta \right) + \left(-\bar{A}_t + \bar{A}_\theta \right) d\Theta \end{aligned} \tag{328}$$

are the right regularization because they do not change the volume of the torus located at $\rho, \rho - \rho_+ << 1$ for the rotating BTZ black hole. By evaluating the $\int A \wedge dA$ term and taking the derivative in terms of α, we get the final expression,

$$S = -2\pi i k \mathrm{Tr} \left[A_+ \left(\tau A_+ - \bar{\tau} A_- \right) \right] - 2\pi i k \mathrm{Tr} \left[\bar{A}_- \left(\tau \bar{A}_+ - \bar{\tau} \bar{A}_- \right) \right]. \tag{329}$$

It is straightforward to verify that this yields agreement with (325).

C Formula for quantum quneches

here we summarize the general formulas of quantum quenches. As discussed in section 2, a quantum quench is specified by an associated Riemann surface Σ with boundary or the conformal map which maps Σ into half plane. Let $W^{\pm}(x^{\pm})$ be the corresponding Lorentzian map derived by a Wick rotation.

The time evolution of entanglement entropy in CFT side is given by

$$\begin{aligned}S_{CFT}(l_1,l_2,t) = &\frac{c}{6}\log\left[W^+(l_1+t)-W^+(l_2+t)\right]\left[W^-(l_1-t)-W^-(l_2-t)\right]\\ &+\frac{c}{6}\log\left[W^+(l_1+t)+W^-(l_1-t)\right]\left[W^+(l_2+t)+W^-(l_2-t)\right]\\ &-\frac{c}{6}\log\left[W^+(l_1+t)+W^-(l_2-t)\right]\left[W^+(l_2+t)+W^-(l_1-t)\right]\\ &-\frac{c}{6}\log a^2\sqrt{\frac{dW^+}{dx^+}(l_1+t)\frac{dW^-}{dx^-}(l_1-t)\frac{dW^+}{dx^+}(l_2+t)\frac{dW^-}{dx^-}(l_2-t)}\\ &\quad , \end{aligned} \tag{330}$$

where a denotes UV cut off of the CFT. The contribution of the connected surface to the holographic entanglement entropy is

$$\begin{aligned}S_c(l_1,l_2,t) = &\frac{c}{6}\log\left[W^+(l_2+t)-W^+(l_1+t)\right]\left[W^-(l_2-t)-W^-(l_1-t)\right]\\ &-\frac{c}{6}\log a^2\sqrt{\frac{dW^+}{dx^+}(l_1+t)\frac{dW^-}{dx^-}(l_1-t)\frac{dW^+}{dx^+}(l_2+t)\frac{dW^-}{dx^-}(l_2-t)}\\ &\quad . \end{aligned} \tag{331}$$

The contribution of the disconnected surface is

$$\begin{aligned}S_{dc}(l_1,l_2,t) = &\frac{c}{6}\log\left[W^+(l_1+t)+W^-(l_1-t)\right]\left[W^+(l_2+t)+W^-(l_2-t)\right]\\ &-\frac{c}{6}\log a^2\sqrt{\frac{dW^+}{dx^+}(l_1+t)\frac{dW^-}{dx^-}(l_1-t)\frac{dW^+}{dx^+}(l_2+t)\frac{dW^-}{dx^-}(l_2-t)}\\ &\quad . \end{aligned} \tag{332}$$

D A Derivation of Two Point Functions on Cylinder

Here we would like to present an explicit derivation of two point functions (180) on cylinder. We work in the description of a massless scalar field X via the bosonization of the Dirac fermion. We set $\alpha' = 2$ in string theory convention and follow [82] about the notations of the mode expansions of a scalar field and the definitions of theta functions.

We employ the complex coordinate $(y, \bar{y})$ on the cylinder defined by (179). In the operator formalism, the scalar field is quantized as usual

$$X_L = x_L - ip_L y + i\textstyle\sum_{m\neq 0}\frac{\alpha_m}{m}e^{-my}, \quad X_R = x_R - ip_R\bar{y} + i\displaystyle\sum_{m\neq 0}\frac{\tilde{\alpha}_m}{m}e^{-m\bar{y}},$$

where the commutation relations are given by

$$[x_L, p_L] = i, \quad [x_R, p_R] = i, \quad [\alpha_m, \alpha_n] = m\delta_{n+m,0}, \quad [\tilde{\alpha}_m, \tilde{\alpha}_n] = m\delta_{n+m,0}. \tag{333}$$

At the compactification radius R, the momenta are quantized as follows

$$p_L = \frac{n}{R} + \frac{wR}{2}, \quad p_R = \frac{n}{R} - \frac{wR}{2}, \tag{334}$$

in terms of the integers n (momentum) and w (winding). The (un-normalized) two point function of the normal ordered vertex operator $V_{(k_L,k_R)} =: e^{ik_L X_L + ik_R X_R} :$ is written as follows

$$\begin{aligned} &\langle V_{(k_L,k_R)}(y_1,\bar{y}_1) V_{(-k_L,-k_R)}(y_2,\bar{y}_2)\rangle_{cylinder} \\ &= \langle B| e^{-\frac{\beta}{2}H} V_{(k_L,k_R)}(y_1,\bar{y}_1) V_{(-k_L,-k_R)}(y_2,\bar{y}_2)|B\rangle. \end{aligned} \tag{335}$$

The Hamiltonian is given in terms of the Virasoro generators as $H = L_0 + \bar{L}_0 - \frac{1}{12}$.

D.1 Neumann Case

The boundary state $|B\rangle$ for the Neumann boundary condition [89] is given by

$$|B\rangle_N = \mathcal{N}\ e^{-\sum_{n=1}^{\infty} \frac{1}{n}\alpha_{-n}\tilde{\alpha}_{-n}} \sum_{w=-\infty}^{\infty} |w\rangle, \tag{336}$$

where $\mathcal{N}$ is the normalization factor whose explicit value is not necessary for our purpose. For bosonization procedures in the boundary state formalism, refer to [90].

The zero-mode part of (335) can be calculated by using the Baker-Campell-Hausdorff (BCH) formula as follows

$$\begin{aligned} &\textstyle\sum_{w=-\infty}^{\infty} \langle w| e^{-\frac{\beta}{2}H} e^{ik_L(x_L - ip_L y_1) + ik_R(x_R - ip_R \bar{y}_1)} e^{-ik_L(x_L - ip_L y_2) - ik_R(x_R - ip_R \bar{y}_2)} |w\rangle \\ &= \textstyle\sum_{w=-\infty}^{\infty} e^{-\frac{R^2 w^2 \beta}{4}} e^{\frac{R}{2}(k_L w(y_1 - y_2) - k_R w(\bar{y}_1 - \bar{y}_2))} e^{\frac{k_L^2}{2}(y_1 - y_2) + \frac{k_R^2}{2}(\bar{y}_2 - \bar{y}_1)}. \end{aligned} \tag{337}$$

The massive modes can be computed by employing the BCH formula, leading to the identity

$$\langle 0| e^{-\hat{\alpha}\hat{\beta} z} e^{a_L \hat{\alpha} + a_R \hat{\beta}} e^{b_L \hat{\alpha}^+ + b_R \hat{\beta}^+} e^{-\hat{\alpha}^+ \hat{\beta}^+} |0\rangle = \frac{1}{1-z} \cdot e^{\frac{a_L b_L + a_R b_R - a_L a_R - z b_L b_R}{1-z}}, \tag{338}$$

where we assume the commutation relation $[\hat{\alpha}, \hat{\alpha}^+] = [\hat{\beta}, \hat{\beta}^+] = 1$. Especially we can perform the calculations for massive parts by taking $z = e^{-n\beta}$ and

$$\begin{aligned} a_L = -\tfrac{k_L}{\sqrt{n}}(e^{-ny_1} - e^{-ny_2}), \quad a_R = -\tfrac{k_R}{\sqrt{n}}(e^{-n\bar{y}_1} - e^{-n\bar{y}_2}), \\ b_L = \tfrac{k_L}{\sqrt{n}}(e^{ny_1} - e^{ny_2}), \quad b_R = \tfrac{k_R}{\sqrt{n}}(e^{n\bar{y}_1} - e^{n\bar{y}_2}), \end{aligned} \tag{339}$$

in (338). By expanding $(1-e^{-n\beta})^{-1}=\sum_{m=0}^{\infty}e^{-4mn\beta}$ and changing the order of the summation w.r.t n and m, eventually we can factorized the result into θ functions. The final result is given by

$$\begin{aligned}
&\langle B|e^{-\frac{\beta}{2}H}V_{(k_L,k_R)}(y_1,\bar{y}_1)V_{(-k_L,-k_R)}(y_2,\bar{y}_2)|B\rangle_N \\
&=\mathcal{N}^2\left[\sum_{w=-\infty}^{\infty}e^{-\frac{R^2w^2\beta}{8}}e^{\frac{R}{2}(k_Lw(y_1-y_2)-k_Rw(\bar{y}_1-\bar{y}_2))}\right]\cdot\frac{1}{\eta\left(\frac{i\beta}{2\pi}\right)} \\
&\cdot\left(\frac{\eta\left(\frac{i\beta}{2\pi}\right)^3}{\theta_1\left(\frac{y_2-y_1}{2\pi i}|\frac{i\beta}{2\pi}\right)}\right)^{k_L^2}\cdot\left(\frac{\eta\left(\frac{i\beta}{2\pi}\right)^3}{\theta_1\left(\frac{\bar{y}_2-\bar{y}_1}{2\pi i}|\frac{2i\epsilon}{\pi}\right)}\right)^{k_R^2}\cdot\left(\frac{\theta_1\left(\frac{y_1+\bar{y}_1}{2\pi i}|\frac{i\beta}{2\pi}\right)\theta_1\left(\frac{y_2+\bar{y}_2}{2\pi i}|\frac{i\beta}{2\pi}\right)}{\theta_1\left(\frac{y_1+\bar{y}_2}{2\pi i}|\frac{i\beta}{2\pi}\right)\theta_1\left(\frac{y_2+\bar{y}_1}{2\pi i}|\frac{i\beta}{2\pi}\right)}\right)^{k_Lk_R}.
\end{aligned}\tag{340}$$

After we substituting the values (179) and the twisted vertex operators (177) at the free fermion radius $R=1$, we find that the second line of the above expression is rewritten as

$$\frac{\sum_{w=-\infty}^{\infty}e^{-\frac{w^2\epsilon}{2}}}{\eta\left(\frac{i\beta}{2\pi}\right)}=\frac{\theta_3\left(0|\frac{i\beta}{2\pi}\right)+\theta_2\left(0|\frac{i\beta}{2\pi}\right)}{\eta\left(\frac{i\beta}{2\pi}\right)},\tag{341}$$

where the first and second term are interpreted as the NS and R-sector of the Dirac fermion. Therefore it is equal to $\langle B|e^{-\frac{\beta}{2}H}|B\rangle$ and can be neglected in order to find the normalized two point functions as we did in (175). In this way we obtain the result (180).

D.2 Dirichlet Case

For the Dirichlet boundary condition, the boundary state is given by

$$|B\rangle_D=\mathcal{N}e^{\sum_{n=1}^{\infty}\frac{1}{n}\alpha_{-n}\tilde{\alpha}_{-n}}\sum_{n=-\infty}^{\infty}|n\rangle.\tag{342}$$

By repeating similar calculations, in the end, we find the two point functions

$$\begin{aligned}
&\langle B|e^{-2\epsilon H}V_{(k_L,k_R)}(y_1,\bar{y}_1)V_{(-k_L,-k_R)}(y_2,\bar{y}_2)|B\rangle_D \\
&=\mathcal{N}^2\left[\sum_{n=-\infty}^{\infty}e^{-\frac{n^2\beta}{2R^2}}e^{\frac{n}{R}(k_L(y_1-y_2)+k_R(\bar{y}_1-\bar{y}_2))}\right]\cdot\frac{1}{\eta\left(\frac{i\beta}{2\pi}\right)} \\
&\cdot\left(\frac{\eta\left(\frac{i\beta}{2\pi}\right)^3}{\theta_1\left(\frac{y_2-y_1}{2\pi i}|\frac{i\beta}{2\pi}\right)}\right)^{k_L^2}\cdot\left(\frac{\eta\left(\frac{i\beta}{2\pi}\right)^3}{\theta_1\left(\frac{\bar{y}_2-\bar{y}_1}{2\pi i}|\frac{i\beta}{2\pi}\right)}\right)^{k_R^2}\cdot\left(\frac{\theta_1\left(\frac{y_1+\bar{y}_1}{2\pi i}|\frac{i\beta}{2\pi}\right)\theta_1\left(\frac{y_2+\bar{y}_2}{2\pi i}|\frac{i\beta}{2\pi}\right)}{\theta_1\left(\frac{y_1+\bar{y}_2}{2\pi i}|\frac{i\beta}{\pi}\right)\theta_1\left(\frac{y_2+\bar{y}_1}{2\pi i}|\frac{i\beta}{2\pi}\right)}\right)^{-k_Lk_R}.
\end{aligned}$$

After we substituting the values (179) and the twisted vertex operators (178) at the free fermion radius $R=1$, we find that the second line of the above expression is rewritten as

$$\frac{\sum_{n=-\infty}^{\infty}e^{-n^2\frac{\beta}{2}}}{\eta\left(\frac{i\beta}{2\pi}\right)}=\frac{\theta_3\left(0|\frac{i\beta}{2\pi}\right)}{\eta\left(\frac{i\beta}{2\pi}\right)},\tag{343}$$

which includes only the NS-sector.

References

[1] T. Ugajin, arXiv:1311.2562 [hep-th].

[2] T. Takayanagi and T. Ugajin, "Measuring Black Hole Formations by Entanglement Entropy via Coarse-Graining," JHEP **1011**, 054 (2010) [arXiv:1008.3439 [hep-th]].

[3] P. Kraus and T. Ugajin, "An Entropy Formula for Higher Spin Black Holes via Conical Singularities," JHEP **1305**, 160 (2013) [arXiv:1302.1583 [hep-th]].

[4] K. Schwarzschild; "Uber das Gravitationsfeld eines Massenpunktes nach der Einsteinschen Theorie" Sitzungsberichte der Koniglich Preussischen Akademie der Wissenschaften .Berlin (Math.Phys.) 1916 (1916) 189-196

[5] Bekenstein, Jacob D. "Black Holes and Entropy" Physical Review D, vol. 7, Issue 8, pp. 2333-2346

[6] Bardeen, J. M.; Carter, B.; Hawking, S. W. "The four laws of black hole mechanics" Communications in Mathematical Physics, Volume 31, Issue 2, pp.161-170

[7] A. Strominger and C. Vafa, "Microscopic origin of the Bekenstein-Hawking entropy," Phys. Lett. B **379**, 99 (1996) [hep-th/9601029].

[8] S.W. Hawking "Breakdown of Predictability in Gravitational Collapse" Phys.Rev. D14 (1976) 2460-2473

[9] A. Almheiri, D. Marolf, J. Polchinski and J. Sully, "Black Holes: Complementarity or Firewalls?," JHEP **1302**, 062 (2013) [arXiv:1207.3123 [hep-th]].

[10] Y. Sekino and L. Susskind, "Fast Scramblers," JHEP **0810**, 065 (2008) [arXiv:0808.2096 [hep-th]].

[11] L. Susskind, L. Thorlacius and J. Uglum, "The Stretched horizon and black hole complementarity," Phys. Rev. D **48**, 3743 (1993) [hep-th/9306069].

[12] K. Papadodimas and S. Raju, "An Infalling Observer in AdS/CFT," JHEP **1310**, 212 (2013) [arXiv:1211.6767 [hep-th]].

[13] K. Papadodimas and S. Raju, "The Black Hole Interior in AdS/CFT and the Information Paradox," arXiv:1310.6334 [hep-th].

[14] G. Festuccia and H. Liu, "Excursions beyond the horizon: Black hole singularities in Yang-Mills theories. I.," JHEP **0604**, 044 (2006) [hep-th/0506202].

[15] P. Kraus, H. Ooguri and S. Shenker, "Inside the horizon with AdS / CFT," Phys. Rev. D **67**, 124022 (2003) [hep-th/0212277].

[16] L. Fidkowski, V. Hubeny, M. Kleban and S. Shenker, "The Black hole singularity in AdS / CFT," JHEP **0402**, 014 (2004) [hep-th/0306170].

[17] I. Heemskerk, D. Marolf, J. Polchinski and J. Sully, "Bulk and Transhorizon Measurements in AdS/CFT," JHEP **1210**, 165 (2012) [arXiv:1201.3664 [hep-th]].

[18] G. 't Hooft, "Dimensional reduction in quantum gravity," gr-qc/9310026.

[19] L. Susskind, "The World as a hologram," J. Math. Phys. **36**, 6377 (1995) [hep-th/9409089].

[20] J. M. Maldacena, "The Large N limit of superconformal field theories and supergravity," Adv. Theor. Math. Phys. **2**, 231 (1998) [hep-th/9711200].

[21] S. Ryu and T. Takayanagi, "Holographic derivation of entanglement entropy from AdS/CFT," Phys. Rev. Lett. **96**, 181602 (2006) [hep-th/0603001]. JHEP **0608**, 045 (2006) [hep-th/0605073]

[22] V. E. Hubeny, M. Rangamani and T. Takayanagi, "A Covariant holographic entanglement entropy proposal," JHEP **0707**, 062 (2007) [arXiv:0705.0016 [hep-th]].

[23] P. Figueras, V. E. Hubeny, M. Rangamani and S. F. Ross, JHEP **0904**, 137 (2009) [arXiv:0902.4696 [hep-th]].

[24] M. Headrick, "Entanglement Renyi entropies in holographic theories," Phys. Rev. D **82**, 126010 (2010) [arXiv:1006.0047 [hep-th]].

[25] T. Nishioka, S. Ryu and T. Takayanagi, "Holographic Entanglement Entropy: An Overview," J. Phys. A **42**, 504008 (2009) [arXiv:0905.0932 [hep-th]].

[26] T. Hirata and T. Takayanagi, "AdS/CFT and strong subadditivity of entanglement entropy," JHEP **0702**, 042 (2007) [hep-th/0608213].

[27] M. Headrick and T. Takayanagi, "A Holographic proof of the strong subadditivity of entanglement entropy," Phys. Rev. D **76**, 106013 (2007) [arXiv:0704.3719 [hep-th]].

[28] J. D. Brown and M. Henneaux, "Central Charges in the Canonical Realization of Asymptotic Symmetries: An Example from Three-Dimensional Gravity," Commun. Math. Phys. **104**, 207 (1986).

[29] A. Lewkowycz and J. Maldacena, "Generalized gravitational entropy," JHEP **1308**, 090 (2013) [arXiv:1304.4926 [hep-th]].

[30] H. Casini, M. Huerta and R. C. Myers, "Towards a derivation of holographic entanglement entropy," JHEP **1105**, 036 (2011) [arXiv:1102.0440 [hep-th]].

[31] R. Emparan, "AdS / CFT duals of topological black holes and the entropy of zero energy states," JHEP **9906**, 036 (1999) [hep-th/9906040].

S. Aminneborg, I. Bengtsson, S. Holst and P. Peldan, "Making anti-de Sitter black holes," Class. Quant. Grav. **13**, 2707 (1996) [gr-qc/9604005].

D. R. Brill, J. Louko and P. Peldan, "Thermodynamics of (3+1)-dimensional black holes with toroidal or higher genus horizons," Phys. Rev. D **56**, 3600 (1997) [gr-qc/9705012].

L. Vanzo, "Black holes with unusual topology," Phys. Rev. D **56**, 6475 (1997) [gr-qc/9705004].

R. B. Mann, "Pair production of topological anti-de Sitter black holes," Class. Quant. Grav. **14**, L109 (1997) [gr-qc/9607071].

D. Birmingham, "Topological black holes in Anti-de Sitter space," Class. Quant. Grav. **16**, 1197 (1999) [hep-th/9808032].

R. Emparan, Phys. Lett. B **432**, 74 (1998) [hep-th/9804031].

[32] T. Hartman and J. Maldacena, "Time Evolution of Entanglement Entropy from Black Hole Interiors," JHEP **1305**, 014 (2013) [arXiv:1303.1080 [hep-th]].

[33] S. H. Shenker and D. Stanford, "Black holes and the butterfly effect," arXiv:1306.0622 [hep-th].

[34] J. M. Maldacena, "Eternal black holes in anti-de Sitter," JHEP **0304**, 021 (2003) [hep-th/0106112].

[35] Thermodynamics of black holes in anti-de Sitter space Hawking, S. W.; Page, Don N. Communications in Mathematical Physics, vol. 87, Issue 4, p.577-588

[36] J. Abajo-Arrastia, J. Aparicio and E. Lopez, "Holographic Evolution of Entanglement Entropy," JHEP **1011**, 149 (2010) [arXiv:1006.4090 [hep-th]].

[37] J. Aparicio and E. Lopez, "Evolution of Two-Point Functions from Holography," JHEP **1112**, 082 (2011) [arXiv:1109.3571 [hep-th]].

[38] T. Albash and C. V. Johnson, "Evolution of Holographic Entanglement Entropy after Thermal and Electromagnetic Quenches," New J. Phys. **13**, 045017 (2011) [arXiv:1008.3027 [hep-th]].

[39] V. Balasubramanian, A. Bernamonti, J. de Boer, N. Copland, B. Craps, E. Keski-Vakkuri, B. Muller and A. Schafer *et al.*, "Thermalization of Strongly Coupled Field Theories," Phys. Rev. Lett. **106**, 191601 (2011) [arXiv:1012.4753 [hep-th]].

[40] V. Balasubramanian, A. Bernamonti, J. de Boer, N. Copland, B. Craps, E. Keski-Vakkuri, B. Muller and A. Schafer *et al.*, "Holographic Thermalization," Phys. Rev. D **84**, 026010 (2011) [arXiv:1103.2683 [hep-th]].

[41] H. Liu and S. J. Suh, "Entanglement Tsunami: Universal Scaling in Holographic Thermalization," arXiv:1305.7244 [hep-th].

[42] H. Liu and S. J. Suh, "Entanglement growth during thermalization in holographic systems," arXiv:1311.1200 [hep-th].

[43] A. Buchel, L. Lehner, R. C. Myers and A. van Niekerk, "Quantum quenches of holographic plasmas," JHEP **1305**, 067 (2013) [arXiv:1302.2924 [hep-th]].

[44] A. Buchel, R. C. Myers and A. van Niekerk, "Universality of Abrupt Holographic Quenches," arXiv:1307.4740 [hep-th].

[45] M. Nozaki, T. Numasawa and T. Takayanagi, "Holographic Local Quenches and Entanglement Density," JHEP **1305**, 080 (2013) [arXiv:1302.5703 [hep-th]].

[46] M. M. Roberts, "Time evolution of entanglement entropy from a pulse," arXiv:1204.1982 [hep-th].

[47] V. Balasubramanian and P. Kraus, "A Stress tensor for Anti-de Sitter gravity," Commun. Math. Phys. **208**, 413 (1999) [hep-th/9902121].

[48] M. Henningson and K. Skenderis, "The Holographic Weyl anomaly," JHEP **9807**, 023 (1998) [hep-th/9806087].

[49] S. de Haro, S. N. Solodukhin and K. Skenderis, "Holographic reconstruction of space-time and renormalization in the AdS / CFT correspondence," Commun. Math. Phys. **217**, 595 (2001) [hep-th/0002230].

[50] P. Calabrese and J. L. Cardy, "Entanglement entropy and quantum field theory," J. Stat. Mech. **0406**, P06002 (2004) [hep-th/0405152].

[51] P.Calabrese,J. Cardy "Entanglement and correlation functions following a local quench: a conformal field theory approach" Journal of Statistical Mechanics: Theory and Experiment, Issue 10, pp. 10004 (2007). arXiv:0708.3750 [cond-mat.stat-mech]

[52] P.Calabrese,J. Cardy "Time Dependence of Correlation Functions Following a Quantum Quench" Physical Review Letters, vol. 96, Issue 13, id. 136801 arXiv:cond-mat/0601225

[53] Sotiriadis, Spyros; Cardy, John "Inhomogeneous quantum quenches" Journal of Statistical Mechanics: Theory and Experiment, Issue 11, pp. 11003, 29 pp. (2008)

[54] A. Karch and L. Randall, "Locally localized gravity," JHEP **0105**, 008 (2001) [hep-th/0011156].

[55] O. DeWolfe, D. Z. Freedman and H. Ooguri, "Holography and defect conformal field theories," Phys. Rev. D **66**, 025009 (2002) [hep-th/0111135].

[56] T. Takayanagi, "Holographic Dual of BCFT," Phys. Rev. Lett. **107**, 101602 (2011) [arXiv:1105.5165 [hep-th]].

[57] M. Fujita, T. Takayanagi and E. Tonni, "Aspects of AdS/BCFT," JHEP **1111**, 043 (2011) [arXiv:1108.5152 [hep-th]].

[58] M. Nozaki, T. Takayanagi and T. Ugajin, "Central Charges for BCFTs and Holography," JHEP **1206**, 066 (2012) [arXiv:1205.1573 [hep-th]].

[59] K. Jensen and A. O'Bannon, "Holography, Entanglement Entropy, and Conformal Field Theories with Boundaries or Defects," arXiv:1309.4523 [hep-th].

[60] T. Azeyanagi, A. Karch, T. Takayanagi and E. G. Thompson, "Holographic calculation of boundary entropy," JHEP **0803**, 054 (2008) [arXiv:0712.1850 [hep-th]].

[61] Affleck, Ian; Ludwig, Andreas W. W. "Universal noninteger "ground-state degeneracy" in critical quantum systems" Physical Review Letters, Volume 67, Issue 2, July 8, 1991, pp.161-164

[62] S. W. Hawking, "Breakdown Of Predictability In Gravitational Collapse," Phys. Rev. D **14** (1976) 2460.

[63] P. M. Chesler and L. G. Yaffe, "Horizon formation and far-from-equilibrium isotropization in supersymmetric Yang-Mills plasma," Phys. Rev. Lett. **102**, 211601 (2009) [arXiv:0812.2053 [hep-th]]; "Boost invariant flow, black hole formation, and far-from-equilibrium dynamics in N = 4 supersymmetric Yang-Mills theory," arXiv:0906.4426 [hep-th];

[64] S. Bhattacharyya and S. Minwalla, "Weak Field Black Hole Formation in Asymptotically AdS space-times," JHEP **0909** (2009) 034 [arXiv:0904.0464 [hep-th]].

[65] V. E. Hubeny and M. Rangamani, "A holographic view on physics out of equilibrium," arXiv:1006.3675 [hep-th].

[66] S. R. Das, T. Nishioka and T. Takayanagi, "Probe Branes, Time-dependent Couplings and Thermalization in AdS/CFT," arXiv:1005.3348 [hep-th].

[67] S. Bhattacharyya, V. E. Hubeny, S. Minwalla and M. Rangamani, "Nonlinear Fluid Dynamics from Gravity," JHEP **0802** (2008) 045 [arXiv:0712.2456 [hep-th]]; S. Bhattacharyya *et al.*, "Local Fluid Dynamical Entropy from Gravity," JHEP **0806** (2008) 055 [arXiv:0803.2526 [hep-th]].

[68] L. Bombelli, R. K. Koul, J. H. Lee and R. D. Sorkin, "A Quantum Source Of Entropy For Black Holes," Phys. Rev. D **34**, 373 (1986); M. Srednicki, "Entropy and area," Phys. Rev. Lett. **71**, 666 (1993) [arXiv:hep-th/9303048].

[69] H. Casini and M. Huerta, "A Finite entanglement entropy and the c-theorem," Phys. Lett. B **600**, 142 (2004) [hep-th/0405111].

[70] D. L. Jafferis, I. R. Klebanov, S. S. Pufu and B. R. Safdi, "Towards the F-Theorem: N=2 Field Theories on the Three-Sphere," JHEP **1106**, 102 (2011) [arXiv:1103.1181 [hep-th]].

[71] H. Casini and M. Huerta, "On the RG running of the entanglement entropy of a circle," Phys. Rev. D **85**, 125016 (2012) [arXiv:1202.5650 [hep-th]].

[72] P. Calabrese and J. Cardy, "Entanglement entropy and conformal field theory," J. Phys. A **42** (2009) 504005 [arXiv:0905.4013 [cond-mat.stat-mech]].

[73] H. Casini and M. Huerta, "Entanglement entropy in free quantum field theory," J. Phys. A **42** (2009) 504007 [arXiv:0905.2562 [hep-th]].

[74] R. C. Myers and A. Sinha, "Holographic c-theorems in arbitrary dimensions," JHEP **1101**, 125 (2011) [arXiv:1011.5819 [hep-th]].

[75] P. Calabrese and J. L. Cardy, "Evolution of Entanglement Entropy in One-Dimensional Systems," J. Stat. Mech. **0504** (2005) P010 [arXiv:cond-mat/0503393]; "Entanglement and correlation functions following a local quench: a conformal field theory approach," J. Stat. Mech. (2007) P010004 [arXiv:0708.3750].

[76] P. Calabrese and J. L. Cardy, "Time-dependence of correlation functions following a quantum quench," Phys. Rev. Lett. **96** (2006) 136801 [arXiv:cond-mat/0601225].

[77] S. Sotiriadis, P. Calabrese and J. Cardy, "Quantum Quench from a Thermal Initial State" EPL **87** (2009) 20002, [arXiv:0903.0895 [cond-mat.stat-mech]].

[78] D. N. Page, "Information in black hole radiation," Phys. Rev. Lett. **71** (1993) 3743 [arXiv:hep-th/9306083].

[79] J. M. Maldacena, "Eternal black holes in Anti-de-Sitter," JHEP **0304** (2003) 021 [arXiv:hep-th/0106112].

[80] T. Azeyanagi, T. Nishioka and T. Takayanagi, "Near Extremal Black Hole Entropy as Entanglement Entropy via AdS2/CFT1," Phys. Rev. D **77** (2008) 064005 [arXiv:0710.2956 [hep-th]].

[81] V. E. Hubeny, H. Liu and M. Rangamani, "Bulk-cone singularities & signatures of horizon formation in AdS/CFT," JHEP **0701** (2007) 009 [arXiv:hep-th/0610041].

[82] J. Polchinski, "String theory. Vol. 1 and 2," *Cambridge, UK: Univ. Pr. (1998).*

[83] C. Holzhey, F. Larsen and F. Wilczek, "Geometric and renormalized entropy in conformal field theory," Nucl. Phys. B **424** (1994) 443 [arXiv:hep-th/9403108].

[84] P. Calabrese and J. L. Cardy, "Entanglement entropy and quantum field theory," J. Stat. Mech. **0406** (2004) P002 [arXiv:hep-th/0405152].

[85] G. Festuccia and H. Liu, "The arrow of time, black holes, and quantum mixing of large N Yang-Mills theories," JHEP **0712** (2007) 027 [arXiv:hep-th/0611098].

[86] P. Hayden and J. Preskill, "Black holes as mirrors: quantum information in random subsystems," JHEP **0709** (2007) 120 [arXiv:0708.4025 [hep-th]].

[87] N. Iizuka and J. Polchinski, "A Matrix Model for Black Hole Thermalization," JHEP **0810** (2008) 028 [arXiv:0801.3657 [hep-th]]; N. Iizuka, T. Okuda and J. Polchinski, "Matrix Models for the Black Hole Information Paradox," JHEP **1002** (2010) 073 [arXiv:0808.0530 [hep-th]].

[88] S. S. Gubser, I. R. Klebanov and A. M. Polyakov, "Gauge theory correlators from non-critical string theory," Phys. Lett. B **428**, 105 (1998) [arXiv:hep-th/9802109]; E. Witten, "Anti-de Sitter space and holography," Adv. Theor. Math. Phys. **2**, 253 (1998) [arXiv:hep-th/9802150]; I. R. Klebanov and E. Witten, "AdS/CFT correspondence and symmetry breaking," Nucl. Phys. B **556** (1999) 89 [arXiv:hep-th/9905104].

[89] J. Polchinski and Y. Cai, "Consistency of Open Superstring Theories," Nucl. Phys. B **296** (1988) 91.

[90] M. Frau, L. Gallot, A. Lerda and P. Strigazzi, "Stable non-BPS D-branes in type I string theory," Nucl. Phys. B **564** (2000) 60 [arXiv:hep-th/9903123]; M. Naka, T. Takayanagi and T. Uesugi, "Boundary state description of tachyon condensation," JHEP **0006** (2000) 007 [arXiv:hep-th/0005114].

[91] M. A. Vasiliev, "Higher spin gauge theories: Star product and AdS space," In *Shifman, M.A. (ed.): The many faces of the superworld* 533-610 [hep-th/9910096].

[92] X. Bekaert, S. Cnockaert, C. Iazeolla and M. A. Vasiliev, hep-th/0503128.

[93] I. R. Klebanov and A. M. Polyakov, "AdS dual of the critical O(N) vector model," Phys. Lett. B **550**, 213 (2002) [hep-th/0210114].

[94] E. Sezgin and P. Sundell, "Holography in 4D (super) higher spin theories and a test via cubic scalar couplings," JHEP **0507**, 044 (2005) [hep-th/0305040].

[95] S. Giombi and X. Yin, "Higher Spin Gauge Theory and Holography: The Three-Point Functions," JHEP **1009**, 115 (2010) [arXiv:0912.3462 [hep-th]].

[96] S. Giombi and X. Yin, "Higher Spins in AdS and Twistorial Holography," JHEP **1104**, 086 (2011) [arXiv:1004.3736 [hep-th]].

[97] M. R. Gaberdiel and R. Gopakumar, "An AdS_3 Dual for Minimal Model CFTs," Phys. Rev. D **83**, 066007 (2011) [arXiv:1011.2986 [hep-th]].

[98] A. Campoleoni, S. Fredenhagen, S. Pfenninger and S. Theisen, "Asymptotic symmetries of three-dimensional gravity coupled to higher-spin fields," JHEP **1011**, 007 (2010) [arXiv:1008.4744 [hep-th]].

[99] M. Henneaux and S. -J. Rey, "Nonlinear $W_{infinity}$ as Asymptotic Symmetry of Three-Dimensional Higher Spin Anti-de Sitter Gravity," JHEP **1012**, 007 (2010) [arXiv:1008.4579 [hep-th]].

[100] A. Strominger, "Black hole entropy from near horizon microstates," JHEP **9802**, 009 (1998) [hep-th/9712251].

[101] M. R. Gaberdiel and T. Hartman, "Symmetries of Holographic Minimal Models," JHEP **1105**, 031 (2011) [arXiv:1101.2910 [hep-th]].

[102] M. Ammon, P. Kraus and E. Perlmutter, "Scalar fields and three-point functions in D=3 higher spin gravity," JHEP **1207**, 113 (2012) [arXiv:1111.3926 [hep-th]].

[103] M. R. Gaberdiel, R. Gopakumar, T. Hartman and S. Raju, "Partition Functions of Holographic Minimal Models," JHEP **1108**, 077 (2011) [arXiv:1106.1897 [hep-th]].

[104] M. R. Gaberdiel and R. Gopakumar, "Minimal Model Holography," arXiv:1207.6697 [hep-th].

[105] E. Witten, "(2+1)-Dimensional Gravity as an Exactly Soluble System," Nucl. Phys. B **311**, 46 (1988).

[106] A. Achucarro and P. K. Townsend, "A Chern-Simons Action for Three-Dimensional anti-De Sitter Supergravity Theories," Phys. Lett. B **180**, 89 (1986).

[107] M. P. Blencowe, "A Consistent Interacting Massless Higher Spin Field Theory In D = (2+1)," Class. Quant. Grav. **6**, 443 (1989).

[108] M. Gutperle and P. Kraus, "Higher Spin Black Holes," JHEP **1105**, 022 (2011) [arXiv:1103.4304 [hep-th]].

[109] J. L. Karczmarek, J. M. Maldacena and A. Strominger, "Black hole non-formation in the matrix model," JHEP **0601**, 039 (2006) [hep-th/0411174].

[110] M. Ammon, M. Gutperle, P. Kraus and E. Perlmutter, "Spacetime Geometry in Higher Spin Gravity," JHEP **1110**, 053 (2011) [arXiv:1106.4788 [hep-th]].

[111] A. Castro, E. Hijano, A. Lepage-Jutier and A. Maloney, "Black Holes and Singularity Resolution in Higher Spin Gravity," JHEP **1201**, 031 (2012) [arXiv:1110.4117 [hep-th]].

[112] H. -S. Tan, "Aspects of Three-dimensional Spin-4 Gravity," JHEP **1202**, 035 (2012) [arXiv:1111.2834 [hep-th]].

[113] J. R. David, M. Ferlaino and S. P. Kumar, "Thermodynamics of higher spin black holes in 3D," arXiv:1210.0284 [hep-th].

[114] P. Kraus and E. Perlmutter, "Probing higher spin black holes," arXiv:1209.4937 [hep-th].

[115] P. Kraus and E. Perlmutter, "Partition functions of higher spin black holes and their CFT duals," JHEP **1111**, 061 (2011) [arXiv:1108.2567 [hep-th]].

[116] M. R. Gaberdiel, T. Hartman and K. Jin, "Higher Spin Black Holes from CFT," JHEP **1204**, 103 (2012) [arXiv:1203.0015 [hep-th]].

[117] A. Perez, D. Tempo and R. Troncoso, "Higher spin gravity in 3D: black holes, global charges and thermodynamics," arXiv:1207.2844 [hep-th].

[118] A. Perez, D. Tempo and R. Troncoso, "Higher spin black hole entropy in three dimensions," arXiv:1301.0847 [hep-th].

[119] M. Banados, C. Teitelboim and J. Zanelli, "Black hole entropy and the dimensional continuation of the Gauss-Bonnet theorem," Phys. Rev. Lett. **72**, 957 (1994) [gr-qc/9309026].

[120] V. Iyer and R. M. Wald, "A Comparison of Noether charge and Euclidean methods for computing the entropy of stationary black holes," Phys. Rev. D **52**, 4430 (1995) [gr-qc/9503052].

[121] S. N. Solodukhin, "Entanglement entropy of black holes," Living Rev. Rel. **14**, 8 (2011) [arXiv:1104.3712 [hep-th]].

[122] D. V. Fursaev and S. N. Solodukhin, "On the description of the Riemannian geometry in the presence of conical defects," Phys. Rev. D **52**, 2133 (1995) [hep-th/9501127].

[123] H. S. Tan, "Exploring Three-dimensional Higher-Spin Supergravity based on sl(N —N - 1) Chern-Simons JHEP **1211**, 063 (2012) [arXiv:1208.2277 [hep-th]].

[124] M. Ammon, M. Gutperle, P. Kraus and E. Perlmutter, "Black holes in three dimensional higher spin gravity: A review," arXiv:1208.5182 [hep-th].

[125] A. Castro, R. Gopakumar, M. Gutperle and J. Raeymaekers, "Conical Defects in Higher Spin Theories," JHEP **1202**, 096 (2012) [arXiv:1111.3381 [hep-th]].

[126] W. Israel, "Thermo field dynamics of black holes," Phys. Lett. A **57**, 107 (1976).

[127] V. Balasubramanian, P. Kraus, A. E. Lawrence and S. P. Trivedi, "Holographic probes of anti-de Sitter space-times," Phys. Rev. D **59**, 104021 (1999) [hep-th/9808017].

[128] R. M. Wald, "Black hole entropy is the Noether charge," Phys. Rev. D **48**, 3427 (1993) [gr-qc/9307038].

[129] D. Bak, M. Gutperle and A. Karch, "Time dependent black holes and thermal equilibration," JHEP **0712**, 034 (2007) [arXiv:0708.3691 [hep-th]].

[130] D. Bak, M. Gutperle and S. Hirano, "Three dimensional Janus and time-dependent black holes," JHEP **0702**, 068 (2007) [hep-th/0701108].